September, 1960

TABLE OF CONTENTS

		Page
I.	INTRODUCTION	
	A. Purpose of the Report	I - 1
	B. General Description of the Plant	I - 1
II.	NUCLEAR STEAM SUPPLY SYSTEM	
	A. Design Features of Reactor Components	II - 1
	B. Fission Product Control	II - 9
	C. Fission Product Traps and Helium Purification System	II - 10
	D. Fuel Handling System	II - 17
	E. Primary Coolant System	II - 22
	F. Afterheat Removal System and Emergency Systems	II - 24
	G. Nuclear Design	II - 26
	H. Reactor Instrumentation	II - 31
	I. Control	II - 33
	J. Thermal Design	II - 34
	K. Shielding Criteria	II - 35
	L. Research and Development	II - 37
III.	CONVENTIONAL PLANT AND SERVICES	
	A. General	III - 1
	B. Main Turbine	III - 1
	C. Condensing System	III - 1
	D. Condensate and Feedwater System	III - 1
	E. Circulating Water System	III - 2
	F. Service Water System	III - 2
	G. Water Storage	III - 3

A-574

APPENDIX A

FIGURES

Figure 1 - Plant Perspective

Figure 2 - Pictorial View of 40 EMW High Temperature Gas-Cooled Graphite-Moderated Reactor

Figure 3 - Plant Flow Diagram

Figure 4 - Plot Plan

Figure 5 - Pictorial View of Graphite-Clad Fuel Element

Figure 6 - HTGR Control Rod Assembly (Articulated)

Figure 6A - HTGR Control Rod Assembly (Flexible)

Figure 6B - Control Rod Coolant Flow

Figure 6C - HTGR Hydraulic Motor Control Rod Drive

Figure 7 - Helium Storage, Purification and Supply System Flow Diagram

Figure 8 - Fuel Handling Flow Diagram

Figure 9 - General Arrangement Fuel Handling System

Figure 10 - Fuel Element and Gas Temperatures-Partial Flow Following Scram

Figure 11 - Nuclear Instrumentation Block Diagram

Figure 12 - Fuel Element Surface Temperatures

Figure 13 - Radial Temperature Profiles - Average Fuel Element

Figure 14 - Radial Temperature Profiles - Hottest Fuel Element

Figure 15 - Plant Layout - Ground Floor Plan

Figure 16 - Plant Layout - Operating Floor Plan

Figure 17 - Plant Layout - Longitudinal Section

Figure 18 - Raw Water Flow Diagram

Figure 19 - Containment Equipment and Shield Cooling Flow Diagram

Figure 20 - Containment Ventilation Flow Diagram

Figure 21 - Waste Gas Flow Diagram

Figure 22 - Liquid Waste Flow Diagram

Figure 23 - Fuel Element Temperature - No Coolant Flow

Figure 24 - Fuel Element and Gas Temperatures - Partial Flow Following Scram and One Hour Delay

Figure 25 - Fuel Element Surface Temperature - Reduced System Pressure

Figure 26 - Fuel Element Temperature Rise - Step Insertion of Reactivity - Beginning of Life

Figure 27 - Fuel Element Temperature Rise - Step Insertion of Reactivity - End of Life

Figure 28 - Fuel Element Temperature Rise - Ramp Insertion of Reactivity

Figure 29 - Graphite Thermal Conductivity as a Function of Temperature

Figure 30 - Counterflow Fuel Element Design

Figure 31 - Schematic Diagram of Fuel Element

Figure 32 - Counterflow Vented Element - Activity Level vs. Time

Figure 33 - Counterflow Vented Element - Activity Level vs. Time

Figure 34 - Schematic Diagram of Fuel Element - Cross Section

Figure 35 - Expanded View of Annulus Between Purge Grooves

Figure 36 - Counterflow Fuel Element - Permeation Coefficient vs. Number of Grooves

Figure 37 - Pressure Drop in Purge Annuli

Figure 38 - Pressure Drop in Purge Grooves

Figure 39 - Tensile Thermal Stress in Graphite Outer Sleeve

Figure 40 - F_t, Ratio of Xe Activity Released to Xe Activity Produced at Steady State vs. Half Life

Figure 41 - Adsorption of Krypton on Charcoal

Figure 42 - Adsorption of Xenon on Charcoal

Figure 43 - Adsorption of Xenon on Charcoal

Figure 44 - Adsorption of Krypton on Charcoal

Figure 45 - Flow Diagram for Helium Purification System

Figure 46 - Iodine-Activated Charcoal Adsorption Isotherms

Figure 47 - Heat of Adsorption vs. Loading for I_2-Charcoal System

Figure 48 - Clausius-Clapeyron Plot for I_2 Absorption on Charcoal

Figure 49 - Cesium-Generation Apparatus

Figure 50 - Cesium-Isotherm Apparatus

Figure 51 - Cesium Absorption on Charcoal as a Function of Cesium Vapor Pressure

Figure 52 - Clausius-Clapeyron Plot for Cesium-Charcoal System

Figure 53 - Heat of Adsorption vs. Loading for Cesium-Charcoal System

Figure 54 - Facility Tube and Fuel Diagram

Figure 55 - Section Thru Test Element

Figure 56 - Out-Of-Pool Equipment

Figure 57 - HTGR In-Pile Loop Piping and Instrumentation Diagram

Figure 58 - HTGR Reactor Equipment Test Facility

LIST OF TABLES

TABLE NO.	TITLE	PAGE
1	Technical Data for HTGR Design	II - 2
2	Nuclear Design Characteristics	II - 27
3	Nuclear Parameters Obtained from Cell Calculations for Uniformly Hooded HTGR Core	II - 27
4	Value of Prompt Temperature Coefficient for the Beginning and End of Life	II - 30
4-A	Properties of Uranium and Thorium Carbides and Oxides	II - 40
4-B	Summary of Tests of Graphite for Sleeves and Cans	II - 46
4-C	Results of Irradiation of Capsule GA-311-1	II - 47
4-D	Xenon Permeability Coefficient as Determined from He Permeability and Xe Diffussion Measurements	II - 48
4-E	Capsule 308-2	II - 49
4-F	Capsule 308-3	II - 49
4-G	Capsule 308-4	II - 50
4-H	Summary of Xe^{133} Retention Data	II - 51
4-I	Leakage Tests of Standoff Seals	II - 54
4-J	Fission Product Element Yields and Characteristics	II - 68
4-K	Fiberglass Filter Effectiveness	II - 72
4-L	Typical Loop Operating Parameters	II - 84
5	Gamma Dose Rates from the Containment	VII - 14
6	Integrated Gamma Dose from Containment	VII - 14
7	Relative Atmospheric Dilution Factors	VII - 15
8	Insertion of Reactivity from Credible Accidents	VII - 19
9	Gamma Dose Rates from Containment	VII - 30
10	Integrated Gamma Dose from Containment	VII - 30

II. NUCLEAR STEAM SUPPLY SYSTEM *

A. Design Features of Reactor Components

The proportions and principal operating conditions of the High Temperature Gas Cooled Reactor (HTGR) are summarized in Table 1. The general arrangement for the reactor is shown in pictorial representation in Figure 2.

1. Reactor Core

The active reactor core is a cylinder nine feet in diameter and seven and one-half feet high, comprised of 859 three and one-half inch diameter cylindrical fuel and control elements in a closely pitched equilateral triangular array. Approximately 37 of these elements are control rods, arranged in a symmetrical pattern. The fuel elements are oriented vertically and the coolant gas passes through the tricusp-shaped passages formed by the elements. The bottom and top graphite reflectors, each two feet thick, are made an integral part of the fuel elements. The side reflector which extends the full height of the fuel elements is also two feet thick and is made up of a row of dummy graphite elements and concentric graphite rings which enclose the core.

2. Reflector

The core is surrounded by a graphite reflector approximately 2 feet thick extending the full height of the fuel elements. The inner 3.5 inches of the reflector are made up of dummy graphite elements constituting removable portions of the side reflector. The remainder of the reflector is permanently located in the reactor and consists of two concentric graphite rings, each approximately 10 inches thick. Each ring is constructed of segments, there being approximately 24 segments in each ring. Both the inner and outer segmented rings are attached to a support plate; the inner ring of segments, however, is movable -- each segment being pivoted at the bottom in such a manner that it can tilt inward radially. This tilting allows the reflector to provide lateral support to the fuel elements near their upper ends. The force necessary to provide this lateral support is due to the differential coolant pressure that exists between the inner and outer faces of the tiltable segments at their upper ends. This force provides a rigid yet thermally expansible containment for the core. In order to prevent excessive coolant from bypassing the core by way of the reflector, vertical seals are provided between adjacent segments of the inner ring, and between their tops and a ring supported by the pressure vessel. These seals are presently under development; the objective is to obtain a long-life seal that need not be leak tight, but which limits the coolant bypass to a few per cent of total flow.

---

* In the following discussion of the components of the nuclear steam supply system reference is made to the research and development program pertaining to several of the components. A more detailed discussion of the research and development program is set forth beginning at page II-37.

d. An integral in-pile loop irradiation program will be carried out to test a full diameter prototype fuel assembly under reactor operating conditions. These tests will provide the following information:

1. Physical stability of the fuel assembly under actual reactor operating conditions.

2. The nature and quantity of the fission product release from the fuel element.

3. An evaluation of fission product deposition in loop components.

4. Provide a source of fresh fission products for testing the fission product trapping systems.

The in-pile loop tests are scheduled to begin about January, 1961, with the first results becoming available in the Summer of 1961. The above experiments are expected to establish the final selection of fuel element materials and provide the design information needed for the fission product trapping system in advance of July, 1962, the time fabrication of the first core is scheduled to begin. (See Section II, Part L)

9. Fission Product Venting System

Fission products are removed from each individual fuel element through the stand-off supports previously described which form the connection points for the purge stream between the fuel elements and the fission product venting system. Purge stream pressure inside the stand-offs will be between 5 and 10 psi less than the local primary coolant pressure; hence gas leakage, which is expected to be small, will always be into the venting system. The purge gas from each of the fuel element stand-offs will leave the reactor either through individual small tubes, one from each stand-off, or via a fission product venting system plenum and a single purge line. In the former case, these tubes would leave the pressure vessel in a bundle and would join at a common header outside the pressure vessel to proceed to the fission product trapping system. The design finally chosen depends primarily on the type of fuel element fault location system ultimately adopted. The venting system between reactor and fission product traps will be of high integrity; double containment thereof is being studied as a possible means of accomplishing this.

With the small masses of fission products flowing through the purge line (cf. Section II under Fission Product Traps and Helium Purification System) it is highly improbable that plugging could occur. The system will be designed so that there would be no hazard to the public or to operating personnel if plugging were to occur.

10. Fuel Element Fault Detection and Location Systems

Positive indication of the occurrence of a fault in a fuel element or its standoff connection will be provided by monitoring the primary coolant for fission product activity. Normally the activity in the primary coolant will be relatively low; thus it will be possible to detect even small changes in the gross activity in the system and to determine that such a failure has occurred.

The fuel element fault detection system will not be able to determine the location of the failed fuel element. Several possible schemes are under consideration to serve as a faulty fuel element location device. As long as the activity release from a faulty fuel

L. Research and Development

This section describes the research and development program which it is presently believed will attain the objectives set forth in this section, and a current estimate of the time to accomplish such program. The direction and emphasis of the program may be changed as information becomes available from the program and from other sources.

1. Fuel Element Development

a. Background

Background information is presented here to give perspective to the status of HTGR fuel element development, and to the program outlined for completing and proving out a satisfactory fuel element design. There exists enough information at present to assure that a fuel element of the type described in Section II, p.II-4 can be satisfactorily developed for use at the conditions specified; the exact design characteristics will be forthcoming from the research and development program.

(1) Graphite

There are several important characteristics of graphite which are of interest in high temperature reactor applications: (a) impermeability, (b) irradiation effects, (c) compatibility with the coolant, (d) thermal conductivity, (e) outgassing, and (f) thermal shock resistance.

(a) Low Permeability Graphite

The graphite used as cladding on the HTGR fuel elements is required to be of low permeability in order to control the release of fission products into the primary coolant. For the counter-flow vented fuel element a permeation coefficient (related to helium at room temperature) of about 10^{-5} cm^2/sec is required (see page II - 43).

Methods of producing low permeability graphite have been under investigation for several years at General Atomic and other laboratories and extensive techniques for measurement of permeability have been developed. Graphite with the required permeability is presently available in tubes of the full fuel element diameter and lengths up to four feet. In fact, small size samples with permeabilities in the range of 10^{-7} to 10^{-10} cm^2/sec have been available for more than one year. The scale-up of existing methods to produce long graphite tubes with permeabilities as low as 10^{-6} cm^2/sec is underway both at General Atomic and at several suppliers.

(b) Irradiation Effects

The displaced atoms in graphite resulting from fast neutron bombardment can considerably alter the properties of graphite. The most significant effects that can occur in graphite under irradiation are an increase in stored energy and changes in its physical properties and physical dimensions.

The temperature of irradiation is an important variable in graphite. At temperatures of 650F- 2000F, the stored energy in graphite will not be a problem because the radiation damage will be continually annealed. Dimensional changes can result from high temperature irradiation. Work carried out by Davidson, Woodruff and Yoshikawa[1] at Hanford shows that significant contraction of graphite takes place, particularly when the graphite is irradiated at temperatures of 1470F and 2010F. Lesser contraction, however, occurs in the irradiation temperature range of 650F to 1300F. The amount of contraction in graphite resulting from irradiation at elevated temperatures also depends on the method of manufacture, and can vary from piece to piece in a single block of graphite. It is essential that the graphite be evaluated from the standpoint of these irradiation effects.

General Atomic has been engaged in research and development work on the radiation effects on graphite over a wide temperature range since 1957. Graphite samples supplied by various companies have been investigated and testing will continue as described hereinafter to prove out the material selected for the reactor.

(c) Compatibility with the Coolant

Although helium itself is a chemically inert gas, reaction can take place between the impurities in the helium and the graphite. The significant impurities, oxygen, hydrocarbons, water vapor and carbon dioxide, may be present in the helium as received from the source, or may be added to the coolant from the outgassing of graphite, or may come from in-leakage. These problems have been under study at General Atomic [2,3] and preliminary results indicate that the level of impurities which can be tolerated (p. VII-4) is a practical one.

(d) Thermal Conductivity

Since graphite serves as the fuel matrix, moderator and cladding material, the thermal conductivity is a property of fundamental interest.

As shown on Figure 29 the thermal conductivity of manufactured graphite is high at room temperature and decreases with increasing temperature. The effects of radiation on the thermal conductivity have been measured at Brookhaven National Laboratory by Meyer and Bourdeau [4]. Several types of graphite of interest to the HTGR have been investigated. The thermal conductivity at an exposure of 3.6×10^{19} nvt at a temperature of 680F and 555 F was found to be approximately 50% of the pre-irradiation value. Thermal conductivities measured at 1010F were approximately 10% lower for irradiated specimens than for un-irradiated specimens. The temperature coefficient of thermal conductivity was lower for the specimens exposed to radiation. Thus, the thermal conductivity of irradiated graphite varied only slightly from room temperature to 1010F.

(e) Outgassing of Graphite

The evolution of various gases is a typical characteristic of all graphites when heated. A considerable amount of information has been developed on the outgassing of graphite. In particular, the Oak Ridge National Laboratory has been carrying on an extensive analysis of the evolution of gases from various types over a wide range of temperatures. The principal gases evolved are hydrogen, hydrocarbons, water, carbon dioxide, carbon monoxide and nitrogen. Sufficient information exists to define the problems to be met by the helium purification system in coping with gases evolved from the graphite.

(f) Thermal Shock Resistance

Graphite has been demonstrated to have a satisfactorily high thermal shock resistance. This results from its properties of high thermal conductivity, low modulus of elasticity, low coefficient of thermal expansion, and high Poisson's ratio.

(2) Fuel Compacts

(a) Properties of Uranium-Thorium Carbides

Uranium carbide was selected as fuel material because of its high melting point, high uranium density and high thermal conductivity. Properties of the carbides of uranium and thorium are given in Table 4-A and comparable properties of the oxides have also been included.

A dispersion of uranium and thorium dicarbides in a graphite matrix is a stable chemical system at temperatures of 2700F and as such, was selected as the material for use as the solid homogeneous fuel body. Such a fuel body is stable up to the uranium dicarbide-carbon eutectic at 4400F as shown in the table. Although carbides of uranium and thorium are reactive toward water and oxygen, they are satisfactory for use in this reactor since helium is the primary coolant.

Both the monocarbides and the dicarbides of uranium and thorium are miscible in all proportions and form stable solid solutions at elevated temperatures.

(b) Predicted Irradiation Behavior

Solid fuel bodies, in which the fuel is diluted with a moderator material, are more resistant to irradiation damage than fuel bodies which are made of undiluted fuel. This is because the presence of the moderator furnishes a matrix which dilutes the fissioning species and maintains structural integrity while the fuel burns up. The result is that even a high burnup of the fuel in such a solid homogeneous fuel body corresponds to the fission of only a small fraction of the total atoms comprising the fuel body.

In the HTGR fuel compacts, uranium and thorium carbides are diluted by a graphite matrix. For the design burnup, only

Table 4-A

Properties of Uranium and Thorium Carbides and Oxides

Property	UC	UC_2	UO_2	ThC	ThC_2	ThO_2	UC_2-C Eutectic	ThC_2-C Eutecti
Density, gms/cc	13.63	11.7	10.95	10.67	9.6	10.00		
Uranium content, gms/cc	12.97	10.5	9.65	10.14	8.7	8.79		
Crystal structure	f.c.c.	b.c. tetragonal	f.c.c.	f.c.c.	monoclinic	f.c.c.		
Melting point, °F	4350 - 4550	4260 - 4550	~5070	4760	4800	5800	4430(5)	4550(6)
Thermal expansion, at-1000C, in/in C	14.6×10^{-6}	--	10×10^{-6}	--	--	9×10^{-6}		
Thermal conductivity, cal/cm°C sec	0.059 (700°C)	--	0.008 (1000 C)	--	--	0.007 (1000 C)		

0.14% of the atoms will undergo fission. For this reason, it is expected that the fuel lifetime will not be limited by irradiation damage to the fuel compact, as has been shown by the irradiation capsule experiments carried out thus far (see page II - 49 and 50).

(c) Fission Product Retention in HTGR Fuel Bodies

The HTGR fuel body, which comprises Th-U carbide particles in a graphite matrix, will not completely retain fission products, since high temperatures are involved and the more volatile fission products will tend to come out of the carbide particles and diffuse through the porous graphite matrix. The fission fragments which are generated near the boundaries of the carbide particles at depths equal to or less than the recoil range of fission products (4 to 7 microns) will come out of the particles. Such recoil particles will imbed themselves in the crystallites of the graphite matrix surrounding the particles and will, in the case of fission product elements having sufficient mobility, subsequently diffuse out of these crystallites.

The release of fission products thus depends on the diffusion coefficient of the particular fission product elements in the carbide particles and in the graphite crystallites. Accordingly, the fundamental goal of experimental work on the release rate of fission products from the fuel is to establish the diffusion coefficients, or the related quantity, the characteristic diffusion time, of the various fission product elements as a function of temperature and radiation exposure of fuel bodies. The latter parameter must be investigated during the research and development program because radiation damage caused by fission recoil particles and by gamma radiation could change the character of the fuel materials.

Previous work that is pertinent to the HTGR fuel element development has been carried out by workers at North American Aviation and at Los Alamos National Laboratory on the diffusion of various fission products from uranium-impregnated graphites. Cubicciotti[7] investigated the rate of escape of radioactive xenon from previously irradiated uranium-impregnated graphite, making measurements in the temperature range 1800-2900F. The rate of escape was found to be independent of sample size, and it was concluded that the rate-determining step was diffusion of xenon out of graphite grains or crystallites and that the resistance to diffusion provided by the pores was negligible. Young[8] found in the temperature range of 3300-4000F that barium and strontium diffused very readily from samples, while zirconium diffused very little (2%) at temperatures up to 4000F for a heating period of four hours.

Doyle[9] studied fission-product diffusion from uranium-impregnated graphite at 2700, 3100 and 3450F. Data were taken at selected time intervals up to 24 hours for each element at each temperature. Cesium and strontium were found to diffuse rapidly at 2700F. Barium, tellurium, and iodine diffused rapidly at 3450F. The rare earths diffused slowly even at 3450F except for praseodymium which diffused several times as rapidly as cerium and yttrium. Ruthenium, molybdenum and zirconium were largely retained in the graphite at 3450F.

Barium and praseodymium were found to have diffusion rates dependent on graphite specimen size, but iodine, tellurium, and perhaps strontium diffused at rates independent of specimen size. Escape into the pores of the graphite from interstitial positions in the graphite crystallites was postulated as the rate-limiting process wherever diffusion was independent of specimen size.

Cowan and Orth[10] studied the diffusion of fission products from previously irradiated uranium impregnated graphite after heating the graphite for four minutes at temperatures ranging from 2900 to 4700F. Molybdenum was used as a reference fission product to estimate the number of fissions that had occurred in the samples. It was found that molybdenum and uranium were not appreciably lost at the time and temperatures of the experiments. Their data indicate that refractory (low volatility) elements such as rubidium and rhodium showed very little loss, while on the other hand some rather volatile elements such as bromine and iodine showed a significant retention for short periods up to temperatures of 4700F.

This information indicates the diffusional behavior that may be expected of fission products in the graphite matrix and indicates that the mobile fission products are those which show reasonable volatility at the temperature of fuel element operation. However, it also indicates that the controlling process is not directly related to volatility (vapor phase diffusion throughout the pores) but probably is solid state diffusion. Since most of the fission products in the case of the HTGR fuel element will be imbedded in the U-Th carbide particles, the diffusion of fission products in the carbide crystallites should be the principal rate-determining diffusion step.

References

(1) Davidson, J.M., Woodruff, E.M. and Yoshikawa, H.H., - High Temperature Radiation Induced Graphite Contraction - HW-57900.
(2) H.E. Shoemaker and J.C. Bokros, "Reactor Materials Compatibility with Impurities in Helium," (to be published).
(3) H.E. Shoemaker, "Effect of Impurities on Materials in Helium - Graphite Systems," GA-1367, April 15, 1960.
(4) Meyer, R.A. and Bourdeau, R. - The Thermal Conductivity of Pre and Post Irradiated Graphite as a Function of Temperature - (To be published).
(5) M.G. Bowman, LASL, (unpublished).
(6) H.A. Wilhelm, P. Chiotti, Trans. Amer. Soc. Metals, 42, 1295 (1950)
(7) D.D. Cubicciotti, "The Diffusion of Xenon from Uranium Carbide - Impregnated Graphite at High Temperatures", NAA-SR-194, Oct. 1952.
(8) C.T. Young et al., "Preliminary Experiments on Fission Product Diffusion from Uranium-Impregnated Graphite in the Range 1800 C - 2200 C", NAA-SR-232, March 1953.
(9) L.B. Doyle, "High Temperature Diffusion of Individual Fission Elements from Uranium Carbide-Impregnated Graphite", NAA-SR-255, 41 p. 1953.
(10) George A. Cowan and Charles J. Orth, "Diffusion of Fission Products at High Temperatures from Refractory Matrices", Second U.N. International Conference on the Peaceful Uses of Atomic Energy, A/Conf.15/P/613, June 1958.

b. Criteria and Objectives

(1) Fuel Can and Sleeve

(a) Graphite Permeability Requirements - Diffusion of Fission Products

The specifications for the low permeability graphite in the fuel element are such that less than one part in 10^6 of the fission products enters the primary coolant stream by diffusion through the fuel can and sleeve. For diffusion through a solid material taking place by Knudsen flow, the required graphite permeability can be expressed in terms of a permeation coefficient. The specifications for the can and the sleeve are that the permeation coefficient (related to that for helium at room temperature) be about 10^{-5} cm^2/sec, as will be evident.

Detailed calculations have been carried out on the permeation of fission products through the graphite fuel can and sleeve based initially on a simplified model of the fuel element, shown in Figure 31, in which the purge gas flows in small concentric annular passages. (Figure 30 shows a detailed sectional view of the fuel element.) The resulting fission product activity computed for the main coolant stream for a number of nuclides covering the volatility range in the fission product spectrum is shown on Figure 32 (assuming complete fission product plate-out in the primary circuit) and Figure 33 (assuming no fission product plate-out).

Because of heat transfer and pressure drop considerations, the annular gaps will be supplemented by a series of grooves cut in appropriate surfaces of the cylinders. Therefore, the actual situation will be flow in a small annular gap in parallel with a number of semicircular grooves, shown in Figures 34 and 35. An approximate analysis showing the effect of the purge grooves on the fission product leakage from the fuel element has also been carried out. In this calculation the assumptions that have been made are conservative, leading to an overestimation of the fission product penetration.

The effect of the annular gap thickness and number of purge grooves on the permeation coefficient is shown in Figure 36. In this figure, the fractional leakage of I^{131} is held fixed at one part in 10^6 and the helium purge flow rate is held constant.

For the purge rates being considered, the gas velocities are relatively small and equations for laminar flow may be employed to compute pressure drops. Figure 37 is a graph of the pressure drop through an annular purge gap as a function of gas thickness. The reference purge flow rate per fuel element used was 1/4 lb/hr with average core gas temperatures. The pressure drop in the annulus varies as the first power of the volumetric flow rate.

Figure 38 is a graph of the pressure drop through a purge channel composed of a series of semicircular grooves. The purge flow rate and gas temperature were the same as those used for Figure 37. The pressure drop again varies as the first power of the volumetric flow rate.

Figures 32, 33, 36, 37 and 38 have been calculated on the basis of a primary system pressure of 300 psi. These graphs are easily modified to provide values for other system pressures and other purge flow rates.

(b) Structural Strength

Since the counterflow fuel element is vented internally, there are negligible pressure loads on the graphite components during normal reactor operation. The strength requirements of this fuel element are determined by thermal stress values and by the loads imposed during fuel handling operations. Thermal stress experiments on graphite components will be performed in a high temperature apparatus for which construction is essentially completed. Figure 39 shows the calculated tensile thermal stress in the outer sleeve as a function of thermal conductivity in the graphite.

The maximum pressure loads which can occur on the graphite fuel elements result from a major rupture in the primary system with a rapid depressurization. Under this circumstance the outflow of gas from the purge channels within the fuel elements is somewhat more restricted than that from the primary system, resulting in a significant pressure differential primarily across the outer sleeves. An estimate of the maximum pressure differential to be expected is 100 psi. Even if this estimate were doubled, the hoop stress requirement would only amount to 1300 psi. By comparison, the hoop strength of Hawker-Siddley graphite is 2300 $\pm$ 500 psi which is adequate to meet this requirement.

(2) Fuel Compacts

The design requirements for the fuel compacts are two-fold: 1) Fuel compacts are designed to be able to withstand 65% burnup of U-235 atoms at the maximum operating temperature of 3100F without appreciable change in dimensions or in such properties as thermal conductivity and strength; 2) Fuel compacts will retain essentially all of the non-volatile fission products which are generated during exposure to the above burnup. The accomplishment of these criteria is necessary for an economical operation of the HTGR. The program, as reported in later sections, presents data which indicates that the achievement of the above goals is practical.

(3) Internal Traps

In the preliminary hazards analysis a worst case consideration has been assumed concerning the fission product inventory distributed between fuel compacts, internal fission product traps and external fission product traps, such that no holdup of volatile fission products takes place in the fuel compacts or the internal traps. Nevertheless, the objective of the research and development program is to develop fuel compacts which provide a significant holdup time for the volatile fission products and to develop internal fission product traps which retain a large fraction of these volatile fission products.

The development program with respect to fission product control is discussed in detail under Fission Product Traps page II-76.

(4) End Fittings and Standoff Seal

The requirements for the end fittings are primarily structural, requiring that they maintain physical integrity during fuel handling and under the forces exerted on them when located in the core.

The design requirement for the standoff seal, in addition to positioning the bottom end of the fuel element, is that they must maintain a minimum bypass inleakage of primary coolant. Specifically, the design requirement for these seals is that the total inleakage of primary coolant past all standoff seals shall not exceed 10% of the total purge flow rate itself.

c. Program and Schedule

(1) Research Accomplished

(a) Fuel Can and Sleeve

The significance of the present HTGR design for the fuel element is that it permits the use of graphite of permeability and breaking strength which is attainable on the basis of present technology. Graphite with a permeability of approximately 10^{-5} cm^2/sec is acceptable for use in this fuel element. Such graphites have been produced on a laboratory scale at General Atomic and on a pilot plant scale by others. Four foot lengths of this type of graphite of full diameter have been received from Hawker-Siddeley in England; in the United States, National Carbon and Great Lakes are endeavoring to produce these graphites to HTGR dimensions. In addition, base stock extrusions have been received from Great Lakes for impregnation treatments at General Atomic. Development work is directed toward having graphites of the required permeability and sizes available when needed for fabrication of the first core loading beginning about July, 1962.

Many of the graphite specimens obtained have been thermal cycled and a few have been irradiated; the results indicate that the initial impermeability is retained after these tests. However, in order to insure adequate performance in HTGR, further out-of-pile and in-pile tests are in progress or are to be undertaken as described later. For example, there is a series of sealed capsule tests to evaluate several impermeable graphites for stability, thermal conductivity and strength after irradiation. Also, an integral in-pile loop test is scheduled to begin in December, 1960.

Full diameter, approximately half-length samples of impermeable graphite are presently available from two sources with permeation coefficients in the range required for HTGR. The results of tests performed at GA on these materials are briefly summarized in Table 4-B.

Table 4-B

SUMMARY OF TESTS OF GRAPHITE FOR SLEEVES AND CANS [a].

Properties	Hawker-Siddeley (4 samples)	National Carbon (1 sample)	Great Lakes (1 sample)
Length of sample (in.)	48	22	15
Density as received (g/cc.)	1.77	1.90	1.61
Permeability as received (cm^2/sec)	1×10^{-7}	2×10^{-6}	10^{-3}
Permeability after heating to 3700F (cm^2/sec)	6×10^{-6}	2×10^{-5}	----
Hoop stress (psi)	2300 ± 500	-----	----
Modulus of elasticity (psi)	3×10^6	2×10^6	----
Modulus of rupture (psi)	5×10^3	7×10^3	----
Thermal expansion coefficient (0 to 500 C)			
Parallel	1.5×10^{-6}/°C	-----	----
Perpendicular	2.5×10^{-6}/°C	-----	----
Impregnant graphitized	No	No	----
Base stock			
Available to 10 ft	No	Yes	Will be
Graphitized	Partially	Yes	Yes

[a]Full-diameter stock.

Calculated hoop tension stresses for destructive tests of segments of Hawker-Siddeley specimens are also shown in Table 4-B. These specimens were loaded by inflating a bladder inside the tubes.

Four specimens were also stressed in bending until they fractured. The calculated maximum tensile stresses in the outer fibers varied from 3900 to 5800 psi for the four specimens. The observed modulus of elasticity during loading was very near 3×10^6 psi in each case.

To assist in the evaluation and characterization of graphite and graphite matrices which might be used in the HTGR fuel element as sleeves, cans, or fuel compacts, helium permeability coefficients have been determined experimentally for various materials. To date, GA has carried out measurements at room temperature and at helium pressures up to 120 psi.

Five graphite specimens were tested before and after the irradiation in capsule GA-311-1 in the GETR. These received an estimated fast neutron dosage of 10^{21} nvt. The results are given in Table 4-C.

Table 4-C

RESULTS OF IRRADIATION OF CAPSULE GA-311-1

Sample	Helium Permeability Coefficient (cm^2/sec)	
	Pre-irradiation	Post-irradiation
CEY crucible	4×10^{-7}	4×10^{-7}
CEY (section of hollow graphite cylinder)	2×10^{-6}	6×10^{-6}
HS 145/17	3×10^{-7}	5×10^{-10}
RXLP-2-19	2×10^{-10}	3×10^{-10}
RXLP-2-6	9×10^{-9}	3×10^{-9}

No significant changes in physical appearance were observed except in the case of the Hawker-Siddeley specimen. Additional irradiation tests are planned in which helium permeability measurements will be made before and after irradiation.

Helium permeability measurements were made on six 3 in. lengths of graphite, three of which were cut from each of two full diameter Hawker-Siddeley tubes. No significant difference could be detected between specimens cut from the same tube, and the average permeability in the three lengths from each tube agreed with the results obtained for measurements on the full length tube. The average helium permeability coefficient (K_{He}) for tube No. CP3 was $(4 \pm 2) \times 10^{-8} cm^2/sec$, and for tube No. CP4 was $(7 \pm 2) \times 10^{-7}$ cm^2/sec. One of the 3 in. lengths from tube No. CP3 was retested after it had been given fifty 8 min cycles between 187 C and 1100 C. The permeability coefficient had increased to $(4 \pm 2) \times 10^{-6}$ cm^2/sec.

Attempts to correlate helium permeability results with xenon effusion measurements where irradiated uranium carbide powder was used as a source of xenon were not successful. However, good agreement was obtained using uranium carbide compacts from purge capsule 309 where these are compared with an unsealed capsule compact, as shown in Table 4-D The amount of xenon released vs time was used as the amount of xenon available for diffusion through the graphite. Results of these calculations are also given in Table 4-D. The permeation coefficients of several specimens of graphite with low permeability have been measured and the permeation has been shown to be by Knudsen flow. The results of Table 4-D give support to the extrapolation of the helium permeability results to higher temperatures and larger masses assuming the Knudsen law ($K \propto \sqrt{T/M}$) to be applicable.

Table 4-D

XENON PERMEABILITY COEFFICIENT AS DETERMINED FROM He PERMEABILITY AND Xe DIFFUSION MEASUREMENTS

Sample No.	He Permeability Coefficient at Room Temperature (cm^2/sec)	Xe Effusion at 1200C (fraction/day)	Xe Permeability Ceofficient at 120 C (cm^2/sec)	
			From Xe Effusion	Predicted from He Data
Unsealed capsule compact	--	0.013	--	--
P117	4×10^{-6}	0.006	1.1×10^{-6}	1.5×10^{-6}
P125	2.5×10^{-5}	0.019	1.3×10^{-5}	9.6×10^{-6}

(b) Fuel Compacts

a. Radiation Stability

As part of the program to evaluate the irradiation performance of fuel compacts, three irradiation capsules containing a total of 18 fuel compacts have been examined thus far in the General Atomic Hot Cell.

One capsule contained 6 solid cylindrical fuel bodies of approximately 1 in. diameter and 1.1 in. length completely converted to uranium-thorium dicarbide. Three of these fuel bodies were obtained from the National Carbon Co. and three were fabricated at General Atomic by warm pressing and sintering techniques. The starting material for the fuel compacts made at General Atomic was uranium-thorium oxide which was converted to the dicarbide during the sintering operation. The approximate fuel content for National Carbon compacts was 11 wt %, while that for the GA samples was 10 wt %. Temperatures, measured during irradiation on the graphite cans that held the fuel, were between 1050F at one end of the capsule to 1550F in the region of highest flux. The maximum calculated burnup was 16.7% U^{235} or 48,000 mwd/T, which is equivalent to 210 $\frac{kw\text{-}hr}{cm^3}$.

On visual inspection it was found that the general physical appearance of all the fuel bodies was excellent. The dimensional measurements of the fuel bodies were checked against the pre-irradiation values and are given in the following table:

Table 4-E

Capsule 308-2

Manufacturer	Compact Location (top to bottom)	Irr. Temp. (of Graphite Can) °F	Fuel Body* Temp., °F	Nominal Size Diameter	Nominal Size Length	%ΔL	%ΔD
NCC	1	1065	1550	1.00 in.	1.10in.	-0.7	-1.7
NCC	2	1280	1750	1.00	1.10	-0.7	-1.7
NCC	3	1390	2100	1.00	1.10	-1.4	-1.5
GA	4	1500	2200	1.00	1.10	0	-0.2
GA	5	1525	2200	1.00	1.10	-0.1	-0.1
GA	6	1430	1900	1.00	1.10	0	0

* Calculated centerline temperatures

It will be noted that the National Carbon compacts, whose fuel particle sizes were approximately 4 microns, reveal the greatest dimensional changes, i.e., contraction in a longitudinal and diametral direction. It is believed that this contraction is due to fission recoil damage of the graphite.

The fuel compacts in the second capsule were annular in shape, rather than cylindrical as in the previous test. These fuel bodies were made at General Atomic by the warm press and sinter technique. The estimated exposure for these bodies was 18% U^{235} burnup or 600 kw-hr./cm^3. The pertinent data are given in Table 4-F; the physical appearance of all compacts after irradiation was good.

Table 4-F

Capsule 308-3

Sample	Compact Dimensional Changes Dia %	L%	Fuel Particle Size, μ	Graphite Can Temp. °F	Fuel Body* Temp. °F	Δ Dia., Can, %
1	0	+0.2	250-500	1200-1400	2000	NM
2	-0.2	+0.2	110-250	1350-1550	2400	NM
3	-1.7	+2.2	50	1550-1650	2550	NM
4	-2.2	+3.0	50	1650-1700	2700	NM
5	-0.3	-.1	110-250	1400-1550	2200	NM
6	0	+.1	250-500	1300-1450	2100	NM

*Calculated centerline temperature

It will be observed that the largest variations in dimensions occurred in the fuel compacts which contained fuel particle sizes of less than 50 microns. The graphite cores in these annular fuel compacts, which were made from graphite of high nuclear purity and low permeability, suffered no physical degradation.

The fuel bodies irradiated in the third capsule were identical in composition and dimensions to those of the second capsule; however, these compacts prepared at General Atomic were made from silicide fuels. The conversion of the silicide to dicarbide was accomplished by sintering. The estimated exposure of these fuel bodies is 3×10^{20} nvt resulting in a burnup of approximately 18% U^{235} (600 $\frac{kw\text{-}hr}{cm^3}$ or 51,000 $\frac{mwd}{T}$). Table 4-G summarizes the results of this irradiation.

Table 4-G

Capsule 308-4

Sample	Compact Dimensional Changes Dia. %	L %	Fuel Particle Size, μ	Graphite Can Temp. °F	Fuel Body Temp. °F	Δ Dia. Can %	Remarks
1	-0.9	+3	< 50	1200-1400	2000(1)	0	Appearance good
2	0	+0.3	250-500	1300-1450	2350	0	Appearance good
3	-0.8	+0.8	< 50	1450-1600	2500	0	Surface spalling
4	-0.1	< +0.1	110-250	1600-1700	2700(2)	0	Appearance good
5	0	+0.1	250-500	1450-1550	2250	0	Slight longitudinal crack
6	0	+0.1	110-250	1350-1500	2150	0	Appearance good

(1) Center line temperature as measured by thermocouple.
(2) Determined by melt wire analysis.

The calculated centerline temperatures of these fuel bodies range up to at least 2700F. These fuel bodies contained 22 wt% of combined uranium-thorium in a ratio of 1 U: 2.5 Th atoms. The particle sizes range from 50 to 500 microns.

The physical appearance of these compacts after irradiation was generally good; however, surface spalling was noted on one fuel body. The exact cause of this spalling is not known at this time; the general appearance of all the fuel compacts prior to irradiation was good.

The dimensional changes indicate the importance of particle size, because the dimensional stability of the compacts is affected by fuel particle size. In this capsule, one fuel compact with small size fuel particles was placed in the cold region and another in a hot region. The contraction effects were nevertheless similar to that observed for other capsules.

The data obtained from these three irradiation capsules indicate that the compacts are acceptable in terms of the dimensional and physical integrity criteria previously discussed. The burnups experienced to date are in the range of 60 to 75% of that expected for the HTGR fuel. The starting material, whether oxide or silicide, did not affect the irradiation stability.

Irradiation testing of fuel compacts will be continued until fuel compacts are developed capable of withstanding exposures of 65% burnup of U-235 (which is that expected for HTGR fuel over a core life) without deleterious effects to the compacts, in accord with the schedule shown in this section.

b. Fission Product Retention

Information to date on the fission product release from HTGR prototype fuel compacts has principally been obtained from annealing experiments carried out on irradiated prototype fuel bodies. In general the prototype samples had a diameter of 1 in. and a length of 1 in. to 2 in. and comprised dispersions of uranium-thorium carbides in a graphite matrix. In general, the particle sizes ranged from 100 to 250 μ. For comparison purposes, a few annealing runs were also carried out on uranium-impregnated graphite and extruded UO_2-graphite admixture fuel elements prepared at Los Alamos. To date quantitative data have been obtained only on Xe^{133} release. However, some qualitative observations have been made on cerium, barium, tellurium and iodine release.

Data obtained in some preliminary tests follows; in the table the subscripts s, m and f designate the slow, medium and fast components of a characteristic diffusion time.

Table 4-H

Summary of Xe^{133} Retention Data

Sample (Compact No.)	Temperature °C	Fraction of Component c_s	c_m	c_f	Characteristic Diffusion Time (hours) T_s	T_m	T_f
23B	1300	0.83	0.16	0	550	2.2	-
24A	1400	0.64	0.30	0.06	167	3.7	<0.1
22B	1550	0.58	0.38	0.04	161	4.9	<0.1
23A	1700	0.71	0.20	0.09	70	3.0	<0.1
22A	1700	0.39	0.40	0.21	550	5.0	≤ 0.07

More recent data on prototype compacts have given indications of much better retention. A prototype compact No. 73A at 2800F gave a curve which could be represented by a single component of 122 hours. Thus, there appeared to be a negligible fast release component in this case and the data could be quite well approximated by a single component or with a fairly long characteristic diffusion time. In the case of a diffusional behavior characterized by one or more components, the expected steady state release function corresponding to a reactor operating at steady power is given by

$$F_T(\lambda) = \sum_i c_i \frac{3}{A_i}\left(\coth A_i - \frac{1}{A_i}\right) = \frac{\text{activity outside of fuel body}}{\text{Total activity}}$$

where:

$$A_i = \pi\sqrt{T_i \lambda} \quad \text{and}$$

$$\lambda = 0.693/\tau_{1/2}; \quad \tau_{1/2} = \text{half-life of given fission product}$$

In order to make an estimate of the release of the various volatile fission products into the HTGR reactor at steady state conditions, the following parameters were assumed to apply which gave the release function corresponding to Figure 40.

	f	m	s
c_i	0.1	0.4	0.5
T_i (hr)	0.03	3.0	100

The parameters were chosen to give a conservative estimate of fission product release that might be expected under reactor conditions. Recent data obtained from the laboratory annealing experiments indicates this is indeed so; however, the effect of irradiation damage on release is as yet unknown.

Experiments are underway in the GETR using purge capsules 309-1, -2, -3 to determine fission product release under reactor operating conditions. In the purge capsule experiments Kr and Xe fission product gas activities are periodically sampled by purging the capsules containing prototype fuel compacts with and without tight graphite cans. These experiments are in an early stage of development and techniques are still being worked out to obtain reliable F values for xenon and krypton as a function of λ under in-pile conditions.

(c) End Fittings

The primary strength data on graphite components comes from the materials development effort where basic stress values were measured on graphite samples. In addition structural tests were carried out on specific components of the fuel element.

Four specimens of graphite were machined to the dimensions of the top grappler knob of a fuel element and loaded to destruction in a tensile testing machine. This test simulated a type of

load which could be applied to fuel elements during fuel handling. All four specimens had similar appearing fractures. The following are the loads at which rupture occurred:

Specimen	Graphite Type	Load at Rupture, lb
1	AGOT	1750
2	AGOT	1785
3	ATJ	1600
4	ATJ	1650

The normal tensile load due to the weight of the element is about 90 lb.

A threaded graphite joint was loaded to destruction in tension. This specimen consisted of a 3.50 in. OD, 2.75 in. ID cylindrical wall section threaded to a solid graphite end piece. Failure took place at the root of the thread relief in the wall section of the sleeve. The tensile load at failure was 2850 lb.

These tests performed to date have indicated that the forces required to break the top end fittings and typical threaded joints are greater than any loads which may be expected during fuel handling. The particular types of graphite to be used for end fittings in the actual HTGR will have strength characteristics as good as, and very likely better than, the graphites used in experimental tests described above.

Bowing of fuel elements in the reactor could have an effect on the forces required to remove a fuel element from the core. The thermal gradient in a fuel element in a worst bowing condition is calculated to cause a deflection of 0.38 in. approximately midway between the stand-off and the top spacing ring above the active fuel zone. The lateral force necessary to straighten this deflection is 115 lb. For this worst case the bowing stress may be assumed to creep out at operating temperatures and then reappear in the opposite direction at shutdown temperatures. Under these conditions, the force necessary to overcome friction during removal of the fuel element is 35 lb, assuming a coefficient of friction of 0.30.

The lateral force required to break an element restrained from tilting at the standoff is 61 lb, exerted at the pickup head. This force causes a deflection at the top of 6.1 inches. The calculation is made for a flexural strength of graphite of 3400 psi, and assuming that the stress is carried by the outer sleeve only.

(d) Graphite Joints

Test brazed joints between graphite components of the diameter of the fuel element outer sleeve have been made using zirconium, titanium, and other metals as brazing materials. Zirconium, titanium, and silicon showed good wetting and bonding characteristics, resulting in tight joints. It has been possible to obtain quite consistently permeation

coefficients of 10^{-5} cm^2/sec using zirconium and silicon and 10^{-4} cm^2/sec using titanium when the graphite starting material has a permeation coefficient of 10^{-6} cm^2/sec before machining.

Brazed end-caps on in-pile irradiation capsules (GA306 series) have been examined metallographically and no structural changes were evident as a result of irradiation.

Cemented joints made at GA have shown permeation coefficients as high as 1×10^{-6} cm^2/sec for joined cylindrical specimens.

(e) Standoff Seal

A model of a spigot type standoff joint was fabricated from carbon steel, and models of the female cylindrical sleeve which slips over the standoff have been fabricated from both carbon steel and graphite. In the fuel element design, only graphite will be used for the female coupling. However, a metal one was made so that leak measurements could be made under conditions where no helium was permeating through the cylinder walls.

Leak tests on these model joints showed the following leak rates through the cylindrical gaps:

Table 4-I

Leakage Tests of Standoff Seals

Sleeve	Temperature, °F	Differential Pressure, psi	Helium Leakage, $ft^3/hr.$
Steel	70	3	0.06
Steel	70	5	0.11
AGOT	70	3	3.81
AGOT	70	5	5.96
AGOT	700	3	0.44
AGOT	700	5	0.67
Imp. EY 9	70	3	0.44
Imp. EY 9	70	5	0.70

The design leak rate for these experimental seals is 0.10 ft^3/hr at 700F. The AGOT graphite was extremely porous; therefore, a large fraction of helium is presumed to have passed through the graphite walls, rather than through the gap. The length of the sealing surface for these specimens was 6.8 inches. The diametric clearances between the sleeve and the standoff were 0.001 in. for the steel sleeve, 0.006 in. for the AGOT sleeve and .002 in. for the impregnated EY 9 at room temperature. The EY 9 specimen fractured from axial expansion of the standoff when the joint was heated to 700F; therefore, no leak data is available for this

specimen at 700 F. A modified design is being fabricated for further leak tests.

As part of the standoff seal development, tests are being conducted on components of the standoff joint for mechanical strength. The stresses on these joint components is that induced by the difference in thermal expansion between the graphite fitting and the metal standoff.

(2) Future Program

The development of the reactor fuel elements involves the design and development of the individual components of the fuel element, the testing of these components, establishment of methods for their manufacture, and the development of methods for assembly of the components into the final element. Specifically, the individual parts of the fuel element development program are as follows:

1. The development of a source for the low permeability graphite tubes out of which the sleeves and cans of the fuel element will be made.

2. The development of a process for fabrication of the fuel compacts.

3. The development of a process for fabrication of the internal fission product traps.

4. The development of a method of inclusion of burnable poison in the reactor core.

5. The establishment of a final mechanical design of the entire element and the determination of its suitability under reactor conditions.

6. The development of fuel element assembly techniques.

This program will involve the fabrication of a large number of trial specimens of the individual components of the fuel element and their testing by a series of out-of-pile and in-pile experiments. The actual reactor fuel handling mechanism will be set up at the General Atomic Laboratory and prototype fuel elements will be handled by it as they will be in the actual loading and unloading of the reactor.

(a) Development of a Source of Supply for Graphite Tubes

a. The development of low permeability graphite has been under way by manufacturers outside of General Atomic for several years. These manufacturers will continue to submit samples of developmental graphite tubes to GA for evaluation in comparison to the requirements for the HTGR fuel elements. These samples are evaluated for permeability, thermal conductivity, strength and chemical purity. Some of these specimens will be tested after exposure to the reactor environment of temperature and radiation as part of the capsule irradiation program.

b. Simultaneously GA will continue its own program to develop a satisfactory grade of graphite tubes. This program involves the impregnation of various grades of graphite base stock obtained from outside sources of supply with various organic materials such as furfural alcohol.

c. The test specimens produced by General Atomic or by other manufacturers will be tested as to their suitability in comparison with the following specifications:

1. Permeation coefficient - maximum value 10^{-5} cm^2/sec.

2. Tensile strength - minimum value 1800 psi.

3. Thermal conductivity - minimum value approximately 15 btu/ft.-hr.-°F under operating conditions.

4. Dimensional tolerance - the tubes must have such physical dimensions that they can be assembled into complete fuel elements. The exact dimensional tolerances will be established at the time that fabrication of the tubes is begun.

It is the purpose of tests made on the original material to establish the ability of the test specimens to meet the above specifications. In addition, specimens will be evaluated as to their ability to meet these same specifications after exposure to thermal cycling in the absence of irradiation.

Further, selected specimens which have passed the out-of-pile tests will be exposed to the reactor environment at core operating temperature and irradiated in the capsule program (GA-311 Series). Such specimens will be tested after the radiation exposure as to their ability to meet the specifications stated above.

A small number of graphite tubes will be fabricated into full diameter fuel elements for use in the in-pile loop program. Operation in the in-pile loop will provide the final test of suitability for use in fabrication of the actual reactor elements.

d. A decision as to the source of supply for the graphite tubes which will be used in fabrication of the reactor fuel elements is scheduled to be made by July 1, 1961.

(b) Development of a Method of Fabrication for the Fuel Compacts

a. Trial fuel compacts will be produced at General Atomic by various procedures. These trial fabrication experiments will concentrate on a procedure involving warm pressing and sintering of the starting material. Compacts will be fabricated from uranium and thorium in the chemical form of oxides and alternatively as carbides. Some of the experiments will start with carbide particles coated with pyrolytic carbon.

b. The trial compacts produced in this program will be tested in regard to their ability to meet the following specifications:

1. Dimensional tolerances adequate to permit assembly and to provide for adequate heat transfer and purge flow.

2. Uranium and thorium conversion to carbides.

3. Uniformity of fuel distribution.

4. Determination of other physical or chemical properties, as shown to be necessary by other parts of the development program.

Although not a specification, it is an important design objective to obtain a hold up of a major fraction of the volatile fission products within the fuel compacts for a time of at least one hour at core operating temperature. This point is discussed more fully in the fission product trap section of this report. The delay of about one hour in the release of volatile fission products from the fuel compacts is desirable to reduce the heat load on the external trapping system.

c. Irradiation Testing Program

1. Sealed capsule program

Specimen fuel compacts will be exposed to the reactor environment in a series of sealed capsule irradiations. The compacts after irradiation exposure will be examined for their ability to continue to meet the specifications outlined above.

2. Purge capsule program

Specimen fuel compacts will be exposed in a series of purge capsule irradiations. In these capsules there will be provision for sampling the fission gases released during neutron irradiation. These experiments will provide information on the fission product release and on the change, if any, during burn-up. The fuel compacts will be examined after removal from the test reactor.

3. In-pile loop program

A small number of specimen fuel compacts will be fabricated into full diameter fuel elements and irradiated as part of the in-pile program. This program is treated in detail on page II-83. Fission product release measurements will be made during irradiation, and post-irradiation examination of the fuel compacts will also be carried out.

A decision on the fabrication process for the reactor fuel compacts is scheduled to be made by April 1, 1962. Fabrication of the fuel compacts is scheduled for completion April 1, 1963.

(c) Development of the Design and Method of Fabrication of the Internal Fission Product Traps.

This subject is treated in detail on page II-78, dealing specifically with the fission product traps. A decision as to the design and method of fabrication of these traps is scheduled to be made by November 1, 1961.

(d) Development of a Method of Inclusion of Burnable Poison in the Reactor Core

Boron as a burnable poison will be loaded in the reactor core to compensate for part of the reactivity change resulting from fuel burn-up. This boron will be included either in the fuel compacts or will be incorporated in separate elements which have the same external dimensions as the fuel elements, but which do not contain fuel. The program for specifying the form of the burnable poison will include the following parts:

a. Nuclear engineering calculations to specify the quantity of burnable poison to be included in the core. Such calculations will give the weight of boron to be included and the physical form, i.e., whether or not the boron is to be self-shielded.

b. Measurements in the GA critical facility to verify the results of the above calculations on the amount of boron required.

c. As part of the materials program, specimen fuel compacts containing the desired amount of boron will be fabricated. These compacts will be tested regarding their stability under the reactor conditions of temperature and thermal cycling by experiments such as the following: The reactivity worth of the compacts will be measured in the General Atomic critical assembly; the compacts will then be heated to temperatures representative of exposure in the reactor core for extended periods of time and then remeasured in the critical assembly to ascertain that no change in reactivity beyond specifications has occurred.

d. A decision is scheduled to be made by March 1, 1962, as to the amount and form of the burnable poison to be used.

(e) Development of Mechanical Design of the Fuel Element

The following tests will assist in the final design of the fuel element:

a. A one-half scale mechanical model of the reactor vessel and core is under construction. Operations with this model are scheduled to begin in December, 1960. The primary purpose of the model is to measure the flow distribution within the reactor vessel. However, in addition, operations with the model will provide data on the structural forces applied to the fuel elements during reactor operation. As a part of the tests, the lateral compressive force exerted against the fuel elements by the tilting side reflector will be measured. The operations of insertion and removal of fuel elements into and from the core will be

carried out with the model and necessary changes in detailed design of the end fittings will be made.

b. The reactor fuel handling equipment will be set up at the General Atomic Laboratory in advance of its erection at the Peach Bottom site. A test rig for operating the fuel handling equipment is under construction at the present time. (This test rig will accommodate the control rod drive tests as well. A sketch of the rig is shown in Figure 58). During this test the fuel handling equipment will load and unload prototype full size fuel elements into and out of a mock-up of a portion of the reactor core. These tests will provide information on the suitability of the fuel element design (particularly the end fittings) for the loading operation. The fuel element design will be modified as necessary in the light of these tests.

c. Investigation of fuel element vibration characteristics. An apparatus is being designed for measuring vibration characteristics of a bundle of fuel elements. In this experiment the fuel elements would be restrained in the same manner as in the reactor. The amplitude and frequency of vibration will be measured for flow conditions simulating the ρv^2 (mass flow times velocity squared) and approximate viscosity values for the HTGR. Data from this experiment are scheduled to be available in January, 1961. The data will indicate any tendencies of the graphite components to abrade or to suffer fatigue under the present fuel element design.

d. Investigation of design of fuel element standoff seal. Experimental tests of alternative designs of the seal between the fuel element and the metal standoff on the grid plate are in progress to select the best design. Such tests will continue during 1961. The standoff seal design is scheduled to be completed by March 1, 1962.

e. In-pile loop program. A full diameter fuel element will be tested in the in-pile loop. The details of this test are given on page II-84. The suitability of the overall fuel element design will be demonstrated by this test.

f. A decision as to the final fuel element design is scheduled to be made by March 1, 1962.

(f) Development of Fuel Element Assembly Techniques

a. The operations of assembling the components of the fuel element, i.e. fuel compacts, internal trap, graphite tubes and end fittings, into a complete fuel element will be investigated by a test assembly program. This program is already under way and will continue during 1961. It will include the continued investigation of the brazing of graphite components by the use of zirconium and other brazing materials.

Brazed and cemented joints can presently be made to the permeabilities required for the HTGR fuel elements. Therefore, the development program on graphite joints is aimed at determining the effects of

the reactor environment on the integrity of the joints. To obtain this information, brazed specimens are being irradiated in the GA-309 series of capsule tests. Also, brazed or cemented joints will be included in the in-pile loop experimental element test.

b. A decision as to the final assembly operations for the fuel elements is scheduled to be made by March 1, 1962.

(3) Schedule

The charts on the following pages outlines the target schedule for the fuel element development program.

HTGR PROJECT
TARGET SCHEDULE
FUEL ELEMENT DEVELOPMENT

LEGEND

- ● INFORMATION TRANSMITTED
- ■ COMPLETION OR DECISION
- ▲ DELIVERY
- ⊗ PLACE ORDER FOR COMPONENT

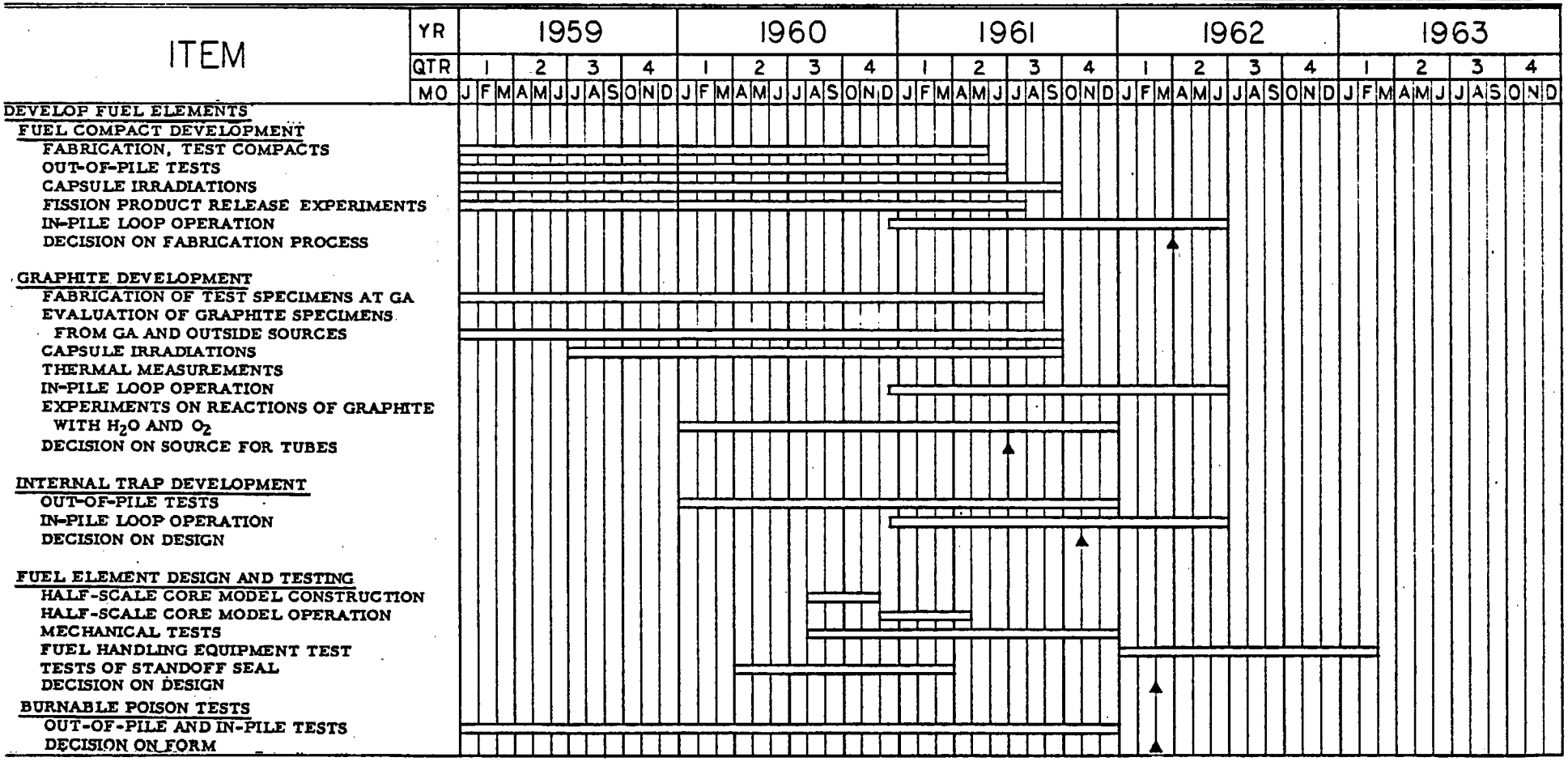

September, 1960

HTGR PROJECT
TARGET SCHEDULE
FUEL ELEMENT DEVELOPMENT

LEGEND

- ● INFORMATION TRANSMITTED
- ■ COMPLETION OR DECISION
- ▲ DELIVERY
- ⊗ PLACE ORDER FOR COMPONENT

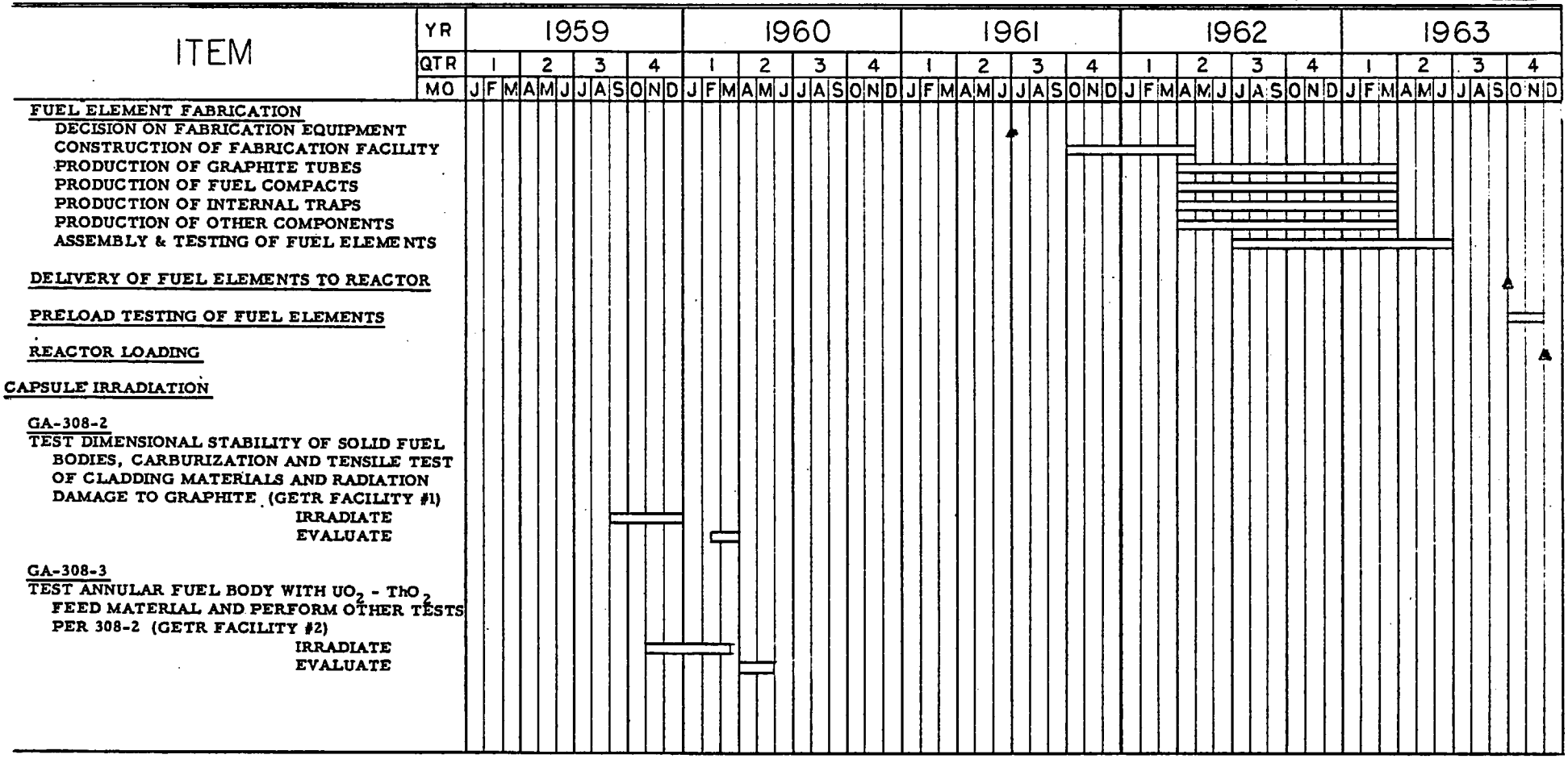

September, 1960

HTGR PROJECT
TARGET SCHEDULE
FUEL ELEMENT DEVELOPMENT

LEGEND

- ● INFORMATION TRANSMITTED
- ▣ COMPLETION OR DECISION
- ▲ DELIVERY
- ⊗ PLACE ORDER FOR COMPONENT

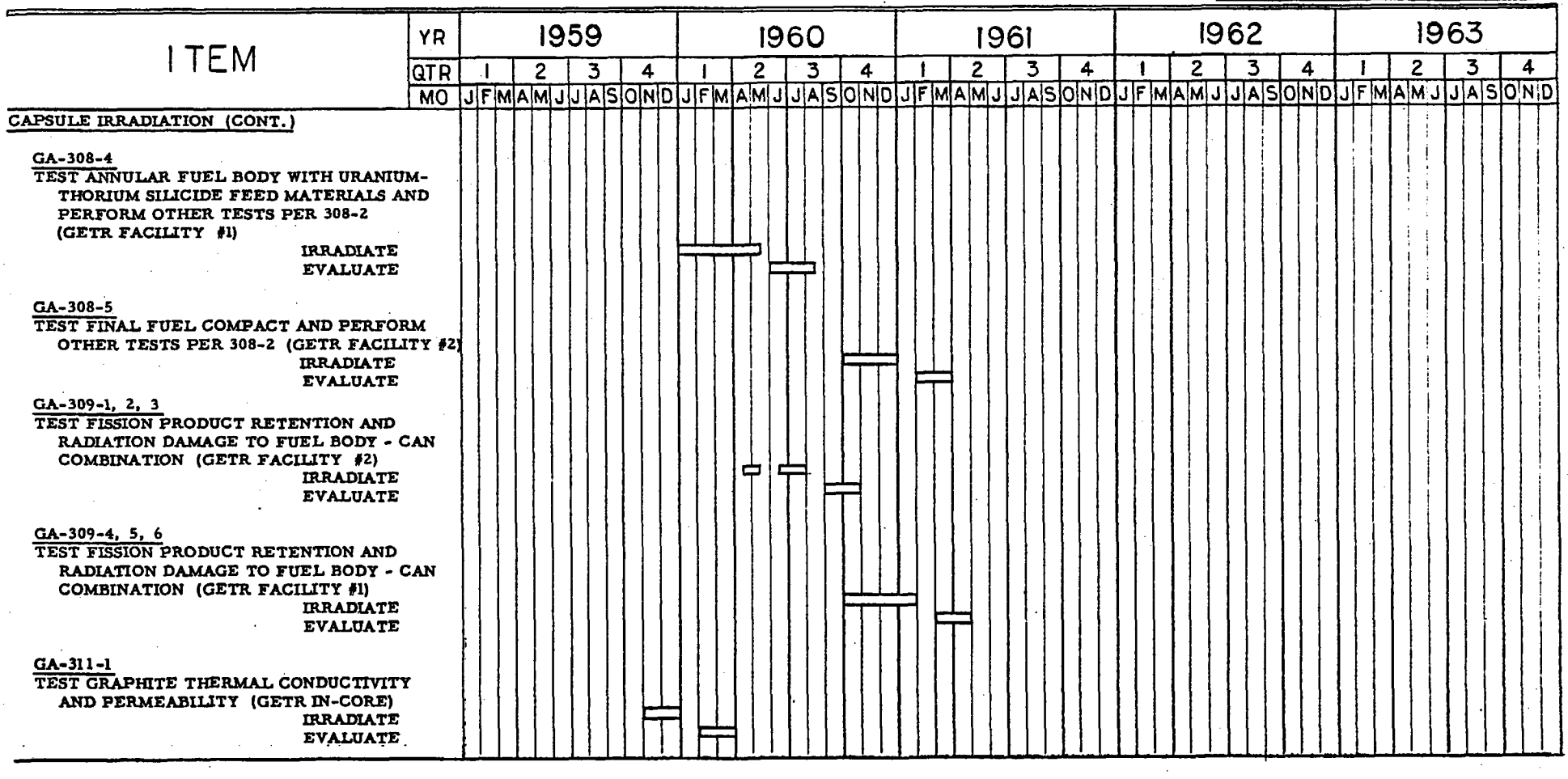

HTGR PROJECT
TARGET SCHEDULE
FUEL ELEMENT DEVELOPMENT

LEGEND

- ● INFORMATION TRANSMITTED
- ■ COMPLETION OR DECISION
- ▲ DELIVERY
- ⊗ PLACE ORDER FOR COMPONENT

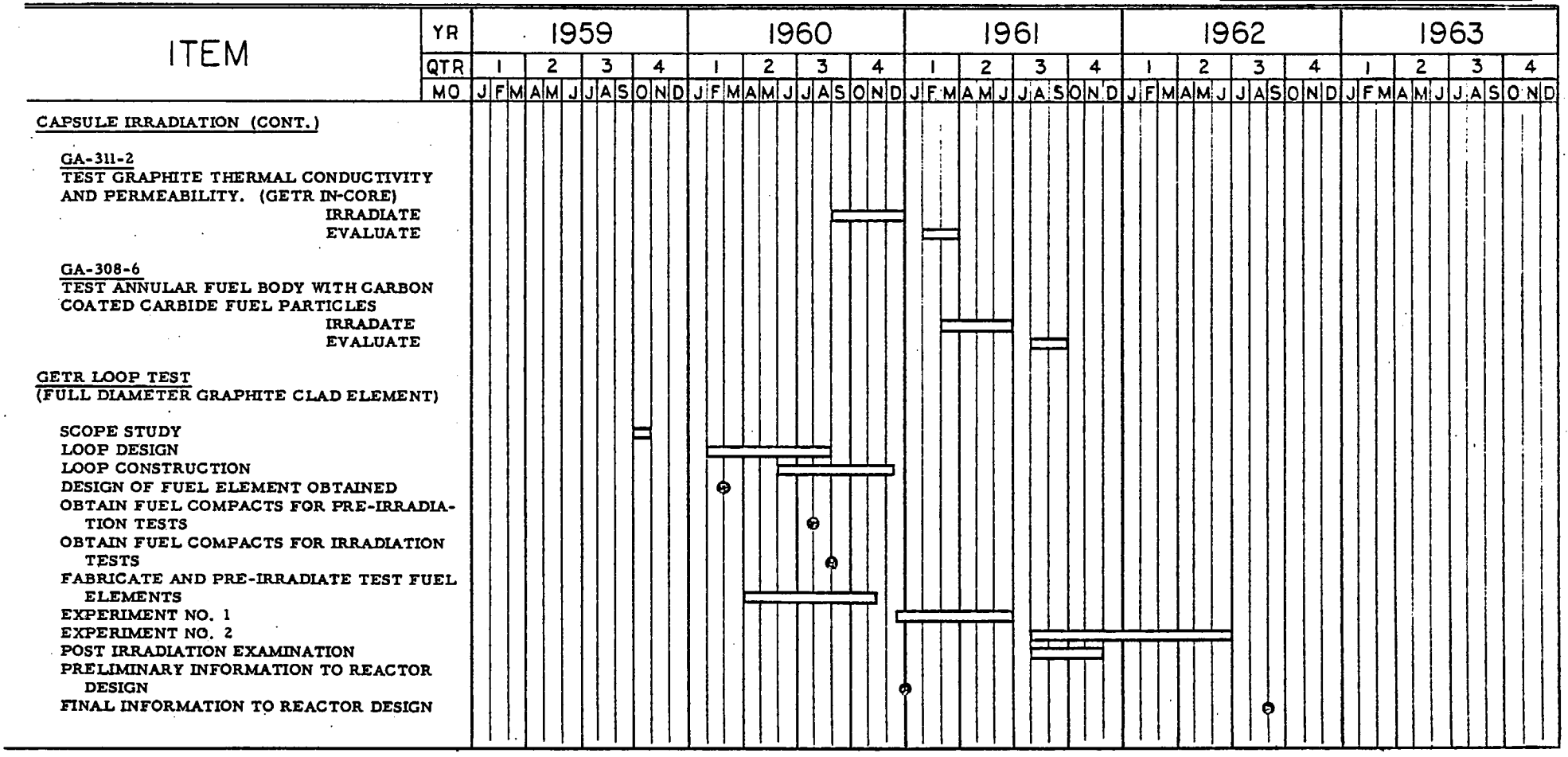

September, 1960

HTGR PROJECT
TARGET SCHEDULE
FUEL ELEMENT DEVELOPMENT

LEGEND

- ● INFORMATION TRANSMITTED
- ■ COMPLETION OR DECISION
- ▲ DELIVERY
- ⊗ PLACE ORDER FOR COMPONENT

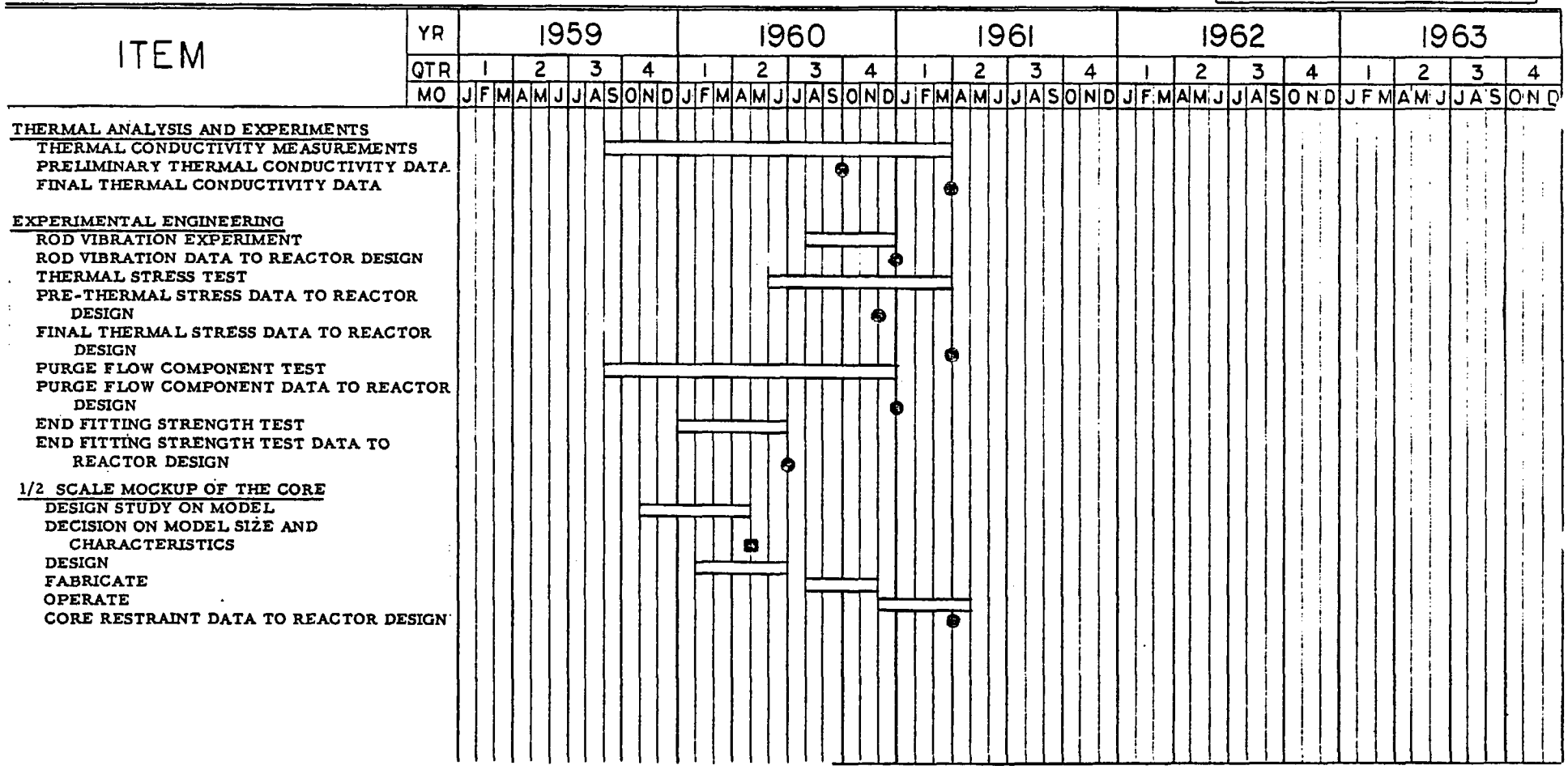

September, 1960

HTGR PROJECT
TARGET SCHEDULE
FUEL ELEMENT DEVELOPMENT

LEGEND

- ● INFORMATION TRANSMITTED
- ■ COMPLETION OR DECISION
- ▲ DELIVERY
- ⊗ PLACE ORDER FOR COMPONENT

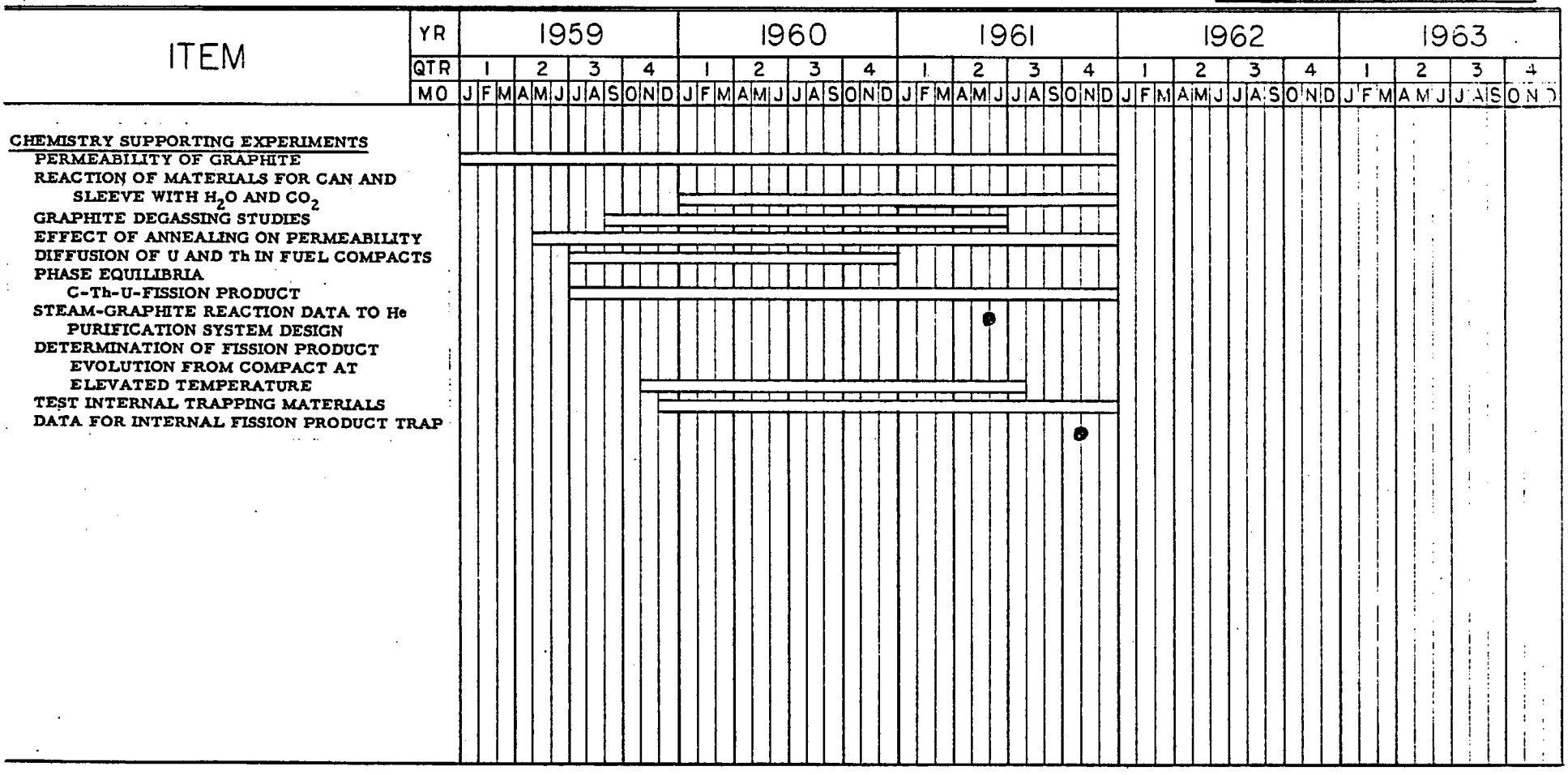

September, 1960

2. Fission Product Traps

a. Introduction

The design objective for the fission product trapping system is to obtain a significant delay of volatile fission products within the fuel compacts and a retention within the internal fission product traps of a major fraction of the fission products passing through. The fission product load on the external trapping system will then be significantly reduced. The following section presents the existing background technology applicable to the trapping of volatile fission products; in particular iodine, krypton and xenon, and the research and development program directed at finding ways to optimize the retention of fission products within the fuel compact and the internal fission product traps.

The information presented here and under the Fuel Element Development Program substantiates that the present design for the fission product trapping system is capable of handling the largest fission product trap load that can be anticipated. The actual amount of products to be handled by the traps will be defined by the research and development program and will be significantly less.

Further, the development of the detailed design of the system outlined herein is primarily one of economical operation of the reactor and not one on which the degree of hazards is dependent. In other words, there is ample information available for the basic design of the fission product trapping system, and the research and development program is designed to develop information to permit the most economical external system as to fission product load, size, lifetime, and maintenance and operational procedure.

b. Background Technology

(1) Fission Product Release from Fuel Compacts

As discussed on pages II - 42-43, the retention or delay of the fission products is determined by solid state diffusion. More specifically, the fraction of a particular fission product nuclide which escapes is a decreasing function of $\sqrt{\lambda\tau}$ where λ is the radioactive decay constant of the nucleus and τ is the characteristic diffusion time of the given nuclide (element) which is determined by the diffusion constant and dimensions of the material from which the nuclide escapes. In general, there can be several components and associated characteristic diffusion times which are required to specify the diffusional behavior. The fraction of a component escaping will be approximately 1 if $\tau << 1/\lambda$ and approximately 0 if $\tau \gg 1/\lambda$. The characteristic diffusion time τ will be measured for the important volatile fission product elements as part of the research and development program.

The volatility characteristics of the thirty-five predominant fission product elements have been studied at General Atomic.(1) Seventeen of the thirty-five elements from germanium to dysprosium may be considered non-volatile at HTGR operating temperatures. These elements

Table 4-J

Fission Product Element Yields and Characteristics

Volatility Category of Element*	Element	Fission Yield of Element $\leq$ Y (%)	b.p. (°K) of Element	Temp. (°K) at which Carbide Vapor Pressure $< 10^{-7}$ atm.
2	Ge	0.00232	3,100.	
1	As	0.0008	866.	
1	Se	0.485	958.	
1	Br	0.14	331.4	
1	Kr	5.86	119.75	
1	Rb	3.5	974.	
2	Sr	9.4	1,640.	
3	Y	4.8	(3,500.)	2000
3	Zr	31.0	4,650.	2500
3	Nb	0	5,200.	2500
3	Mo	24.5	5,100.	2500
3	Tc	6.1	4,900.	
3	Ru	11.29	(4,000.)	
3	Rh	3.0	(4,000.)	
3	Pd	1.173	3,400.	
2	Ag	0.03	2,450.	
1	Cd	0.097	1,038.	
2	In	0.011	2,320.	
3	Sn	0.095	2,960.	
2	Sb	0.058	1,910.	
1	Te	2.42	1,260.	
1	I	1.03	456.	
1	Xe	22.3	165.04	
1	Cs	18.0	958.	
2	Ba	5.7	1,910.	
3	La	6.2	3,640.	2000
3	Ce	12.4	3,200.	1500
3	Pr	6.0	3,290.	1500
3	Nd	21.17	3,360.	1500
3	Pm	2.4	(3,000.)	1500
2	Sm	1.92	(1,860.)	
2	Eu	0.183	(1,700.)	
3	Gd	0.015	(3,000.)	1500
3	Tb	0.0011	(2,800.)	1500
3	Dy	0.00005	2,600.	1500

*Volatility Category:
1. b.p. $<1500°K$
2. Intermediate between 1 and 3
3. v.p. of element or carbide $< 10^{-7}$ atm at 1500°K

comprise volatility category 3 in Table 4-J. In addition, it should be noted that the following elements form carbides of moderate to great stability.*

Y	La	Pm
Zr	Ce	Gd
Nb	Pr	Tb
Mo	Nd	Dy

The formation of the fission product carbides significantly lowers the vapor pressure of the element. It is expected, therefore, that these elements will remain fixed in the fuel compacts, or at worst diffuse out only at extremely slow rates. Their disposition will be determined in the in-pile loop program as described on pages II-84 ff.

The remaining fission products are either gases at reactor temperatures or have appreciable vapor pressures at the operating temperatures. These volatile fission product elements are the ones that must be retained in the trapping systems.

The fission yields of elements given in Table 4-J correspond to the sum of the yields of all mass chains ending with a stable nuclide of the element or a nuclide of the element with a half life greater than one year. This gives the distribution of the elements (the number of atoms produced is proportional to ΣY) corresponding to that obtained when the reactor has run for an extended period of time ($\gg$ one year).

In accordance with these volatility characteristics, the following fission product elements are expected to reach the internal fission product traps in significant quantities: Se, Br, Kr, Rb, Sr, Sb, Te, I, Xe, Cs, Ba, Sm and Eu. These are elements in volatility categories 1 and 2 in Table 4-J. Others in these categories which are unimportant because of low yields are: As, Cd, Ge, Ag and In.

(2) Trapping of Iodine

Activated charcoal has been known for some time to have a high affinity for iodine and bromine. In 1935, Reyerson and Cameron (2) reported studies that indicated activated sorption that is monomolecular in depth of the adsorbed layer. Sorption isotherms were obtained which followed the Langmuir equation.

More recently the effectiveness of charcoal in removing iodine from gas streams has been studied at Hanford and at Oak Ridge. Removal efficiencies have been measured and charcoal capacity and lifetime will be quantitatively evaluated in the research and development program.

* It should be noted that Sr, Ba, Sm and Eu also form carbides. They are not included in the group of carbide-formers since the vapor pressures of the elements themselves are sufficiently high to insure that these elements will volatilize from the fuel compacts.

The removal of iodine from a helium stream by charcoal at room temperature was studied by Finnigan, et al. at Hanford.[3] They observed a decontamination factor of 10^7, i.e., a fractional iodine penetration of 10^{-7}. The iodine was all adsorbed in the first few millimeters of a 4-inch long charcoal bed, and the iodine showed essentially no movement in the bed even after the bed was heated to 80 C.

Similar studies were performed by Adams and Browning at Oak Ridge,[4] using air rather than helium as the carrier gas. A removal efficiency of 99.95 per cent (5×10^{-4} fractional penetration) was observed for a 12-inch long charcoal bed with an air velocity through the bed of 180 ft/min.

In more recent studies,[5] Adams and Browning compared the effectiveness of charcoal and silver-plated copper ribbon in removing iodine from air streams. Removal efficiency of the charcoal was found to be superior to that of the ribbon. Efficiencies of 99.63, 99.89, and 99.99+ per cent were observed for charcoal mesh sizes of 2-4, 4-6, and 6-8, respectively, operating at room temperature. Air velocities from 82 to 275 ft/min showed little effect on efficiency. Use of moist air at 82 per cent relative humidity had no significant effect on efficiency. Use of charcoal containing large amounts of dust reduced the efficiency, indicating penetration of iodine adsorbed on dust particles.

A charcoal bed is currently being used to remove iodine from the off-gas of the RAIA dissolver at the Chemical Processing Plant of the National Reactor Testing Station, Arco, Idaho.[6] Off-gas from the dissolver is air containing I, Kr, and Xe. Total activity content for a single run includes about 30,000 curies of I^{131}, 35,000 curies of I^{132}, and 6,000 curies of I^{133}. The off-gas (16 to 20 cfm) is passed through a 16-inch diameter, 6-foot long bed of charcoal at room temperature to remove iodine. Pellet-type charcoal is used to minimize dusting and breakdown in the adsorber, and the bed is backed up with a 20μ sintered stainless steel filter to separate fines.

Efficiency of the adsorber bed was measured by locating small test traps on bypass lines at the inlet and outlet of the adsorber. The test traps consisted of small charcoal beds followed by glass wool filters. Comparison of total activity in the two test traps indicated inlet to outlet activity ratios which ranged from 12/1 to 33/1. However, most of the activity in the outlet test trap was in the filter section, rather than the charcoal, indicating that much of the activity passed through the adsorber in particulate form. Comparing the activities on the charcoal sections of the test traps gave inlet to outlet ratios greater than 1000/1, indicating that the adsorber bed was quite efficient for removing gaseous iodine.

The adsorber bed has been in operation for two years at Arco during which time about 20 runs have been carried out. The adsorber has not required regeneration or replacement thus far, but provision has been made in the adsorber design to permit insertion of a "vacuum-cleaner" nozzle which would suck out the old charcoal and thus permit replacement with fresh adsorber.

(3) Trapping of Krypton and Xenon

Information on the removal of radioactive krypton and xenon from gas streams by adsorption has been developed in connection with the following three projects: The Homogeneous Reactor Test (HRT) at Oak Ridge National Laboratory, the dissolver off-gas system of the Idaho Chemical Processing Plant, and the AERE Dragon Project in Great Britain. Activated charcoal has been the adsorbent of primary interest in all three cases. Two different types of adsorption processes have been studied. In the first case, an adsorber bed operating in the vicinity of room temperature is used to delay the passage of the fission gases and thus cause decay of the shorter-lived radioactive isotopes; in the second case, an adsorber bed operating near the boiling point of nitrogen (-320F) is used to provide complete retention of the fission gases.

Browning and his associates have carried out fission gas adsorption experiments over a fairly wide range of temperatures, adsorber materials, and carrier gases.(7) Two parallel adsorber beds, each containing 520 pounds of charcoal, are used on the HRT. These tests have shown(8) that these adsorbers provide a krypton holdup of more than 200 hours, with the xenon holdup being about ten times greater.

Experiments on the adsorption of krypton and xenon have also been performed at Harwell in Great Britain, in connection with the fission product trapping system for the Dragon Reactor. Dynamic experiments similar to those of Browning have been performed by Sangster,(9) using hydrogen as the carrier gas. Amphlett and Greenfield,(10) also at Harwell, obtained adsorption isotherms in a static system by direct pressure measurement (no carrier gas.) Amphlett and Greenfield included measurements on irradiated charcoal; results showed either no change with irradiation or a moderate increase in adsorption after irradiation.

Figure 41 shows data for the adsorption of krypton on charcoal taken from a number of sources, including those mentioned above. The data are correlated in terms of the dynamic adsorption coefficient. The spread in data is to be expected, due to the various carrier gases and types of charcoal used. The dashed line has been used for preliminary studies on the HTGR fission product trapping system. A similar plot of xenon adsorption data is shown in Figure 42.

A charcoal bed operating at about -300F has been used to separate krypton and xenon from the dissolver off-gas at the Chemical Processing Plant in Arco, Idaho. The off-gas stream (principally nitrogen) is passed through charcoal-filled tubes, the tubes being submerged in liquid nitrogen. Adsorption data used in the design of the off-gas facility are correlated by Holmes.(13) Holmes also presents data on the mass transfer rates in charcoal beds, expressed in terms of the "height of a transfer unit," which permit adsorber lifetime to be calculated as a function of the required adsorber efficiency. Adsorption isotherms for krypton and xenon on charcoal have been measured by Burdick.(14) Data from Holmes and from Burdick are shown in Figures 43 and 44; volume adsorbed (standard cc/gm) is plotted against partial pressure of the adsorbate gas (mm Hg) for both krypton and xenon.

(4) Filters

Methods of removing radioactive particulate matter from gas streams have been given considerable study at the Hanford Atomic Products Operation. The Hanford work has been summarized by Blasewitz and Judson; (15) they recommend the use of packed glass fiber filters. By arranging the filter in layers of successively finer fibers, relatively long service life can be obtained (filters of this type have operated for over 3 years at Hanford.) Blasewitz and Judson propose the following filter design for a superficial gas velocity of 20 ft/min:

Table 4-K
Fiberglass Filter Effectiveness

Layer	Type Fiberglass	Packing Density (lb./cu.ft.)	Bed Depth (in)	Initial Efficiency (%)	Initial Pressure Drop (in. of water)
Bottom	115K	1.5	12	39	0.10
Second	115K	3.0	10	53	0.24
Third	115K	6.0	20	93	1.34
Clean-up	AA	1.2	1	99.9	2.20
Total			43	99.9	4.0

The filter efficiency is observed to increase as the filter becomes loaded. Quoted efficiencies are for particles in the size range of 0.2 to 0.7 micron. Particles of 0.1 to 1.0 micron diameter are generally the most difficult to remove by filtration.(16)

c. Design Criteria and Objectives for Research and Development Program

The behavior and interaction of three essential features or components of the HTGR fission product trapping system determine the fate (and thus the control) of the fission products generated in the reactor core.

1. The ability of the fuel bodies to hold up volatile or mobile fission products permitting them to decay before leaving the fuel permits them to liberate radiation and heat while still within the reactor core, which is desirable to reduce the heat load on the external traps. Accordingly, the characteristic diffusion times for volatile fission products to be released from fuel bodies are important parameters from the fission product control viewpoint and their measurement is one of the objectives of the research and development program.

Information presently available on the retention of fission products in fuel compacts is discussed at length in the supplementary material on the fuel element development.

2. The ability of the internal traps at the lower end of the individual fuel elements to hold all of the volatile fission product elements except Br and I which are substantially delayed and Kr and Xe which are negligibly delayed also reduced the heat load and inventory in the external traps. The internal trap thus supplements the fuel compacts in retaining fission product decay heat and radiation in the reactor core.

3. The external traps (incorporated as part of the helium purification system) must be designed to remove and retain the residual fission products (mostly Kr and Xe nuclides) in the combined purge gas stream which exits from the fuel elements.

The research and development effort on the fission product traps is directed toward establishing the process design by obtaining necessary information on trapping materials, amounts of trapping material required, number of traps, trap lifetimes, operating temperatures, etc. This data and the resulting process design will serve as the basis for a firm design of the fission product trapping system. Mechanical design of the traps is currently under study. Design requirements for the fission product traps are outlined below, and the major areas in which future development work will proceed are identified.

1. Overall System Criteria

The helium purification system must be sufficiently effective for all fission product elements so that penetration of these fission products through the purification system is comparable to the 10^{-6} fraction which penetrates the fuel element sleeves.

2. Internal Fission Product Traps

The major function of the internal fuel element traps is to remove fission product elements other than krypton and xenon, and thus reduce the activity levels and decay heat generation in the external trapping system. Efficiencies of the order of 99 per cent are adequate for this purpose. By removing the least volatile fission products, the internal traps can also reduce the possibility of fission product condensation in the lines leading to the external traps. Preliminary studies indicate that the internal traps will operate at a temperature level where they will satisfactorily remove elements other than krypton and xenon. Experiments described in this section will establish the actual effectiveness of these traps.

Specifically, results obtained from the experimental program show that approximately 300 cm^3 of trapping reagent comprising about 150 grams of activated charcoal impregnated with 10 to 20 w/o copper or silver metal (in finely divided form) will serve to convert the electronegative fission product elements to relatively stable forms. Thus, with a copper reagent Se, Br, Te and I are respectively converted to CuSe, CuBr, CuTe and CuI. Of these compounds only the copper bromides and iodides are somewhat volatile at these trap temperatures (order of 900F).

Accordingly, selenium and tellurium fission products will be held firmly in the trap, while iodine and bromine will pass through the trap slowly due to the adsorption action of the activated charcoal. A delay time of greater than 5 days is expected for the iodine and bromine; therefore, all the shorter-lived nuclides of these elements will decay in the trap. The research and development program described in this section will determine the actual delay time. As reported below, volatile cesium (and rubidium) can be expected to adsorb strongly on the activated charcoal and be fixed. Substantially all of the other fission products except cadmium (which occurs in very low yield), krypton, and xenon will also condense or be adsorbed in the internal trap.

3. External Fission Product Traps

The water-cooled adsorber trap is designed to remove those fission products other than krypton and xenon which penetrate the internal traps. Allowable fractional penetration for the combined internal trap and water-cooled trap system (concentration leaving water-cooled trap divided by concentration entering internal trap) is tentatively set at 10^{-5} for these condensible fission products (iodine, cesium, etc.). The purpose of this specification is to prevent appreciable quantities of condensible, gamma-emitting isotopes from reaching the low-temperature portions of the system, where they could condense in piping or exchangers. Note that failure to meet this specification will not reduce the net effectiveness of the system since the low-temperature trap will continue to provide final removal of condensibles, although the heat in the low temperature traps would be increased. Information available at this time indicates that the desired efficiency can be obtained for iodine so long as the iodine is in the vapor phase (i.e., no particulates). The fission product bromine which is of secondary importance, will be adsorbed about as well as iodine. Other fission products such as cesium and rubidium are less volatile than iodine and will be adsorbed more strongly. Exact sizing of the water-cooled adsorbers and specification of trap lifetime will depend on more information from the research and development program on the effectiveness of the internal traps. Preliminary studies, which are continuing, indicate that lifetimes of several years are attainable with reasonable trap sizes.

The water-cooled trap must also provide some adsorptive delay of krypton and xenon in order to prevent penetration of short-lived noble gas isotopes which have long-lived gamma-emitting daughters. The most significant isotope in this respect is 3.9-minute Xe^{137}, which decays to 30-year Cs^{137} (Cs^{137} decays to 2.6-minute Ba^{137m}, which emits a gamma ray). A delay time of one hour or more will provide adequate attenuation of Xe^{137}. If the internal traps are reasonably effective, the primary source of decay heat in the water-cooled trap will be short-lived krypton and xenon isotopes. Cooling requirements for the trap will thus depend on release rates of krypton and xenon from the fuel compact.

Some fission products may form aerosols in the purge stream or be adsorbed on dust particles in the gas. In addition to the charcoal beds, a high-efficiency filter follows the water-cooled trap. The filter efficiency should be comparable to that of the adsorber; packed glass fiber filters are capable of meeting this efficiency requirement.

Decay heat generation by krypton and xenon isotopes which penetrate the water-cooled trap is appreciable (in the range of 200,000 to 300,000 btu/hr, based on recent estimates). Strong adsorption of krypton and xenon requires temperatures in the -250F to -300 F range, but removal of such quantities of heat at these temperatures is not economically feasible. For this reason, an intermediate temperature adsorber is interposed between the water-cooled trap and the low-temperature trap. Its purpose is to delay the passage of krypton and xenon, causing all except the longest lived isotopes to decay in transit and thus reducing decay heat generation in the low-temperature trap to an acceptable value. Delay times of about one day for krypton and ten days for xenon (which is adsorbed ten times more strongly than krypton) appear to be roughly the optimum; these values will be confirmed in the research and development program described in this section. With these delay times, only 5.6-day Xe^{133} and 10-year Kr^{85} penetrate the delay traps in any quantity, and decay heat generation in the low-temperature trap is reduced to 8,000 btu/hr. Design studies are being performed to select the optimum operating temperature for the delay trap, based on an economic balance between the larger trap sizes required at high temperature and the greater refrigeration costs at low temperature. Existing adsorption data have permitted preliminary sizing of the traps, but more precise data will be developed for the conditions expected in the HTGR traps.

Final removal of krypton and xenon is accomplished by the low-temperature charcoal trap, operating at a temperature close to -300F. The design objective for this trap is a penetration fraction for Kr^{85} of 10^{-4}, that is, an efficiency of 99.99 per cent. (Note that a penetration fraction of 10^{-3} i.e. only 99.9 per cent efficiency, has been used to predict primary system activities, as a pessimistic estimate of the efficiency actually to be obtained.) Net penetration of other isotopes will be less than that of Kr^{85} because of the delay time in the refrigerated trap. Available data on charcoal capacity indicate that about 100 lb. of charcoal will adsorb one year's production of krypton and xenon. Further experimental data on capacity and efficiency of charcoal for krypton and xenon are required. A high-efficiency filter follows the low-temperature trap to prevent possible penetration of krypton and xenon adsorbed on particulates.

As indicated previously, some preliminary consideration has been given to mechanical design of the trapping system. The major consideration in the internal design of the adsorber beds is decay heat removal. Because the effective thermal conductivity of charcoal beds is very low, it is ineffective to attempt to cool a single large region of charcoal. Two basic alternates are under consideration:

1. Contain the charcoal in small tubes, with coolant circulating outside the tubes.

2. Provide metal conductors, or fins, extending into the charcoal to improve the effective conductivity of the bed.

Important mechanical design factors also arise from considerations of trap shielding and removal of saturated traps. Three

basic approaches are being studied:

1. Locate traps in a water pond and use underwater maintenance techniques.

2. Surround the trap body with sufficient lead shielding to permit direct access and handling after shutdown.

3. Locate the traps in concrete cells and use remote maintenance and handling techniques.

The best choice of these alternatives will be able to be made as a result of the research and development program described in this section.

d. Program of Research and Development on Fission Product Trapping System

As has been emphasized in the preceding background information, the fundamental physical information on which to base the design of the fission product control system exists either in the open literature or in the results of the research and development program to date. The experimental work to be carried out in the future falls into three main categories:

1. Determination of the quantities of various volatile fission products which will be released from the fuel compacts.

2. Experimental measurements and tests which are relevant to the design of the internal traps.

3. Experimental measurements and tests relevant to the design of the external traps.

(1) Release of Volatile Fission Products from Fuel Compacts

A series of measurements of increasing complexity and precision will be carried out to identify the quantities of volatile fission products which will be liberated from the fuel compacts and which will be carried by the purge stream to the internal fission product trap. These measurements are as follows:

(a) Out-of-Pile Measurements Using Radioactive Tracers

In these measurements, specimen fuel compacts are exposed to a low level neutron irradiation in order to produce tracer quantities of volatile fission products in the compacts. The irradiated compact is then inserted quickly into a tube furnace held at the desired operating temperature while a stream of helium is passed over the compact. The fission products vaporized out of the compact are trapped in a refrigerated trap downstream from the furnace. From the radioactivity caught in the trap, a continuous record is made of the fission products released from the compact.

Such measurements have been carried out on specimen compacts during the past six months of 1960 and are expected to continue during the next year. The results of these measurements will be used to select a fabrication process for the fuel compacts which is most satisfactory from the standpoint of fission product retentivity. They will also establish the radioactive content of the helium purge stream which will be incident on the internal fission product traps.

(b) Purge Capsule Experiments

A series of irradiation experiments is in under way in which the volatile radioactive fission products released from sample fuel compacts can be repeatedly sampled during neutron irradiation of the compacts at a flux of approximately 2×10^{13}. These experiments supplement the out-of-pile experiments described above and provide additional information on the following two important points: first, the change of fission product release from fuel compacts due to burnup of the uranium in the compact; and, second, data on the release of various short lived fission products which cannot be studied in the out-of-pile experiments.

The present schedule for the purge capsules is shown on the fuel element development schedule. The data obtained from this series of capsules will extend the data obtained from the out-of-pile experiments.

(c) Fission Product Release from Heavily Irradiated Compacts

The experiments described under (a) above will be repeated using fuel compacts which have been exposed to a burn-up of uranium corresponding approximately to that which will occur during the full fuel element lifetime of the HTGR. These measurements will establish the effect of burn-up on fission product release. These measurements are scheduled to be carried out during 1961.

(d) In-Pile Loop Program

The program for the in-pile loop experiments is described elsewhere in Section II-L.3. As part of this program the fission product release from the specimen full scale fuel element will be determined for selected fission products.

(2) Experiments and Tests Relevant to Development of Internal Fission Product Traps

The information available at the present time shows that activated charcoal will function as a satisfactory trapping material for some of the volatile fission products (such as Cs, Rb, Ba, Sc. Se, Te) for incorporation in the internal trap. In addition, activated charcoal will delay the passage of iodine through the internal trap. The balance of the program consists of: 1) experiments to furnish more precise and specific adsorption data needed to establish the trap behavior, and 2) tests to establish the mechanical design of the internal traps, so that they perform satisfactory under reactor operating conditions. As planned this program consists of the following parts:

(a) Measurements of Adsorption Isotherms

1. Measurements of the adsorption of cesium and iodine on selected grades of activated charcoal (such as Fisher 6/14 and Columbia G). These measurements will select the most satisfactory commercially available charcoal.

2. Measurements will be made of the adsorption behavior of charcoal for copper iodide and silver iodide at lower partial pressures to supplement the data already obtained on these materials.

(b) Dynamic Measurements of Trap Behavior

The experiments which have already been carried out in flow systems, which simulate closely the actual operation of the internal traps, will be continued during 1961. These experiments provide increasingly precise determination of the length of time which iodine will be held up in the internal trap. In addition, the behavior of additional fission product elements such as selenium and tellurium, will be investigated at various operating temperatures.

(c) In-Pile Loop Program

A test of the internal fission product trap will be made during the operation of the in-pile loop in 1961. The full diameter fuel element to be utilized in the loop will contain a prototype of the fission product trap to be incorporated in the reactor fuel elements. Two types of measurements will be made:

1. Samples of the purge helium will be taken downstream from the internal trap for analysis for radioactive fission products. These analyses will indicate directly the efficiency of the trap for removing various elements.

2. After removal of the test element from the loop, the internal trap will be extracted from the element and a post irradiation examination made on it. This examination will establish the physical condition of the trap and will identify the quantities of various fission products which have been retained in the trap.

   This experiment will be a proof test of the actual trap design. Preliminary information from this experiment is scheduled to become available during the early part of 1961 and should continue to be produced during the year. This test is described in detail in Section II-L-3.

(d) Mechanical Tests

Various kinds of physical tests on specimen designs of the internal fission product trap units to establish the ability of these units to withstand the reactor design conditions, as well as to identify possible malfunctions. will be carried out. These tests will include the following:

1. Tests to investigate the possibility of plugging of the passageways through the internal trap by deposition of fission products or other materials. These experiments will be conducted outside of a reactor for the most part, but satisfactory operation of the prototype unit in the in-pile loop will constitute evidence of satisfactory design.

2. Continuing analyses on the problem of satisfactory thermal design of the trap unit. Measurements will be made of thermal conductivity and probable operating temperatures will be established.

(e) Development of Fabrication Procedures

Tests will be carried out to establish the fabrication process for the trap structures themselves and for the active adsorbent.

The trap design must be established by the end of 1961.

(3) Experiments and Tests Relevant to the Design of the External Fission Product Trapping System

The program to be carried out consists of the following:

(a) Determination of Feed Material to the External Trapping System

The experiments described above to establish the

of the internal fuel element fission product traps serve to establish the effluent from these traps, and consequently, the feed material to the external trapping system.

(b) Experiments to Establish the Size and Operating Parameters of the Delay Beds

The delay beds have the function of holding up the radioactive xenon and krypton fission products so that decay of the short-lived isotopes will release heat at a relatively high temperature level. As has been pointed out above, considerable information on this point exists as the result of previous work. However, because of the importance of the experimental data in specifying the size of the delay beds, experiments will use radioactive Kr^{85} as a tracer. These experiments will be essentially a repetition of previous work carried out elsewhere. The experiments will utilize various kinds of commercially available activated charcoal and various bed temperatures. It is anticipated that these experiments will be completed during the first half of 1961.

(c) Design of the Water-cooled Traps

Analytical work will be carried out to establish the size and other parameters of the water-cooled traps, taking into account the feed material on which they must operate, the probable heat loads, and the inventory of radioactive material contained in them. It is believed that the operation of the in-pile loop will provide a satisfactory test of these traps.

(d) Design of the Refrigerated Traps

Analytical work will be carried out to establish the design and operating conditions for the low temperature refrigerated traps. The objective of these studies will be to establish the optimum design temperature level taking into account the fission product inventory and heat load. Operating procedures will be established in the course of this analytical work.

(e) Mechanical Design of the Trapping System

Continuing work will be carried out during 1961 to specify the mechanical design of the components of the fission product trapping system. The process and instrumentation diagrams are scheduled to be available during the latter half of 1961 in order to allow fabrication of the equipment early in 1962.

(f) In-Pile Loop Program

A test of the external fission product trapping system will be carried out on a prototype trapping system as part of the in-pile loop experiments. Information from this program available during 1961 will be used to establish specifications of the final

system to be used on the reactor. It is anticipated that performance of the trapping system in connection with the in-pile loop will demonstrate satisfactory performance or will point out problem areas or deficiencies in design which must be rectified before operation of the reactor is possible.

HTGR PROJECT
TARGET SCHEDULE
FISSION PRODUCT TRAPS

LEGEND

- ● INFORMATION TRANSMITTED
- ■ COMPLETION OR DECISION
- ▲ DELIVERY
- ⊗ PLACE ORDER FOR COMPONENT

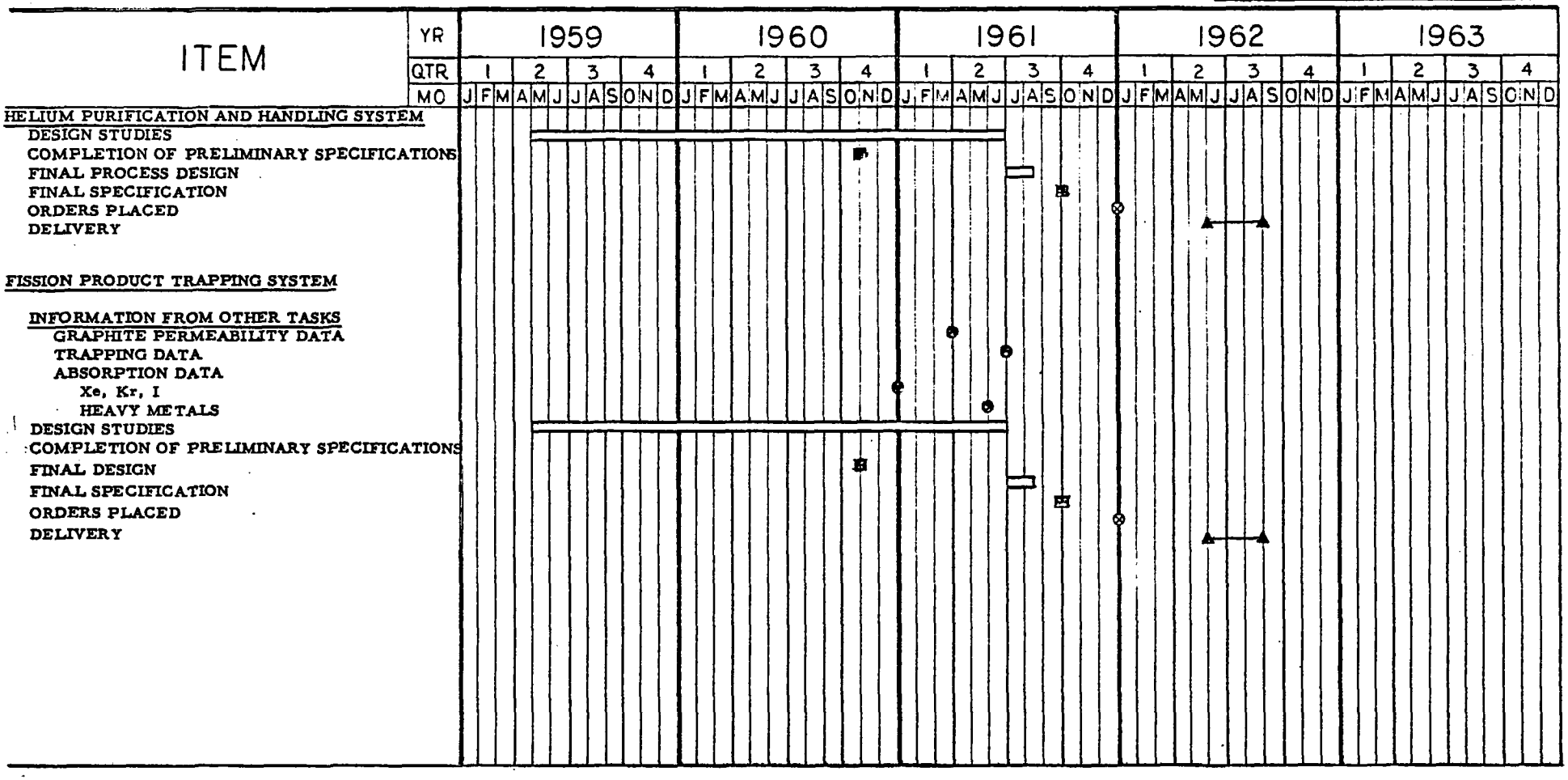

HTGR PROJECT
TARGET SCHEDULE
FISSION PRODUCT TRAPS

LEGEND

- ● INFORMATION TRANSMITTED
- ■ COMPLETION OR DECISION
- ▲ DELIVERY
- ⊗ PLACE ORDER FOR COMPONENT

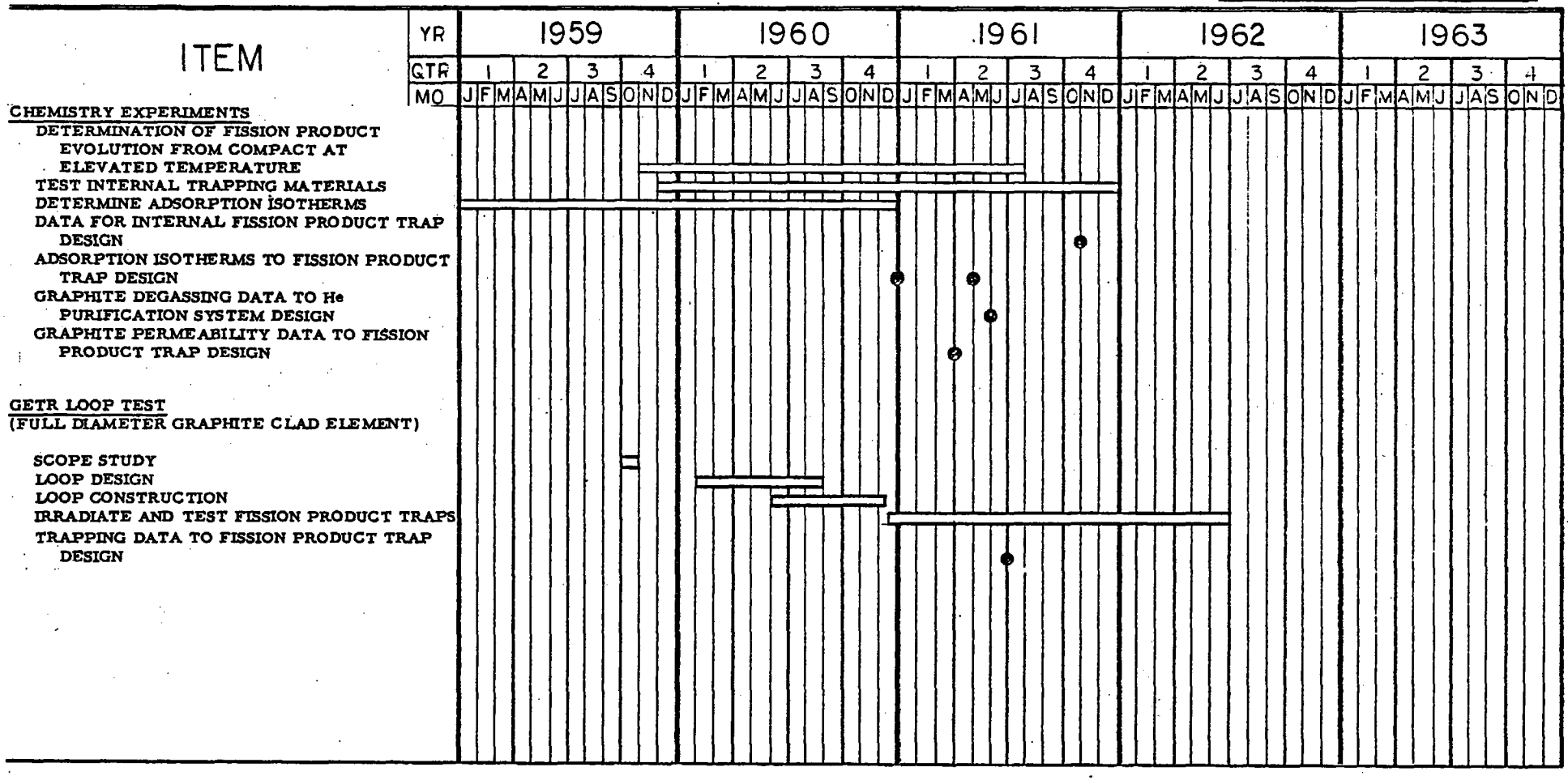

3. In-Pile Loop

a. Introduction

As part of the HTGR development program on the fuel elements and fission product traps, an in-pile loop has been designed and is under construction. This loop will be installed in the General Electric Test Reactor and is scheduled for operation during 1961. The purpose of the HTGR In-Pile Loop is twofold:

(1) To test a graphite-clad fuel element under conditions approximating those in the HTGR core.

(2) To develop operating data for a system containing a vented graphite-clad fuel element.

The facility consists of a single full diameter HTGR fuel element, a closed loop helium gas circulating system, a fission product trapping system, provision for sampling both the main loop and the fission product trapping system, and their required containment cubicles and shielding. A more detailed description of the loop is given below.

b. Operating Parameters

The loop is designed to operate over a fairly wide range of temperatures, flow and pressure. Typical operating conditions are given in Table 4-L.

TABLE 4-L

TYPICAL LOOP OPERATING PARAMETERS

Fuel element diameter, in	3.50
Fuel element length, in	43
Fuel element active length, in	22.50
Fuel element loading of U (93% enriched), g	195
Fuel element loading of Th, g	425
Power generation, kw	76
Fuel element temperature, F	3500
Graphite surface temperature, F	2200
Entrance gas temperature, F	600
Exit gas temperature, F	1400
Helium flow rate, lbs/hr	260
Purge flow rate, lbs/hr	0.24
Helium pressure, psia	350

c. Design Description

(1) In-Pile Equipment

The experiment will be located in the pool of the General Electric Test Reactor adjacent to the reactor pressure vessel, that is, at the core-reflector interface. Figure 54 is a schematic diagram of the facility tube and a section through the facility tube. In order to thermally insulate the hot facility tube from the water in the pool, the entire in-pool portion is located within an aluminum vacuum chamber. A secondary function of the vacuum chamber is that it provides secondary containment for radioactive fission products in case of leakage from the in-pool portion of the loop. A section through the test element is shown full size in Figure 55. The disconnects for the lines connecting the facility tube to the remainder of the system are Marman-type flanges utilizing double seals. The space between the two seals on each flange is evacuated. The leakage, if any, is directed to a leakage collection system.

The facility tube assembly consists essentially of a pressure vessel containing the fuel assembly and flow and thermal baffles, coolant inlet and outlet piping, tempering gas piping, purge gas piping, thermocouples, disconnect joints, and internal shielding. During normal loop operation, the facility tube is located in close proximity to the reactor vessel to take advantage of the high neutron flux. Means are provided, however, to retract the vacuum chamber in the core region up to five inches from the reactor vessel when it is desired to operate the reactor with the loop facility shut down. In the retracted position, a shutter consisting of lead, steel and cadmium shields the fuel in the facility tube to minimize heat generation. During this time helium is provided in the vacuum chamber annulus assuring the necessary conductance for removal of the small amount of heat still being generated.

The fuel element assembly consists of the following: Five HTGR fuel compacts located in a graphite fuel can within a graphite outer sleeve; graphite end plugs, heat insulators, connections and structure; an internal fission product trap; purge lines and thermocouples. Each of the fuel compacts consists of a central core of boron dispersed in graphite and an annular cylinder of U^{235} and Th^{232} dispersed in graphite. Heat is transferred to the helium

coolant at the surface of the outer cylinder and the annular space between the fuel can and outer graphite cylinder is swept by helium gas to purge the fission products entering this space. The helium purge gas enters the outer annulus at the plenum in the lower end of the element, flows upward between the two cylinders to an upper plenum and downward between the fuel compacts and the fuel can. At the lower end, the purge gas flows either through an internal fission product trap or through a trap bypass purge line. The two purge lines are connected to the external fission product trapping system in the main cubicle.

A baffle separates the downward and upward coolant flow and virtually eliminates radiative heat transfer between the graphite and the pressure vessel. Stagnant helium between the baffle walls minimizes heat transfer between the two flowing helium streams. The baffle consists of an outer wall of stainless steel and two walls of Nichrome V.

Thermocouples are provided to measure temperatures of the fuel compact internals, helium at test section inlet, fuel element inlet and fuel element outlet. Six thermocouples are attached to a thermocouple ring on the outlet pipe. Steel shielding is provided in the upper region of the facility tube to minimize radiation in a vertical direction above the fuel.

(2) Out-Of-Pile Equipment

The out-of-pile portion of the primary system is located within a concrete cubicle on the second floor of the GETR. The cubicle is lined inside with steel plate which forms a secondary containment. The cubicle is divided into two levels with the fission product trapping system equipment located on the first level and the primary loop and associated equipment located on the second level as shown in Figure 56. The second level is divided into two compartments, the larger of which is open to the lower level and contains the major loop components, such as the circulators, heat exchanger, cooler, full flow filter, hot helium storage tank, leakage collection hold up tanks, depressurizer tank, cubicle cooling system, ventilation blower, main loop piping and valves and instrumentation. The other compartment on the second level is the pump room which contains the main transfer pump, leakage transfer pump, vacuum chamber pump, purge containment blower, fission product trapping system vacuum pump and depressurizer compressor. Figure 57 is

a piping and instrumentation diagram which shows the relationship of the various components to each other. The pump room is provided to permit access to the pumps for periodic inspection and maintenance. It is shielded from the components in the other compartment and is also surrounded by shielding. Local shielding is provided around the circulators, cooler, full flow filter, hot helium storage tanks and leakage hold up tanks to minimize radiation to personnel entering the cubicle for inspection and maintenance during accessible periods. The cubicle normally operates under a slight negative pressure to minimize out-leakage.

The primary loop main cooler is a single wall gas-to-water type (approximately 7 ft x 1-1/2 ft x 6 ft). The purpose of the main cooler is to transfer heat from the hot helium gas to a closed demineralized secondary water system which in turn transfers heat to the GETR cooling tower water through a secondary heat exchanger. The cooler is designed to operate at 1400 F maximum helium inlet temperature without local boiling on the water side. The maximum capacity of the heat exchanger is 328,000 btu/hr.

A full flow filter is located on a bypass line upstream of the circulators. It will be used to remove graphite fragments from the main loop stream to protect the circulator bearings in case of fuel element erosion. The main loop flow will normally bypass the filter but can be remotely directed through the unit by valves controlled from the main loop panel.

Two circulators of equal capacity are installed to pump the helium coolant around the closed loop. One of the circulators is normally not operated but held as an in line spare in the event of a circulator failure. All rotating parts are carried on self-acting gas bearings which use the circulating fluid as a lubricant. The entire pumping system will be leak tested such that gas leakage will not be detectable with a helium mass spectrometer. Each circulator is designed to meet the following performance conditions.

Inlet temperature	650 F
Inlet pressure	340 psia
Pressure rise	10 psi
Mass flow, maximum	0.15 lbs/sec

A system is provided to collect and contain leakage from points in the system most likely to leak radioactive gas.

The main evacuation pump serves several purposes. During normal operation, this pump is used to maintain a high vacuum on the vacuum chamber to minimize heat losses to the reactor pool water. The same pump also maintains a vacuum on the space between the seals of the facility tube disconnect flanges. Leakage, if any, into the vacuum chamber is directed through a moisture detector, cold trap and vacuum pump to the low pressure hold-up tank. Leakage from the disconnect interseals is also directed to the tank through the same pump. A slight negative pressure is maintained on the purge line containment shell by the purge containment vacuum pump. The sample lines to the junior cave and sample blister are also evacuated by separate pumps to purge the lines of gas which may be radioactive. The gas from the interseals, sample lines and purge line containment discharges through a filter into the 10 cubic foot low pressure hold-up tank. If and when the pressure in this tank reaches 15 psia or over, a leakage transfer pump transfers the gas to the five cubic foot, high pressure hold-up tank. The gas is stored here until it becomes necessary to relieve excess gas through an iodine trap and filter to the main cubicle ventilation exhaust. Radiation detectors are included on the system to monitor activity in the various lines. The main loop may also be evacuated by the main evacuation pump if required during shutdown.

The emergency helium cooling system provides a means of admitting helium to the vacuum annulus of the vacuum chamber which will increase heat loss from the fuel element to the pool. The system is put into operation in case of low coolant flow and/or low coolant pressure in the loop. A cylindrical tank in the system is kept charged with sufficient helium to feed this annular space upon demand. Double valves are used to increase reliability.

A 50 kw capacity electric heater is located downstream of the circulators to control the return gas temperature. The heat output is automatically regulated by a saturable core reactor controlled by the helium temperature downstream of the heat exchanger on the main loop coolant return line to the fuel element. The control equipment for the heater will be located outside the cubicle on the control mezzanine.

The fuel element inlet gas temperature conditions required for the experiment are higher than the maximum permissible operating temperature of the gas circulator. In order to minimize the loop heat losses, a regenerative heat exchanger is used.

Located within the cubicle is a ventilation system designed to maintain a negative pressure on the main cubicle, junior cave, sample blister, pump room and auxiliary equipment containment area; and to isolate the containment system in the event of high activity release from the loop. The ventilation system includes a mechanical blower located in the main cubicle, two high efficiency air filters, an iodine trap, radiation monitors and associated piping.

The mechanical blower takes suction from the main cubicle through a high efficiency filter and discharges to the stack through an iodine trap and the second high efficiency filter. Air flow into the main cubicle is from the GETR containment through the auxiliary containment, junior cave, pump room and sample blister.

Valves, located on all inlets, will close on a signal of high radiation or high pressure in the main cubicle. The valves on the interconnecting lines between the various units being ventilated will open in case the pressure in the units becomes higher than the main cubicle pressure.

(3) Fission Product Trapping System

The external fission product trapping and helium purification system (FPTS) is provided to remove radioactive fission products and gaseous impurities from the fuel element purge stream and to return the essentially clean helium to the main coolant stream. It consists of a series of adsorbent beds and filters, operated at various temperatures, through which the purge stream is passed. This equipment is located on the lower level of the main cubicle.

The main components are:

(a) Charcoal Trap No. 1, water-cooled and contained in a lead cask about nine inches thick. This trap is designed to remove the volatile fission products other than the noble gases.

(b) Charcoal Trap No. 2, whose purpose is to provide a hold-up period for the noble gases, is freon-cooled to -40 F and shielded with six inches of lead.

(c) A Copper-oxide Bed with electric heater and lead brick shielding, to convert carbon monoxide in the coolant to CO_2 and hydrogen to H_2O.

(d) A CO_2-H_2O Trap to remove the CO_2 and H_2O formed, which is cooled by liquid nitrogen and shielded with lead bricks.

(e) Charcoal Trap No. 3, cooled by liquid nitrogen to -320 F and shielded with six inches of lead. This trap is designed to retain the noble gases held up temporarily by Charcoal Trap No. 2.

(f) Emergency Trap No. 1, which is used as a stand-by trap for Charcoal Trap No. 1 and which is water-cooled and shielded with nine inches of lead.

(g) Emergency Trap No. 2, which is liquid nitrogen-cooled and shielded by six inches of lead and which will be used as a stand-by trap for Charcoal Traps No. 2 and No. 3.

Circulation or purge gas is accomplished by taking advantage of the pressure drop across the main loop. A booster pump is used only when the pressure differential is not sufficiently great to obtain the desired flow rate.

The purge lines between the pool penetration flange and the Charcoal Trap No. 1 and Emergency Trap No. 1 are contained in a secondary containment shell to minimize the possibility of excessive leakage to the main cubicle. The purge lines are also connected to the junior cave trapping sampling systems. The water and freon cooling systems for the FPTS are located in the auxiliary containment cubicle.

(4) Junior Cave

A Junior Cave is located outside the main cubicle on the second floor adjacent to the reactor biological shielding. The cave is a shielded containment vessel constructed with the same leak tightness requirements as the main cubicle containment structure. Penetrations are provided on the cubicle face of the cave for sample connections from the purge lines and from sample points at the several locations in the fission product trapping system. To reduce the radiation field to within working limits, the structure is shielded with eight inches of steel plate placed on the top, left and front faces. The remaining faces of the case are shielded by the reactor biological shielding and the main cubicle shielding.

All of the required operations within the cave are performed by a claw-type manipulator. The control mechanism for the equipment is located on the outside front face of the cave and is easily accessible to one operator. The manipulator is designed to operate valves for control of gas flow and to handle and remove the test traps. Observation of operations within the cave is provided for by two high-density lead-glass windows.

Instrumentation within the cave will include provisions for measurement of local gamma activity in the purge line, and gross activity within the cave area.

(5) Gas Sampling

(a) Purge Gas

Within the junior cave, means are provided for sampling the purge gas stream both as it leaves the fuel assembly and after it has passed through various traps within the FPTS. Two separate functions of purge gas sampling are performed within the cave.

a. The study of the efficiency of various trapping materials is accomplished by passing purge gas through small test traps and then removing the traps from the cave for analysis.

b. Analytical study of the purge gas stream at four different locations in the FPTS is carried out by intermittently sampling the gas stream and either analyzing the samples with a gas chromatograph installed in the cave or by external radiochemical means.

(b) Primary Coolant

Main loop samples are handled in a sample blister located adjacent to the main cubicle shield wall on the operating mezzanine. The blister contains stop valves on the piping leading to and from the system sample points, a gas chromatograph analyzer, a liquid nitrogen-cooled charcoal trap, a connection point for a sampling container and miscellaneous piping and valves.

The blister is a steel enclosure normally kept under a slight negative pressure to insure in-leakage. A sealed viewing window and glove ports are provided to permit handling of equipment within the blister. A pass-through chamber is also provided which can be flushed to minimize the probability of internal air escaping to the GETR containment when samples or equipment are passed in and out of the blister.

The sampling equipment is connected to the helium loop at several sample take-off points and one sample return point. Samples can be passed through the gas chromatograph for direct reading of impurity content, or alternatively, samples can be removed from the system in a sample container. While loop gas is recirculating through the sample equipment to purge the sample system prior to taking a sample, the sample system is under loop pressure. After isolation of the system by closing the valves, the gas pressure is reduced to atmospheric by bleeding excess gas through the nitrogen-cooled cold trap where fission products, if any, are trapped. Samples are then removed with the system at atmospheric pressure. The sample container is normally evacuated before filling and therefore draws in a known volume of gas from the sample system.

The sampling system is connected to a clean helium supply and to vacuum pump (which discharges to the leakage collection system). This system is used to purge the sampling system initially.

(6) Gas Charging System

The charging system, which is located outside the main cubicle, is designed for manual operation and supplies high-purity helium for filling and purging of the main loop and subsequent main loop make-up requirements. Through suitable valving, including a back-flow check valve, high purity helium from this charging system can be supplied when required to the junior cave, sample blister, interseal disconnect chambers and Charcoal Trap No. 1 of the fission product trapping system.

The helium purifier in the charging system consists of a 10 micron filter, a molecular sieve cartridge for water vapor removal and an oil vapor cartridge. This unit is designed to limit the impurities in the helium to the following values:

Water Vapor	--	less than 10 ppm/volume
Hydrocarbons	--	less than 10 ppm/weight
Solid particle size	--	less than 6 microns

(7) Instrumentation

All instrumentation needed for the loop is centralized at a local control panel in the experiment area. Critical parameters are repeated and recorded in the reactor control room. An annunciator on the control room panel indicates loop troubles. Additional annunciators on the local panel

indicate the source of the trouble. Critical parameters have two levels of action -- alarm and either scram or rundown of the reactor.

The loop is fully instrumented to measure required fuel element and coolant temperatures, flow rates, and pressures. All measurements of interest throughout the system will be transcribed on recorders, thus providing information for post-operational analyses. Suitable instrumentation is provided for reactor shutdown should a potentially serious condition be indicated. Reactor scram will be initiated by high exit gas temperature, high circulator intake gas temperature, low flow or pressure of main loop gas. In addition, a reactor rundown will be initiated by activity monitors located on the main loop and purge lines. Intermediate levels of these parameters and other warning signals will be annunciated. The general system is laid out in such a way that all parameters concerned with the operation of the system and the contained experiments are under the direct control of the loop system operator. Should a transient occur, the operator will be able to make suitable system adjustments to return the system to equilibrium condition. Fast-acting transients involving temperature, pressure or flow excursions will cause automatic reactor scram should these parameters exceed pre-set limits.

Primary heat exchanger water flow will be metered and low flow will cause an alarm. Discharge water high temperature will also operate an annunciator.

A separate continuous monitoring system is provided to determine cubicle exhaust gas activity before release to the GETR stack.

The controls and instruments allow the reactor operator, in case of an emergency, to introduce emergency cooling which will increase the heat loss from the experiments, thereby reducing the gas and fuel assembly temperature. If the loop fails to respond, the gas coolant may be transferred to the hot helium storage tank, reducing the loop pressure and automatically causing a reactor scram.

(8) Shielding

The shielding design assumptions are that a large percentage of fission products escape from the system to the main cubicle and that large quantities of fission products are plated out in various sections of the loop. Under normal operation, the majority of the fission products will be retained within the fuel element and/or the individually

shielded fission product trapping system traps, which will reduce the dose rates calculated by several orders of magnitude.

The in-pool shielding was based on the maintenance requirements of the reactor and the requirements for direct work on the facility, under the set of assumed conditions listed below; for direct maintenance of the reactor, access to the top head is required 8 to 10 hours after reactor shutdown.

(a) 0.05 curie/cm^3 activity in the main loop coolant.
(b) 50 curie/cm^3 activity in the purge stream.
(c) 0.2% of the potential loop plate-out occurs in the region of the joints ($\sim$190 curies) which region is adjacent to the reactor vessel head.
(d) Direct beaming of radiation from the fuel element up the evacuated secondary containment.
(e) Maximum dosage contribution from all loop components to a man on the reactor vessel head is 100 mr/hr.

The shielding required was calculated to be about 5 inches of lead in certain locations. A shielded radiation detector will be located above the disconnect flanges and calibrated to indicate the dose level at shutdown. The contribution of plate-out to the radiation level indicated, will be estimated from decay curves obtained during reactor shutdown and by comparison with decay curves obtained from detectors located elsewhere in the system.

The cubicle shielding thickness requirements were based on a loop power of 100 kw for about three years operation. The resulting equilibrium fission product activity level for potential helium contaminants having half-lives greater than 10 minutes would be about 1×10^5 curies.

Under normal operation, the fission products will be retained within the main loop piping and in the individually shielded FPTS traps.

For potential accident situations, shielding calculations for the lower level of the main cubicle assumed that 100% of all the equilibrium volatile fission products with half-lives greater than 10 minutes are distributed uniformly in the cubicle. The dose rate through 1-1/2 feet of ferro-phosphorous concrete is about 300 mr/hr under this emergency condition.

(9) System Leak-Tightness

Components of the loop which will be operated under helium pressure are being mass spectrometer leak-tested to a minimum sensitivity of 5×10^{-8} atmospheric cc/sec. During the shop fabrication phase, the out-of-pile portion of the main loop will be pre-assembled and operated at temperature and pressure to verify system performance and leak-tightness. The design objective is to reduce the leakage of the system to less than 1×10^{-5} atmospheric cc/sec, as measured by a mass spectrometer.

d. Purpose and Program

As mentioned earlier, one of the purposes of the in-pile loop is to test a graphite-clad fuel element under conditions approximating those in the HTGR core. Certain specific information will be obtained while the test is going on and other information will be obtained on post-irradiation examination. Three thermocouples are located in the fuel-bearing region of the element, two in the graphite can, two in the graphite sleeve and two in the internal fission product trap. There is some question as to how long these thermocouples will survive in the presence of graphite at high temperature. It is anticipated that they will last at least long enough to obtain a set of temperature readings at full power.

An attempt will be made to determine the efficiency of the internal trap by sampling the effluent gas in the purge line. In addition, a bypass line is provided around the internal trap, which line can also be sampled. An estimate of the diffusion of fission products into the main stream should be obtained, both from gas samples and from radiation monitors on the hot gas line leaving the in-pile section. These measurements would also provide warning of a fuel element failure.

Post irradiation examination is expected to determine the following:

(a) The extent of fuel migration and diffusion.
(b) The extent of fission product migration and diffusion.
(c) Structural stability of the fuel compacts and of the graphite fuel can and sleeve.
(d) The integrity of joints.
(e) Erosion effects.
(f) Possible thermal stress effects.

Another main purpose of the loop is to test the operability of a dynamic system containing a graphite-clad fuel element. In the loop, a synergetic test is made of the fuel element, its environment and the circulating system. Consequently, it is expected to determine the following:

(a) Definition of any unforeseen problems.

b. Determination of the effect of fission products, such as activity buildup in the coolant gas, fission product plate-out, or corrosion caused by selective deposition of fission products. To this end, radiation monitors are located adjacent to each of the major loop components and near the in-pool disconnects.
c. The ability to maintain a clean helium coolant, both from the standpoint of fission product contamination and non-radioactive impurity contamination, will be determined. Sample points are provided after each of the charcoal traps in the fission product trapping system and also following the copper-oxide bed.
d. When equipment is removed for maintenance, it should be possible to get some idea of mass transfer of carbon, as well as of fission product plate-out within components. In addition, it will be possible to test decontamination procedures on such components.
e. The use of various materials in the primary system such as carbon steel and low alloy valves in the cooler portions of the system should help in determining whether these materials will present any unforeseen problems in the HTGR.
f. Since the system is completely sealed, it should be possible to get some idea of leakage by checking pressure loss in the system (gross loss). Air contamination is another qualitative measure of leakage. If leakage is found, it will be necessary to locate the source. This will be done by means of mass spectrometer testing.

e. Target Schedule

The schedule for the in-pile loop is shown on the following chart.

HTGR PROJECT
TARGET SCHEDULE
IN-PILE LOOP

LEGEND

- ● INFORMATION TRANSMITTED
- ■ COMPLETION OR DECISION
- ▲ DELIVERY
- ⊗ PLACE ORDER FOR COMPONENT

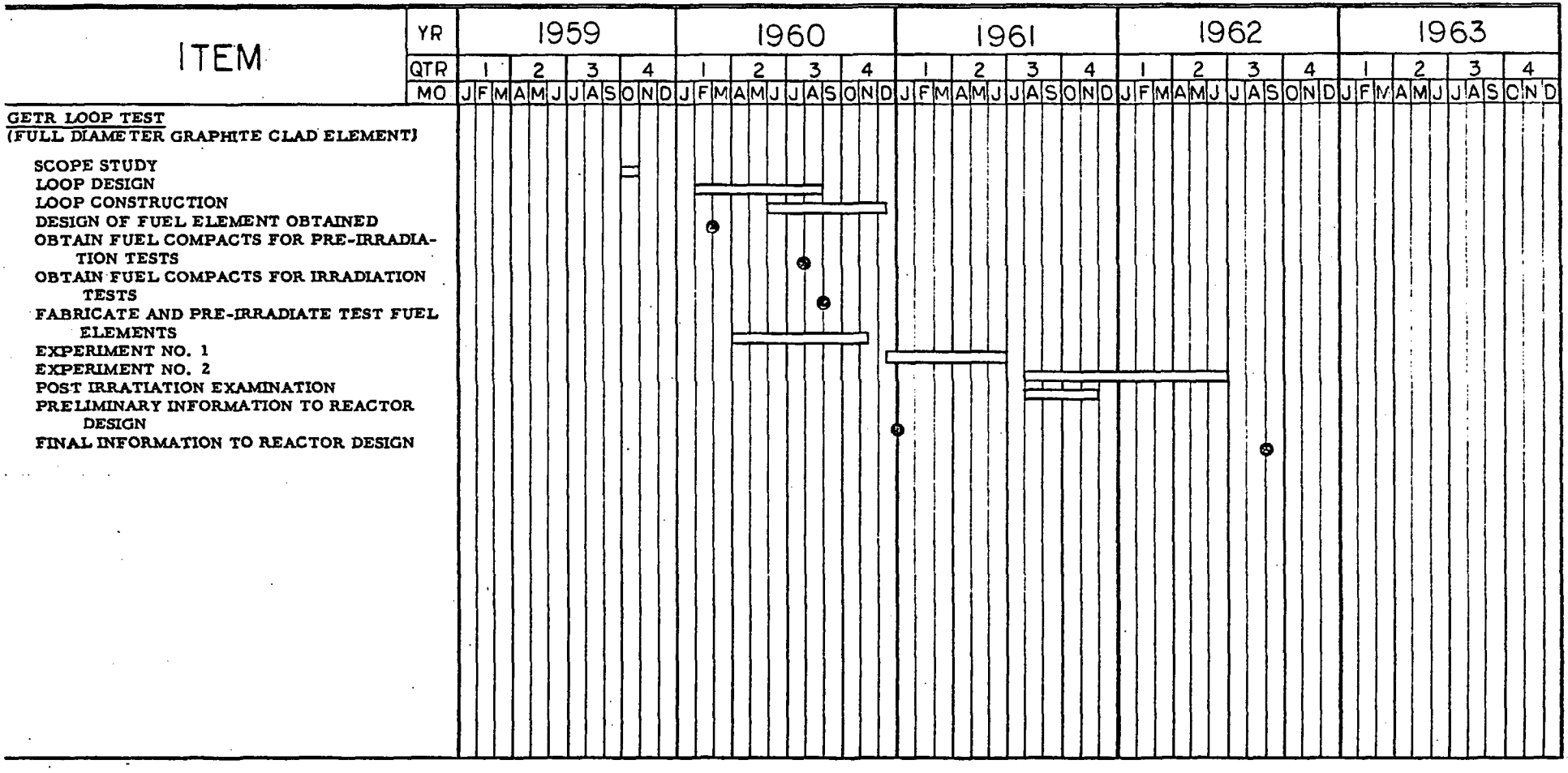

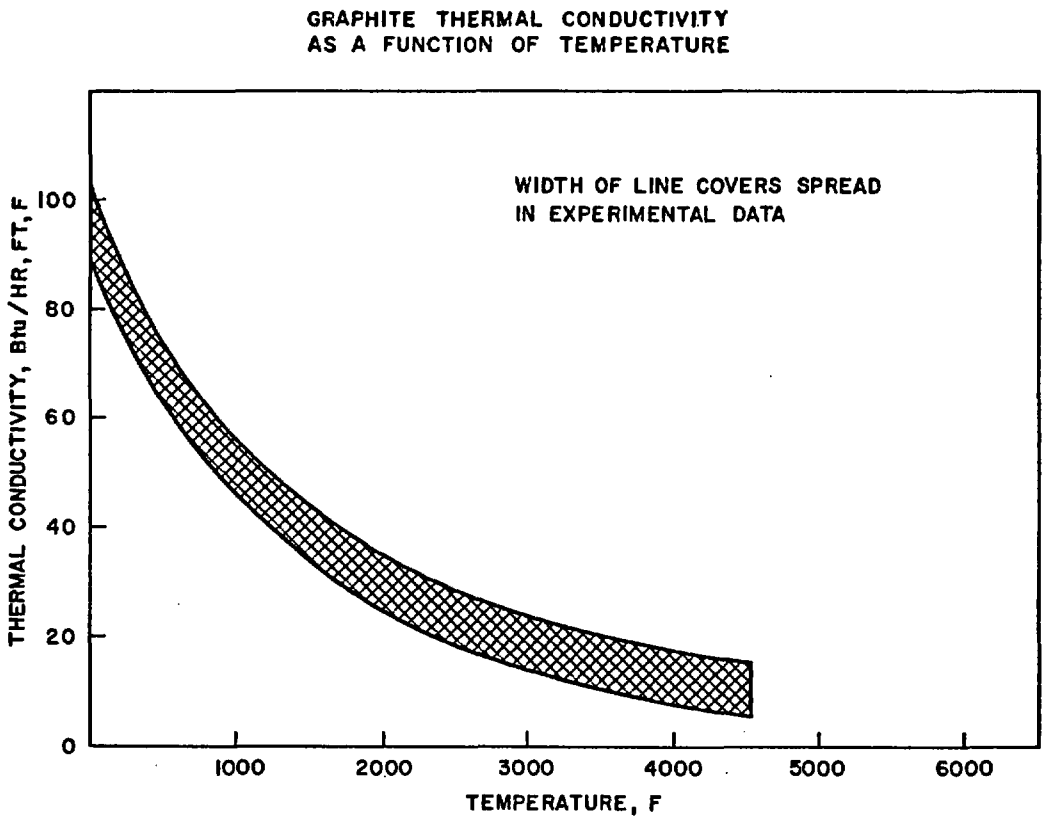
GRAPHITE THERMAL CONDUCTIVITY
AS A FUNCTION OF TEMPERATURE
WIDTH OF LINE COVERS SPREAD
IN EXPERIMENTAL DATA
THERMAL CONDUCTIVITY, Btu/HR, FT, F
0
20
40
60
80
100
1000
2000
3000
4000
5000
6000
TEMPERATURE, F

FIGURE 29

COUNTERFLOW VENTED FUEL ELEMENT DESIGN

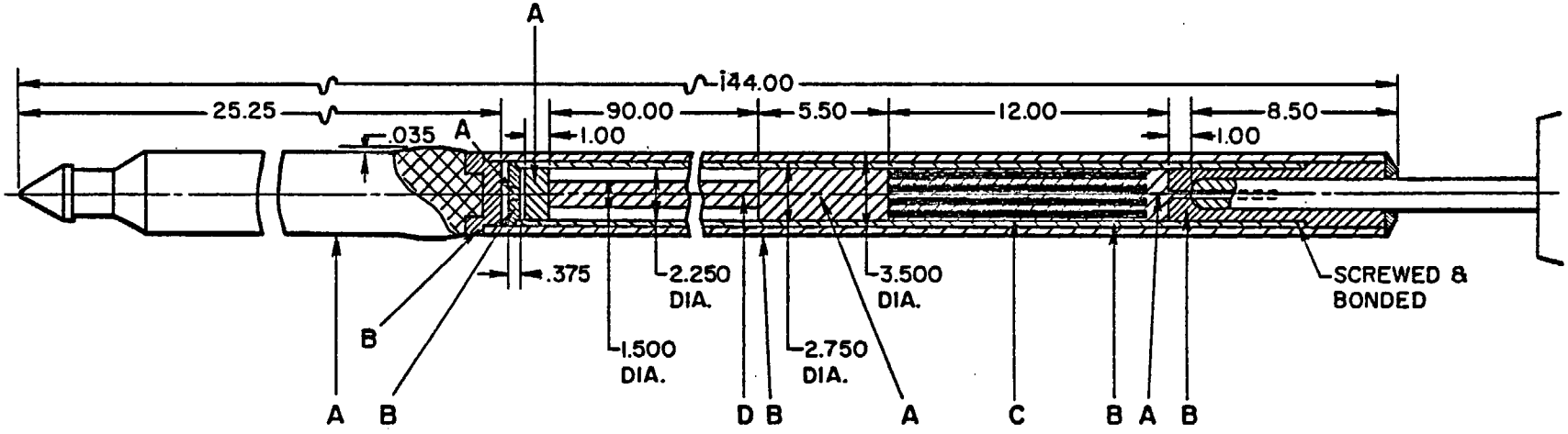

D GRAPHITE CENTER IN FUEL BODY P-1.9 GR/CC
C FISSION PRODUCT TRAPPING AGENT
B IMPERVIOUS GRAPHITE P-1.85 GR/CC
A POROUS GRAPHITE P-1.70 GR/CC

FIGURE 30

SCHEMATIC DIAGRAM OF FUEL ELEMENT

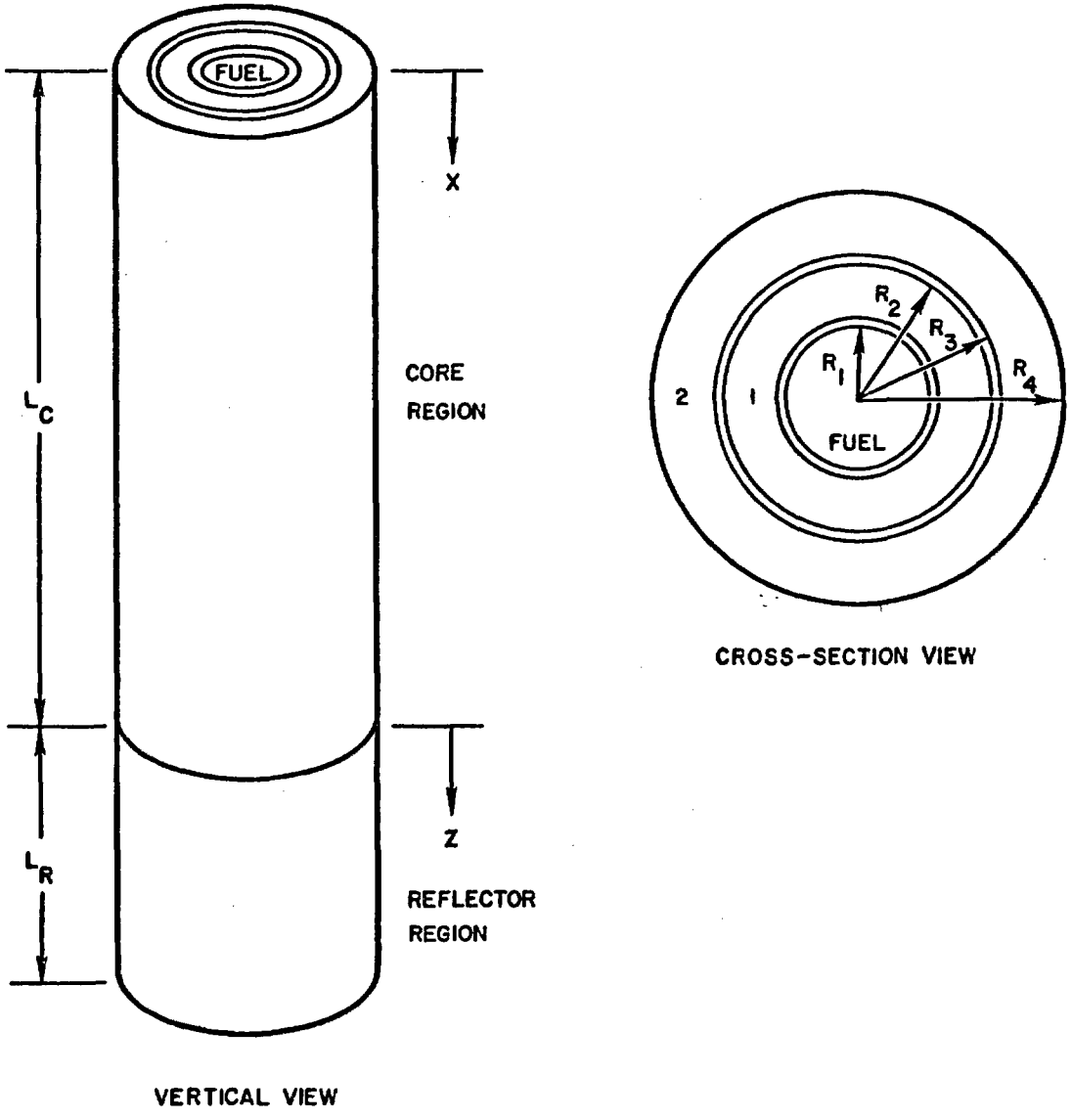

FIGURE 31

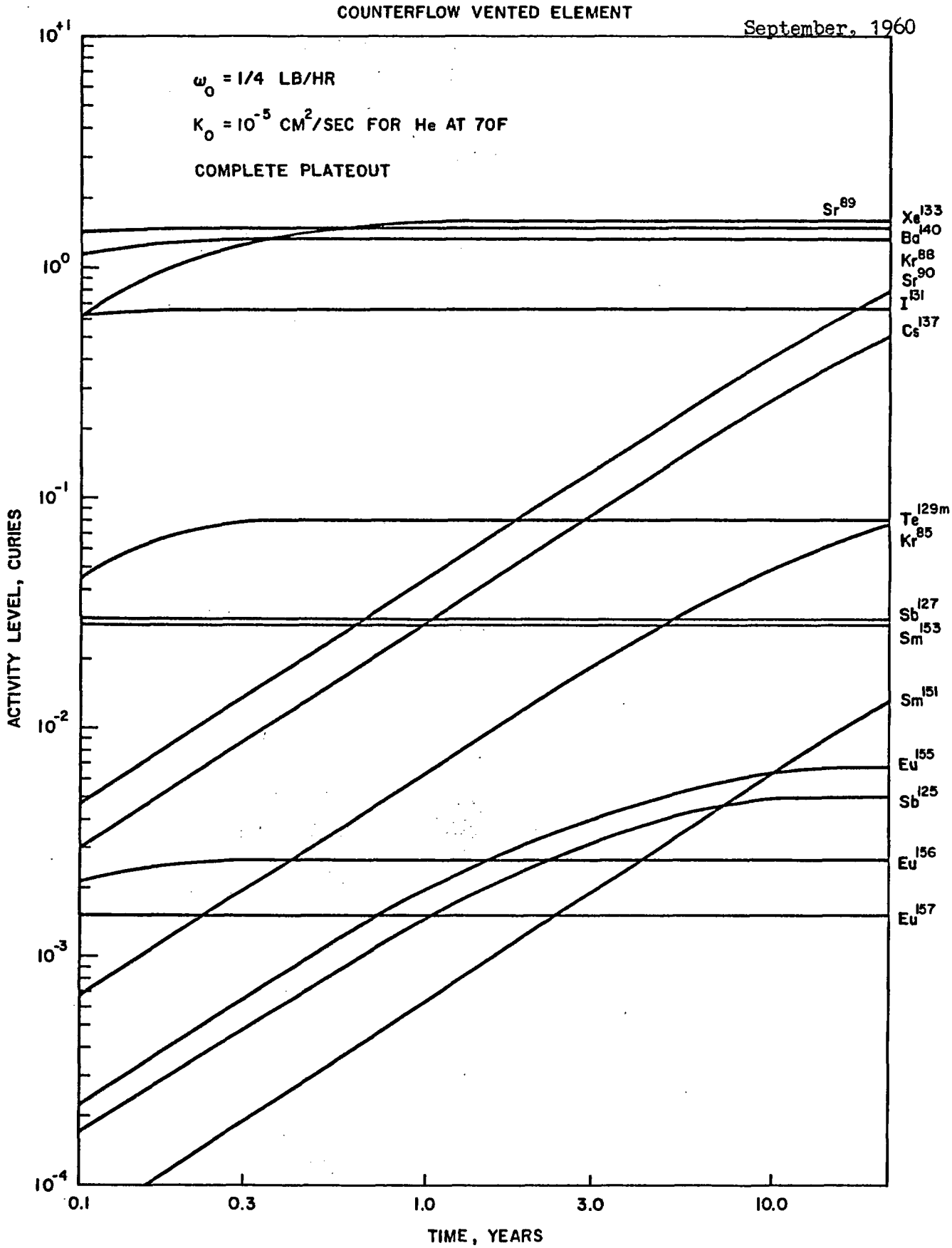
COUNTERFLOW VENTED ELEMENT
September, 1960
ω_0 = 1/4 LB/HR
$K_0 = 10^{-5}$ CM^2/SEC FOR He AT 70F
COMPLETE PLATEOUT
ACTIVITY LEVEL, CURIES
TIME, YEARS
10^{+1}
10^0
10^{-1}
10^{-2}
10^{-3}
10^{-4}
0.1
0.3
1.0
3.0
10.0
Sr^{89}
Xe^{133}
Ba^{140}
Kr^{88}
Sr^{90}
I^{131}
Cs^{137}
Te^{129m}
Kr^{85}
Sb^{127}
Sm^{153}
Sm^{151}
Eu^{155}
Sb^{125}
Eu^{156}
Eu^{157}

FIGURE 32

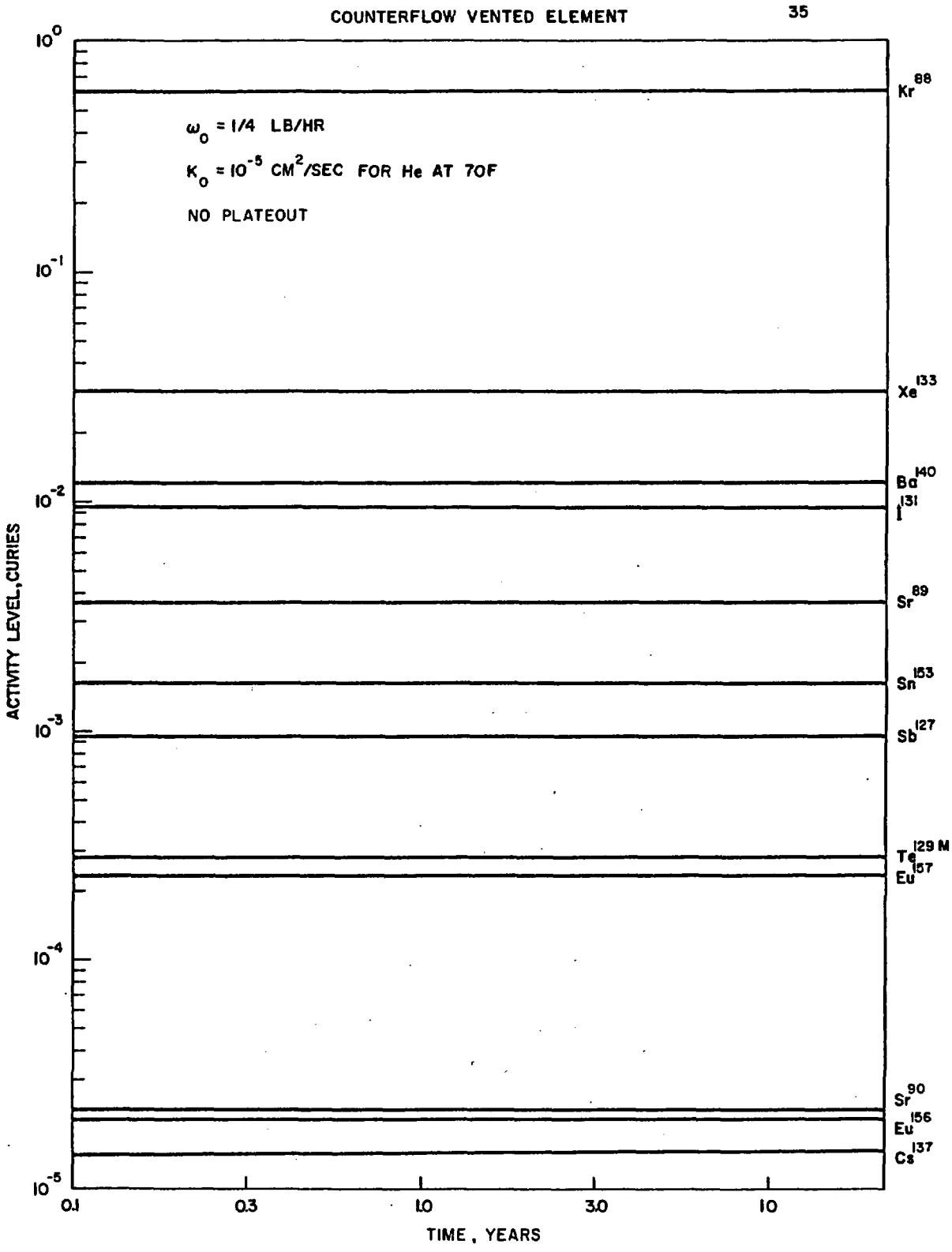
COUNTERFLOW VENTED ELEMENT
35
ω_0 = 1/4 LB/HR
$K_0 = 10^{-5}$ CM^2/SEC FOR He AT 70F
NO PLATEOUT
ACTIVITY LEVEL, CURIES
10^0
10^{-1}
10^{-2}
10^{-3}
10^{-4}
10^{-5}
0.1
0.3
1.0
3.0
10
TIME, YEARS
Kr^{88}
Xe^{133}
Ba^{140}
I^{131}
Sr^{89}
Sn^{153}
Sb^{127}
Te^{129M}
Eu^{157}
Sr^{90}
Eu^{156}
Cs^{137}

FIGURE 33

SCHEMATIC DIAGRAM OF FUEL ELEMENT
CROSS SECTION

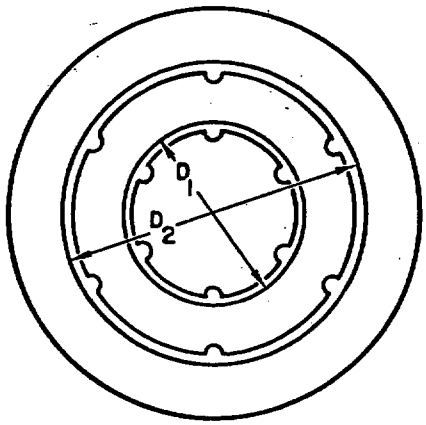

FIGURE 34

EXPANDED VIEW OF ANNULUS
BETWEEN PURGE GROOVES

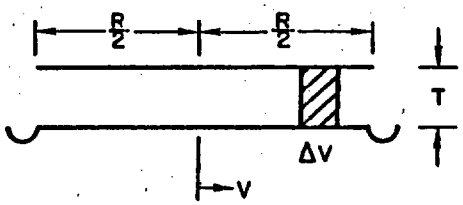

FIGURE 35

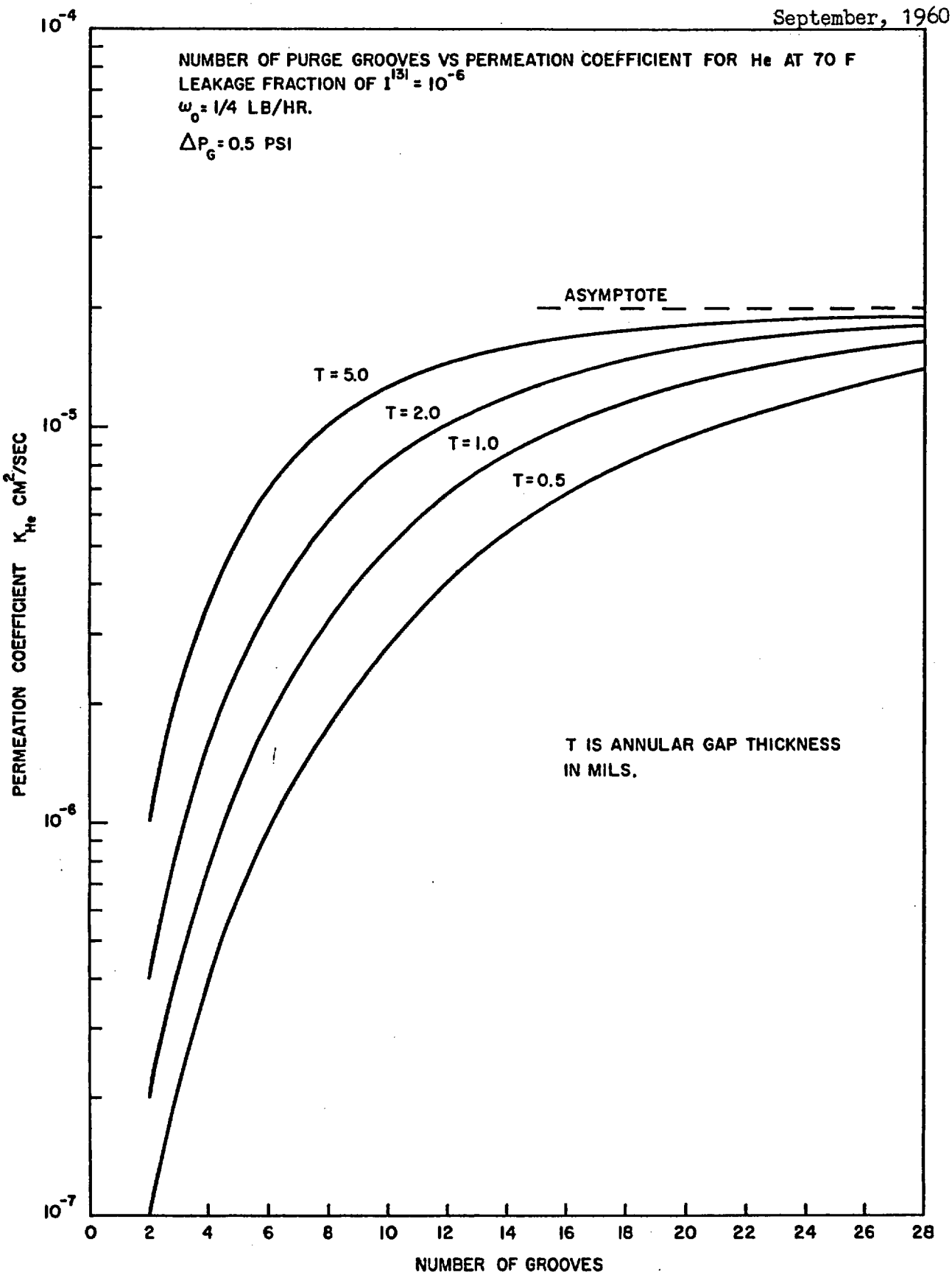
NUMBER OF PURGE GROOVES VS PERMEATION COEFFICIENT FOR He AT 70 F
LEAKAGE FRACTION OF $I^{131} = 10^{-6}$
$\omega_0 = 1/4$ LB/HR.
$\Delta P_G = 0.5$ PSI
ASYMPTOTE
T = 5.0
T = 2.0
T = 1.0
T = 0.5
T IS ANNULAR GAP THICKNESS IN MILS.
PERMEATION COEFFICIENT K_{He} CM^2/SEC
10^{-4}
10^{-5}
10^{-6}
10^{-7}
0
2
4
6
8
10
12
14
16
18
20
22
24
26
28
NUMBER OF GROOVES

FIGURE 36

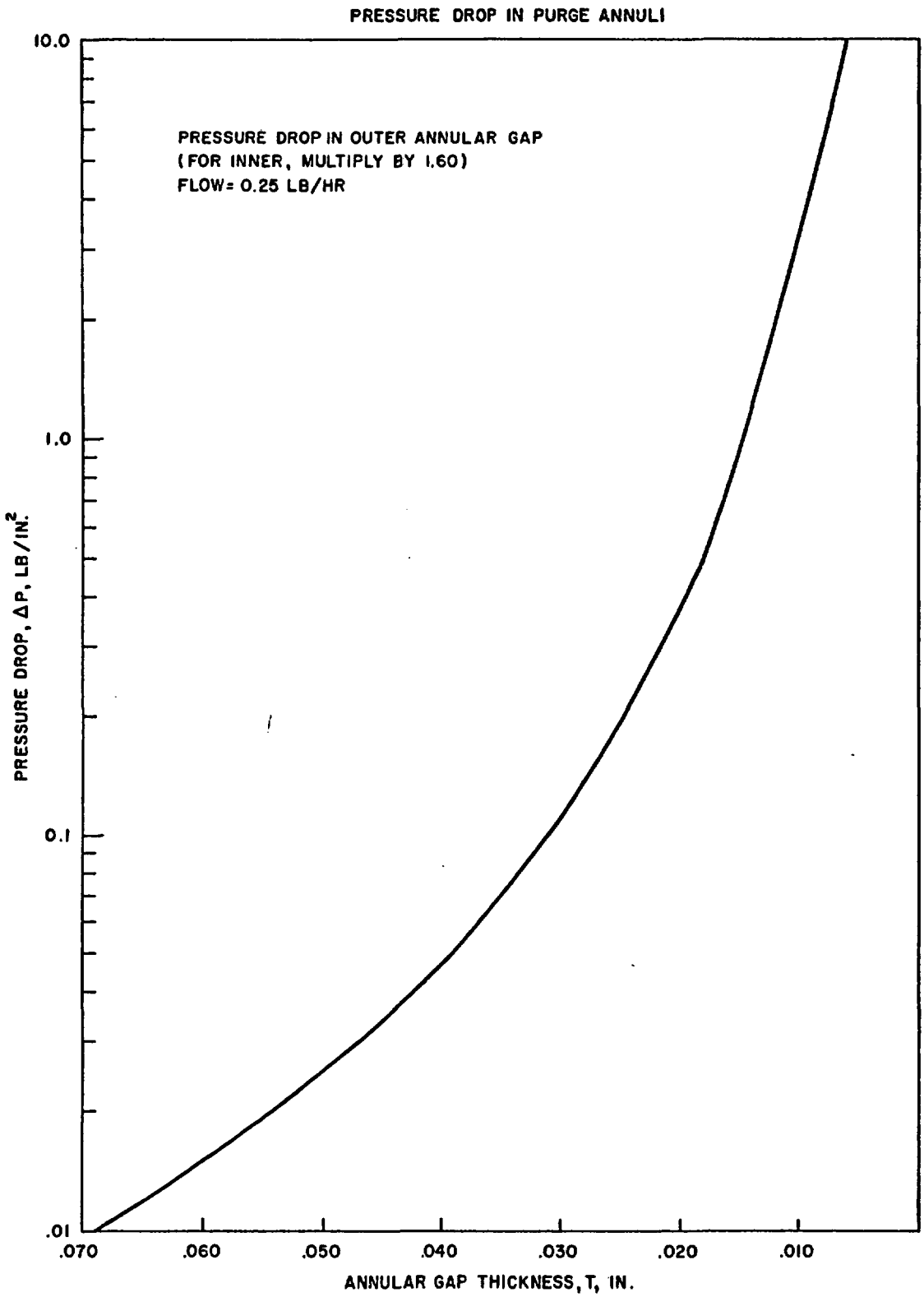
PRESSURE DROP IN PURGE ANNULI
PRESSURE DROP IN OUTER ANNULAR GAP
(FOR INNER, MULTIPLY BY 1.60)
FLOW= 0.25 LB/HR
10.0
1.0
0.1
.01
PRESSURE DROP, ΔP, LB/IN.²
.070
.060
.050
.040
.030
.020
.010
ANNULAR GAP THICKNESS, T, IN.

FIGURE 37

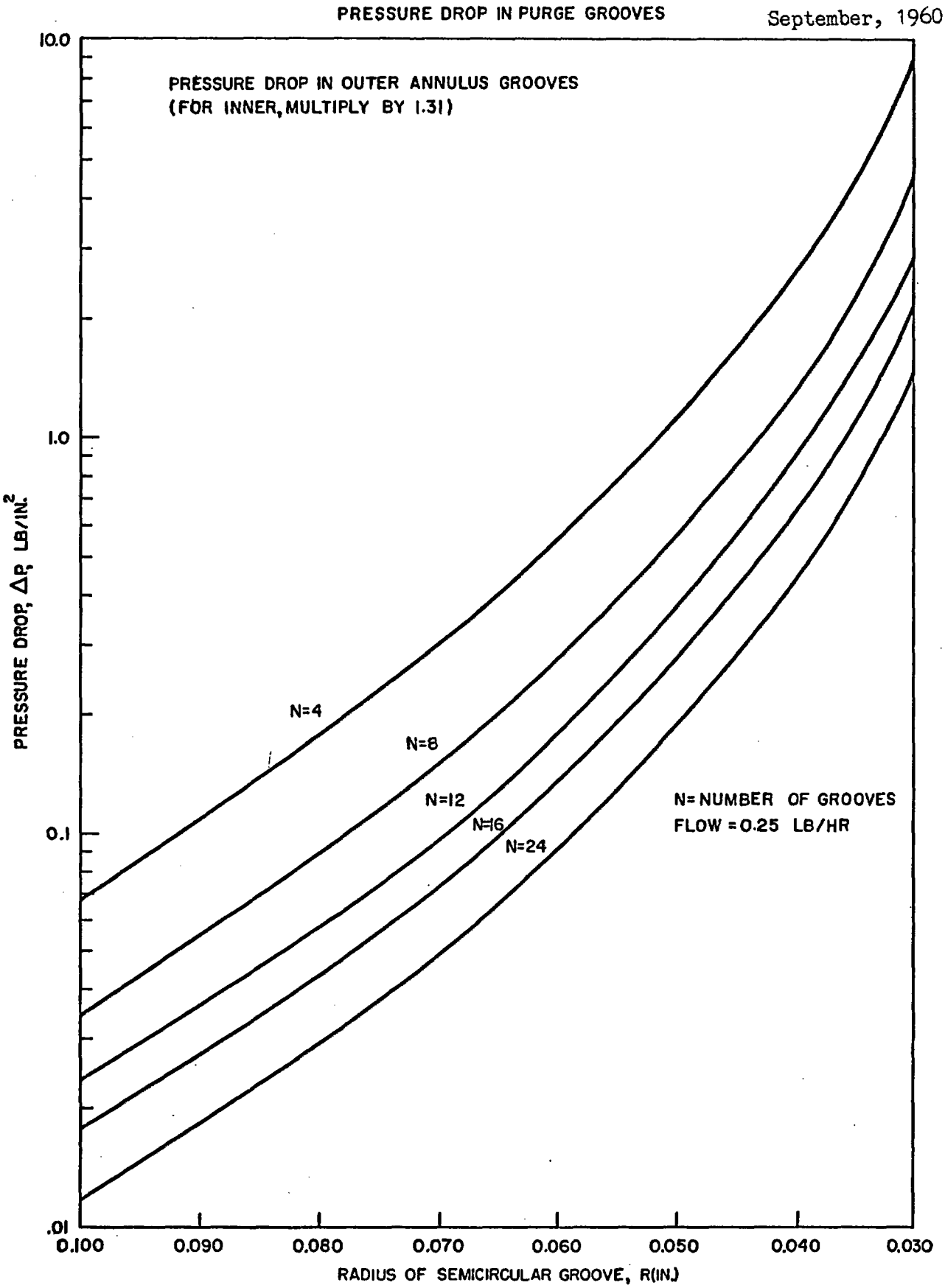
PRESSURE DROP IN PURGE GROOVES
PRESSURE DROP IN OUTER ANNULUS GROOVES
(FOR INNER, MULTIPLY BY 1.31)
10.0
1.0
0.1
.01
PRESSURE DROP, ΔP, LB/IN.²
N=4
N=8
N=12
N=16
N=24
N= NUMBER OF GROOVES
FLOW = 0.25 LB/HR
0.100
0.090
0.080
0.070
0.060
0.050
0.040
0.030
RADIUS OF SEMICIRCULAR GROOVE, R(IN.)

FIGURE 38

TENSILE THERMAL STRESS IN GRAPHITE OUTER SLEEVE

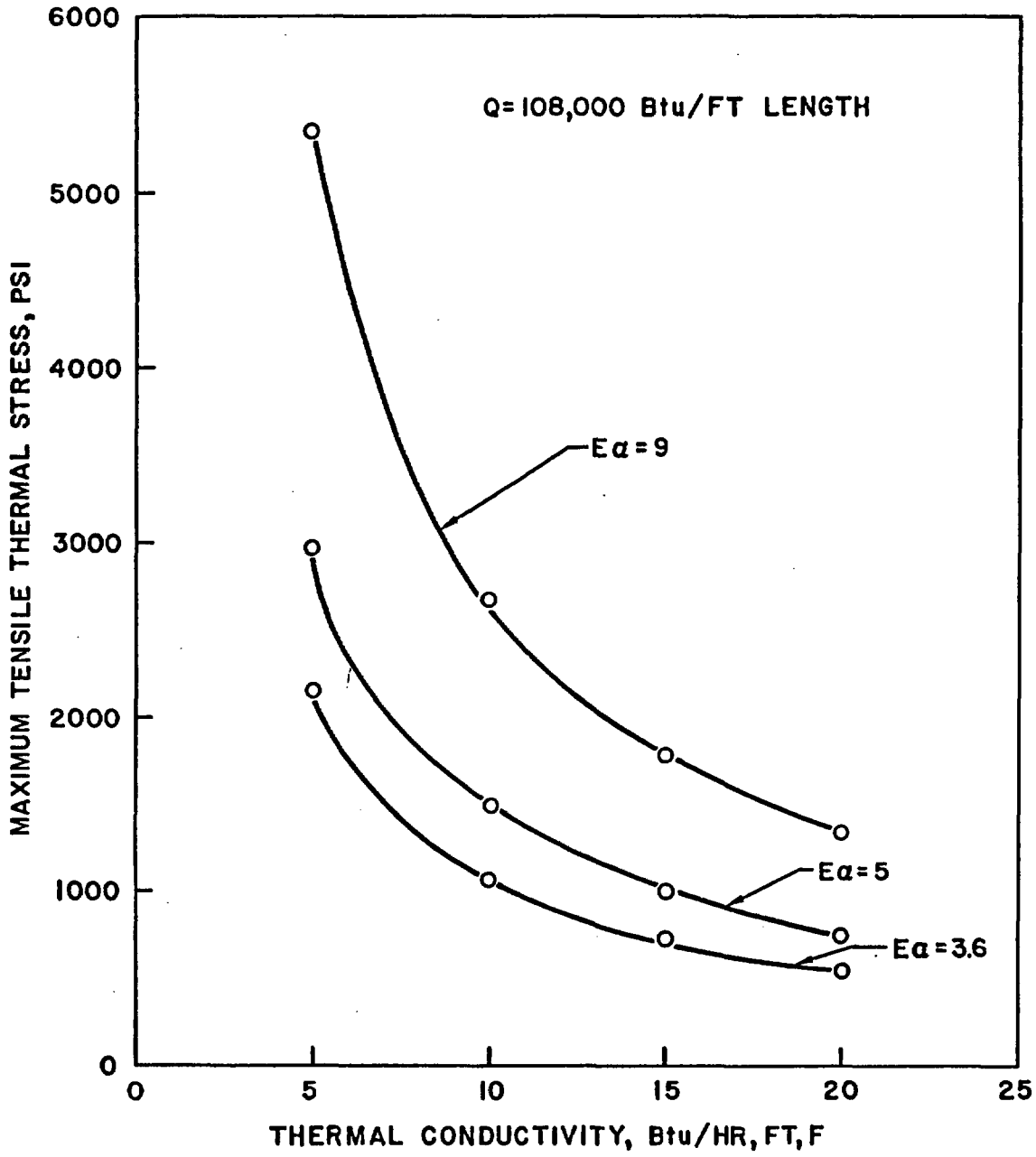

FIGURE 39

F_T, RATIO OF Xe ACTIVITY RELEASED TO Xe ACTIVITY PRODUCED AT STEADY STATE VS. HALF LIFE

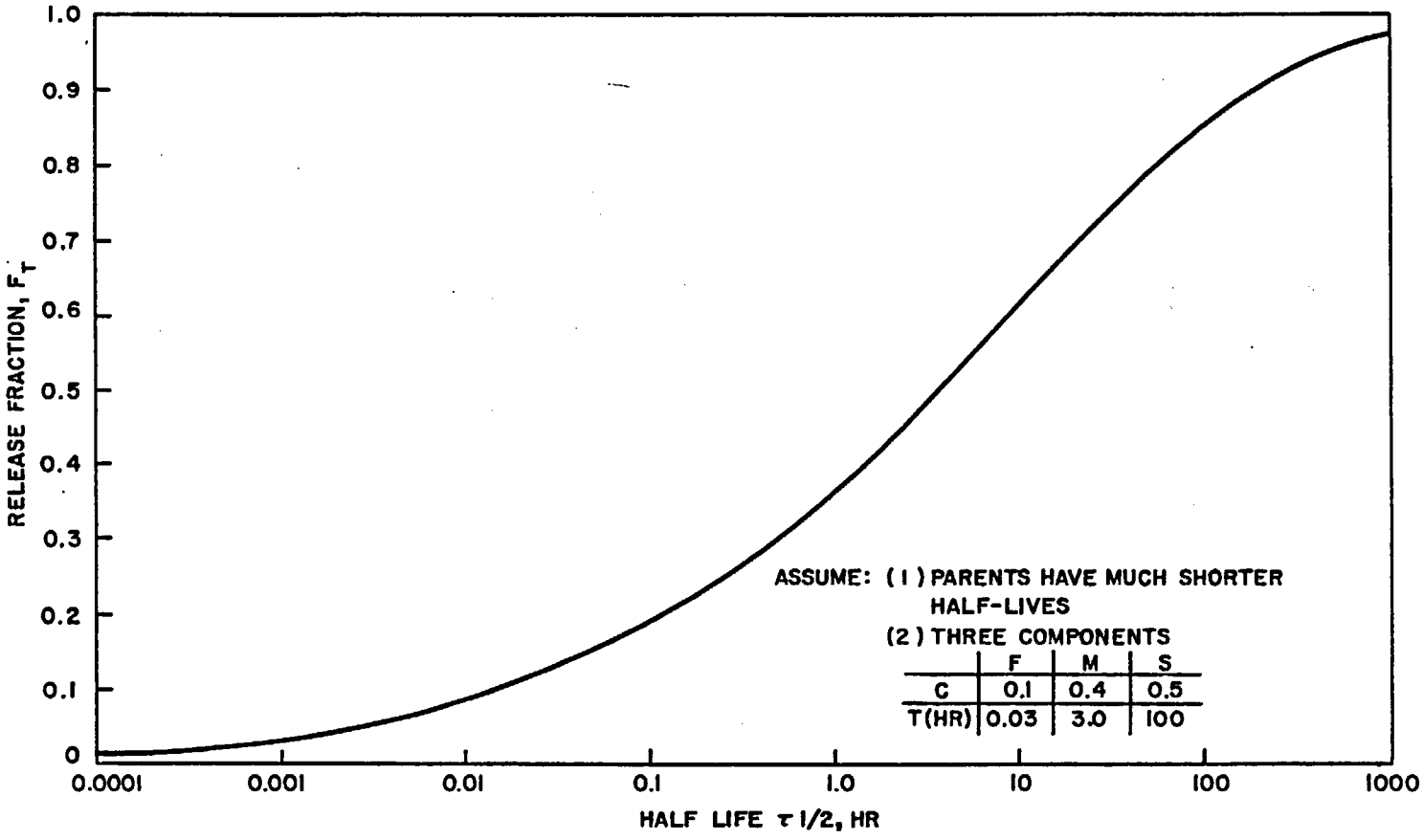

	F	M	S
C	0.1	0.4	0.5
T(HR)	0.03	3.0	100

FIGURE 40

September, 1960

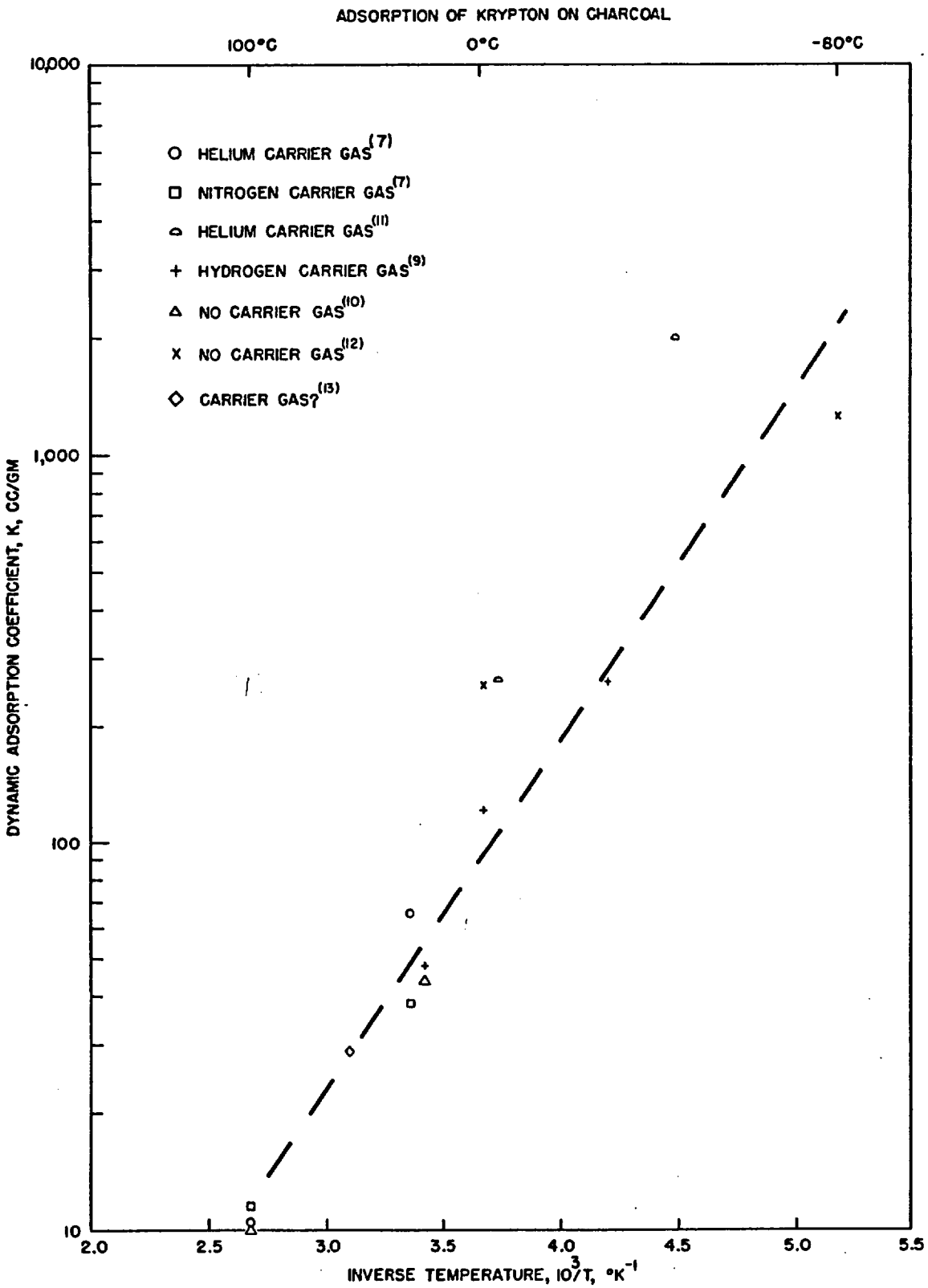
ADSORPTION OF KRYPTON ON CHARCOAL
100°C
0°C
-80°C
10,000
1,000
100
10
DYNAMIC ADSORPTION COEFFICIENT, K, CC/GM
HELIUM CARRIER GAS(7)
NITROGEN CARRIER GAS(7)
HELIUM CARRIER GAS(11)
HYDROGEN CARRIER GAS(9)
NO CARRIER GAS(10)
NO CARRIER GAS(12)
CARRIER GAS?(13)
2.0
2.5
3.0
3.5
4.0
4.5
5.0
5.5
INVERSE TEMPERATURE, 10³/T, °K⁻¹

FIGURE 41

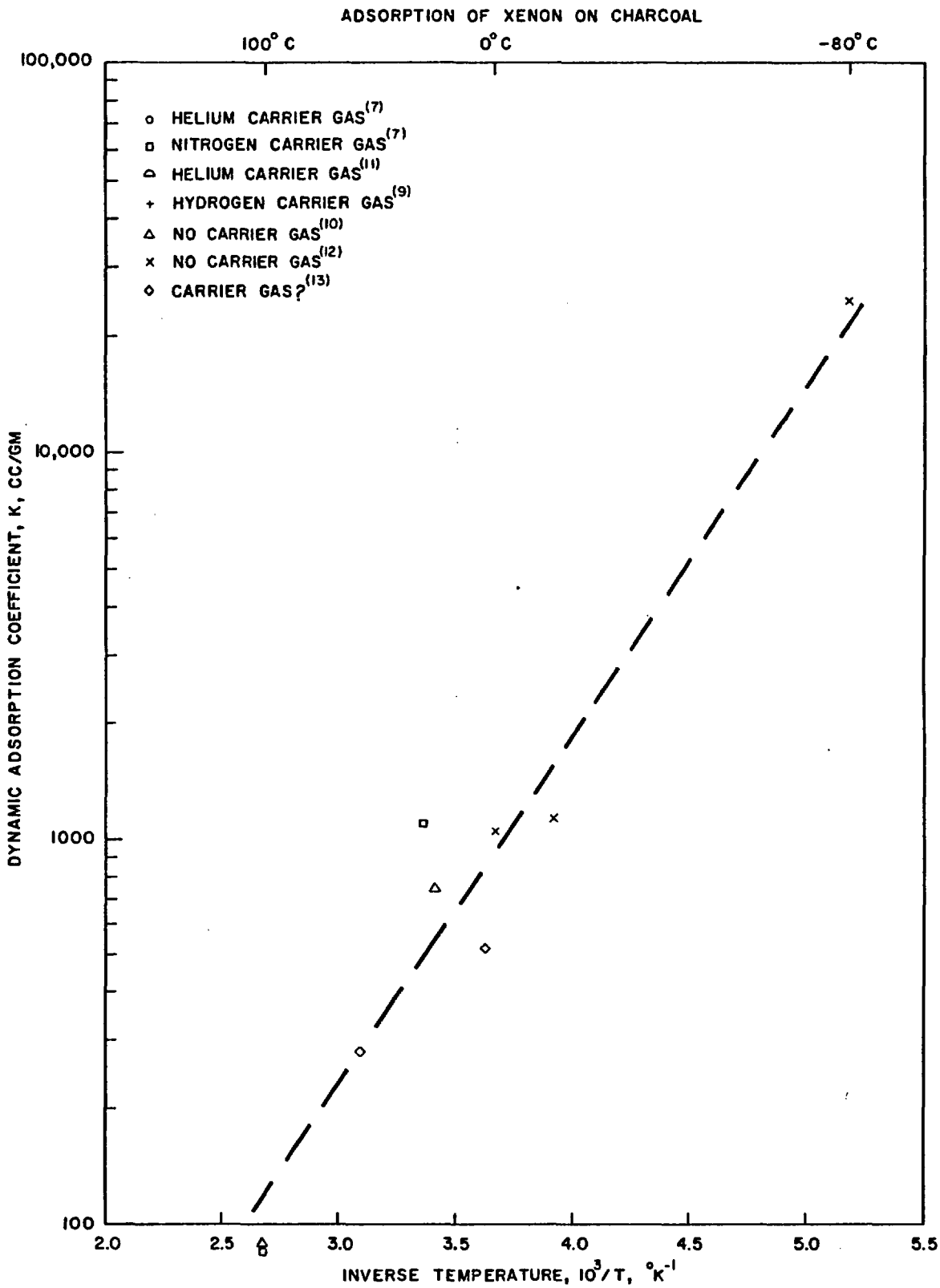
ADSORPTION OF XENON ON CHARCOAL
100° C
0° C
-80° C
100,000
10,000
1000
100
HELIUM CARRIER GAS(7)
NITROGEN CARRIER GAS(7)
HELIUM CARRIER GAS(11)
HYDROGEN CARRIER GAS(9)
NO CARRIER GAS(10)
NO CARRIER GAS(12)
CARRIER GAS?(13)
DYNAMIC ADSORPTION COEFFICIENT, K, CC/GM
2.0
2.5
3.0
3.5
4.0
4.5
5.0
5.5
INVERSE TEMPERATURE, 10³/T, °K⁻¹

FIGURE 42

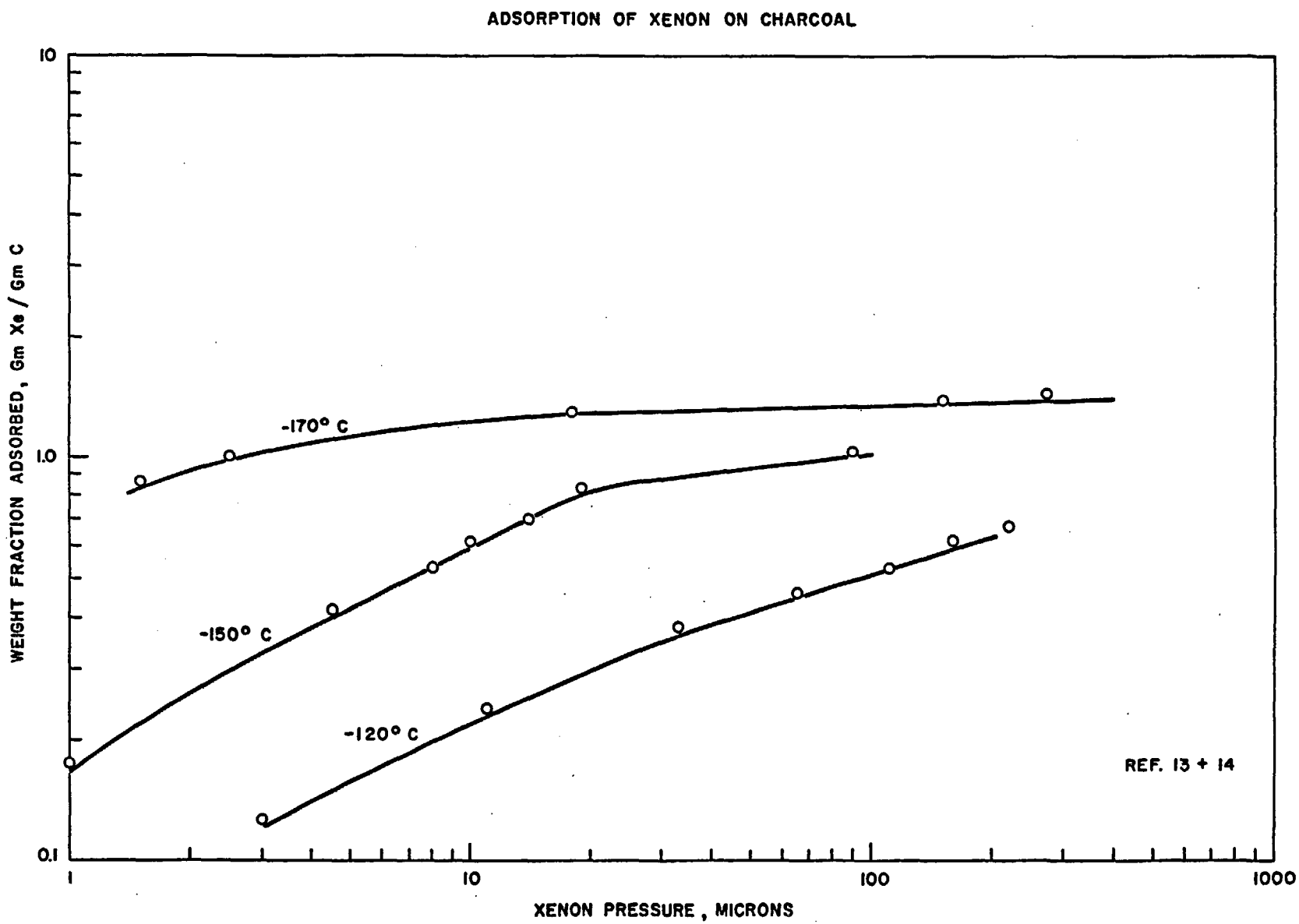

FIGURE 43

September, 1960

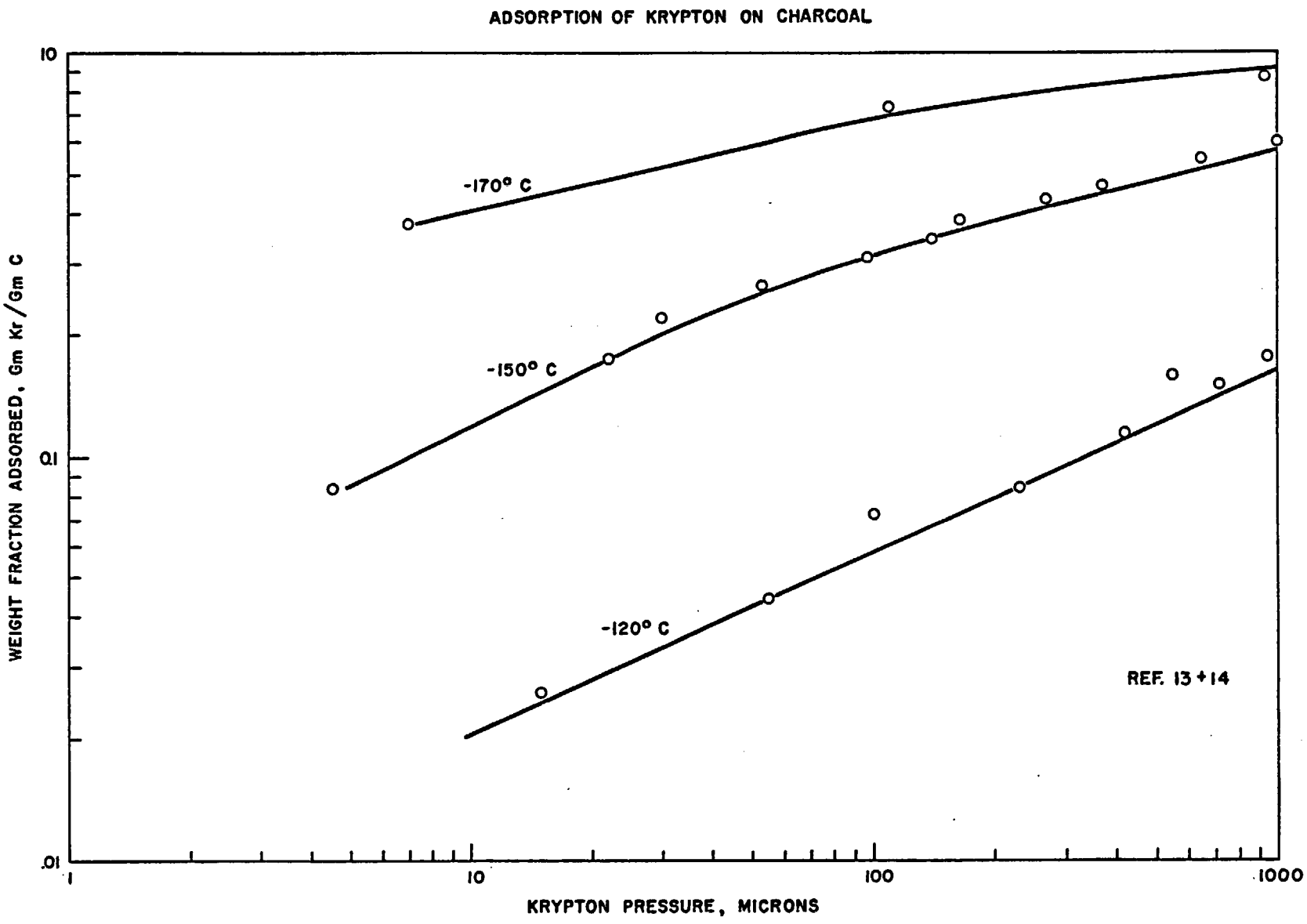
ADSORPTION OF KRYPTON ON CHARCOAL
WEIGHT FRACTION ADSORBED, Gm Kr/Gm C
10
.1
.01
-170° C
-150° C
-120° C
REF. 13 + 14
1
10
100
1000
KRYPTON PRESSURE, MICRONS

FIGURE 44

FLOW DIAGRAM FOR HELIUM PURIFICATION SYSTEM

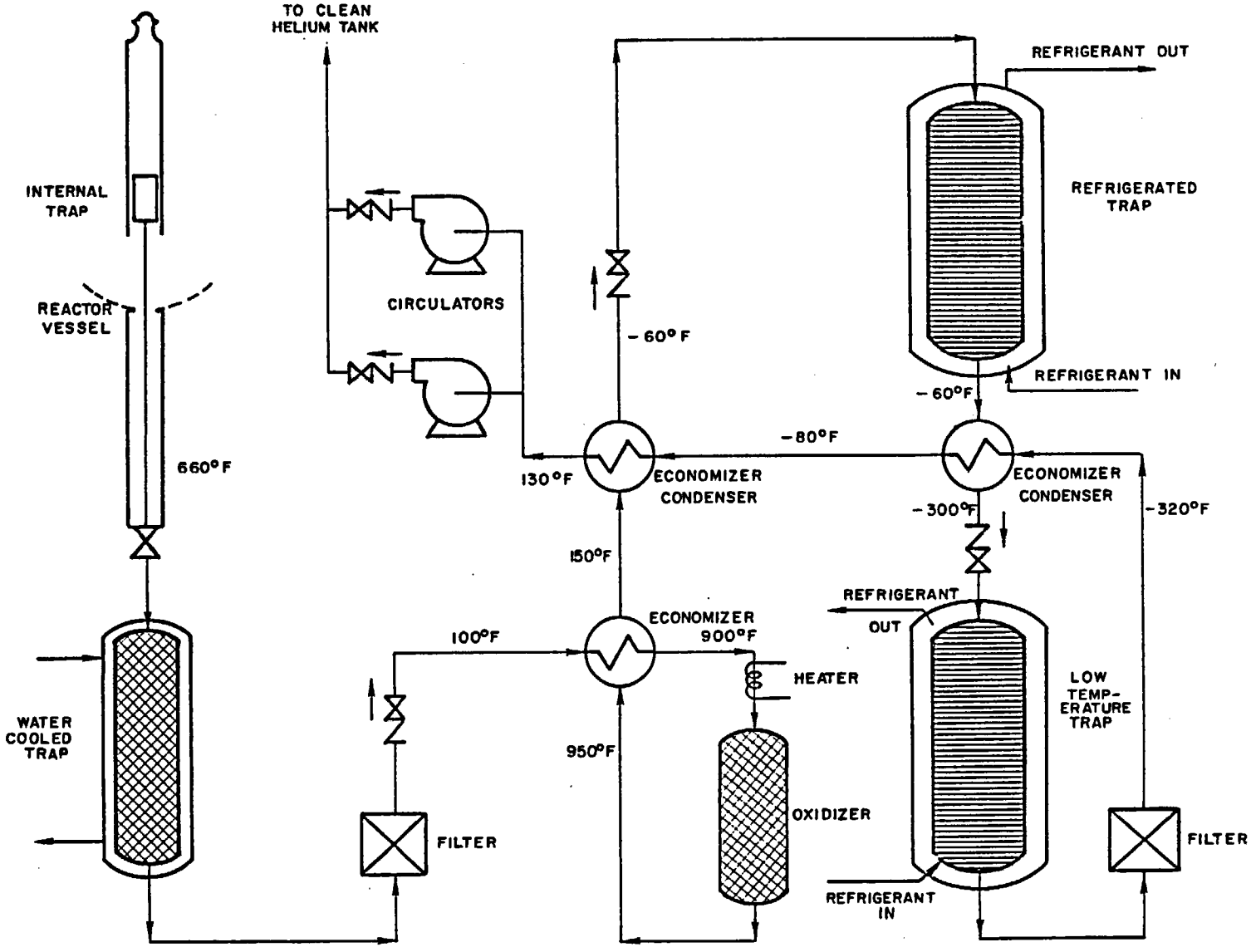

FIGURE 45

September, 1960

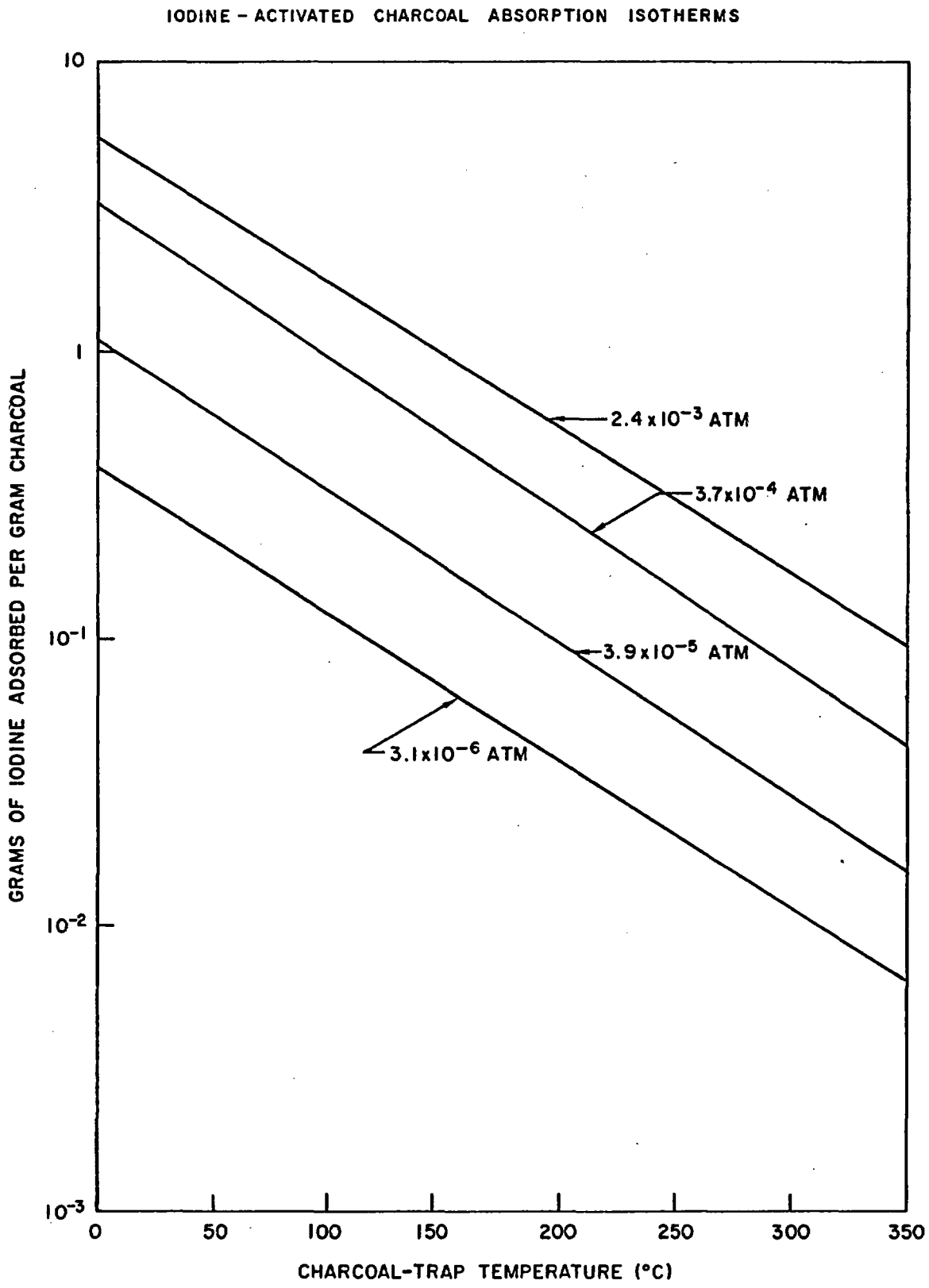
IODINE - ACTIVATED CHARCOAL ABSORPTION ISOTHERMS
GRAMS OF IODINE ADSORBED PER GRAM CHARCOAL
10
1
10⁻¹
10⁻²
10⁻³
2.4 x 10⁻³ ATM
3.7x10⁻⁴ ATM
3.9 x 10⁻⁵ ATM
3.1x10⁻⁶ ATM
0
50
100
150
200
250
300
350
CHARCOAL-TRAP TEMPERATURE (°C)

FIGURE 46

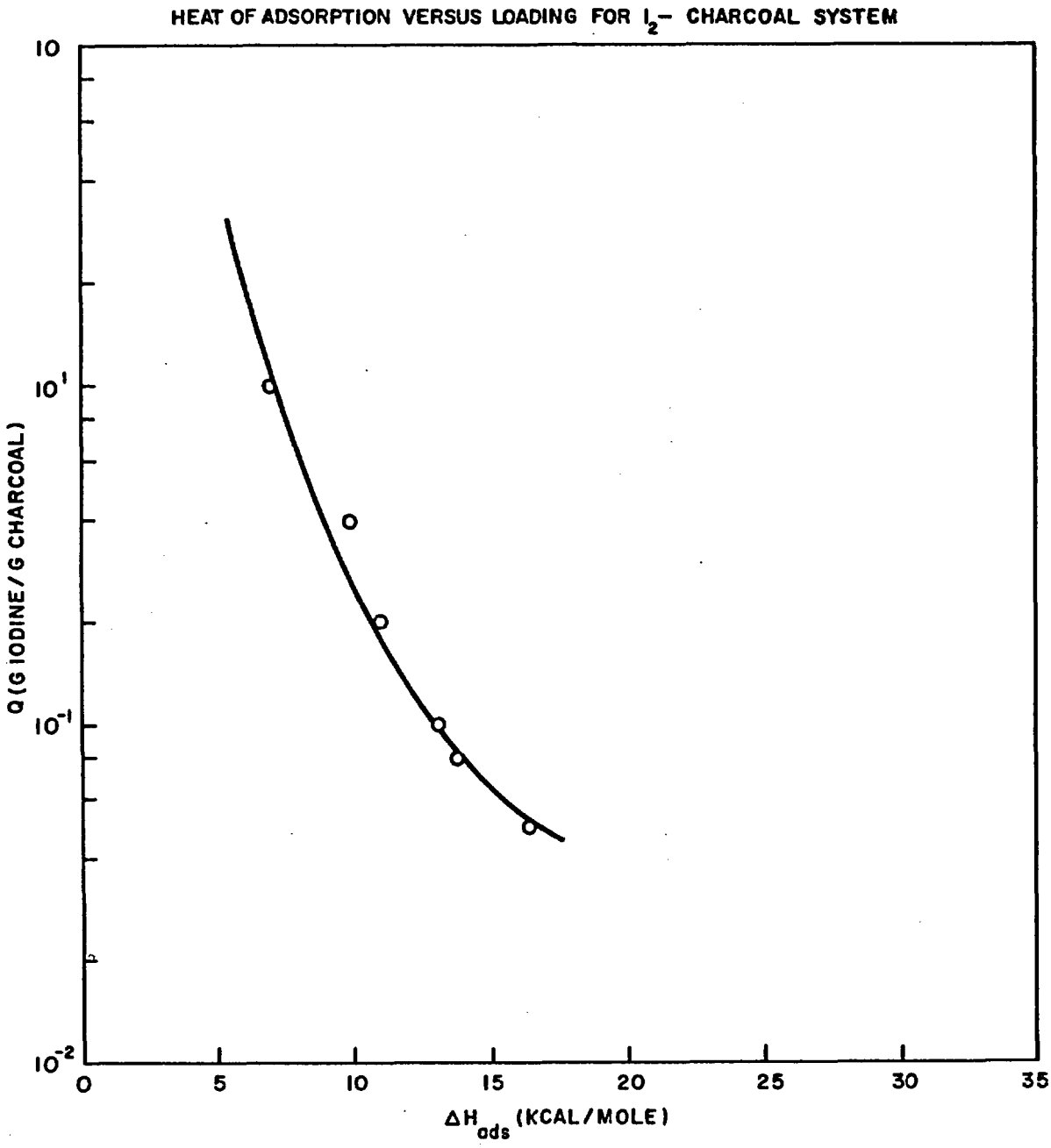
HEAT OF ADSORPTION VERSUS LOADING FOR I_2– CHARCOAL SYSTEM
Q (G IODINE / G CHARCOAL)
10
10^1
10^{-1}
10^{-2}
0
5
10
15
20
25
30
35
ΔH_{ads} (KCAL/MOLE)

FIGURE 47

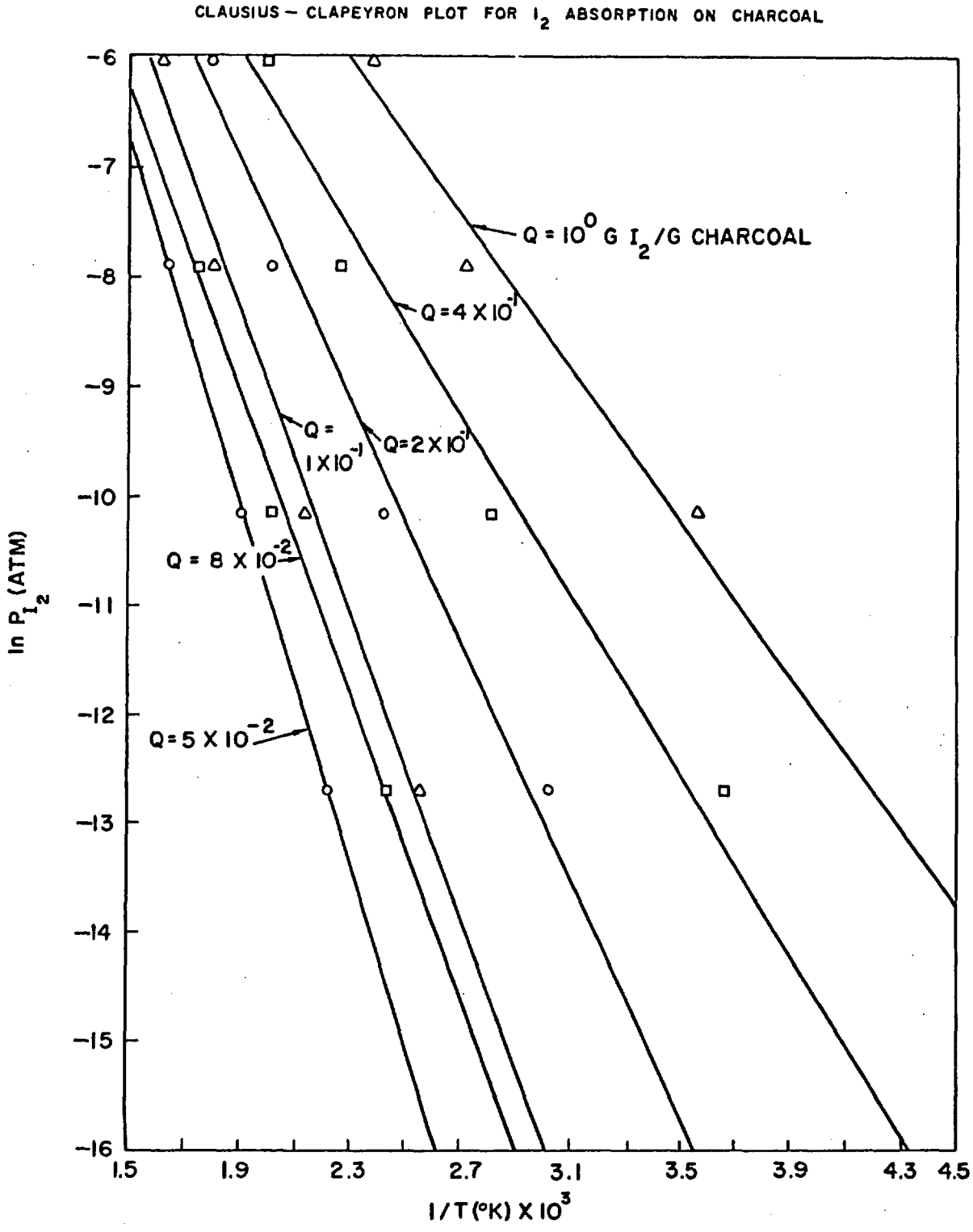
CLAUSIUS – CLAPEYRON PLOT FOR I_2 ABSORPTION ON CHARCOAL
Q = 10^0 G I_2/G CHARCOAL
Q = 4 X 10^{-1}
Q = 1 X 10^{-1}
Q = 2 X 10^{-1}
Q = 8 X 10^{-2}
Q = 5 X 10^{-2}
ln P_{I_2} (ATM)
-6
-7
-8
-9
-10
-11
-12
-13
-14
-15
-16
1.5
1.9
2.3
2.7
3.1
3.5
3.9
4.3
4.5
1/T (°K) X 10^3

FIGURE 48

CESII -GENERATION APPARATUS

September, 1960

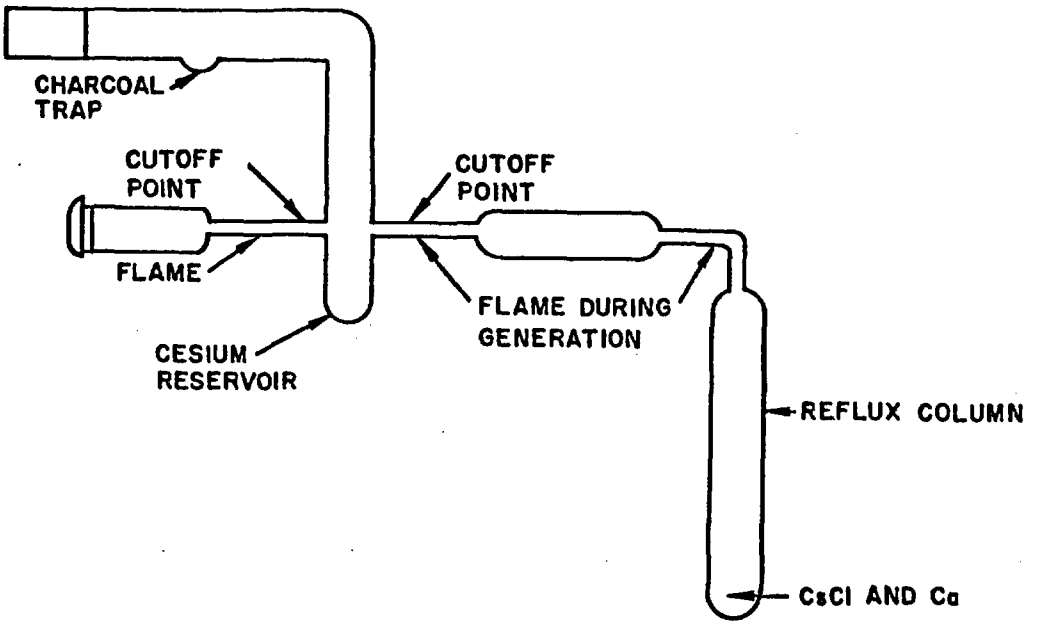

FIGURE 49

CESIUM - ISOTHERM APPARATUS

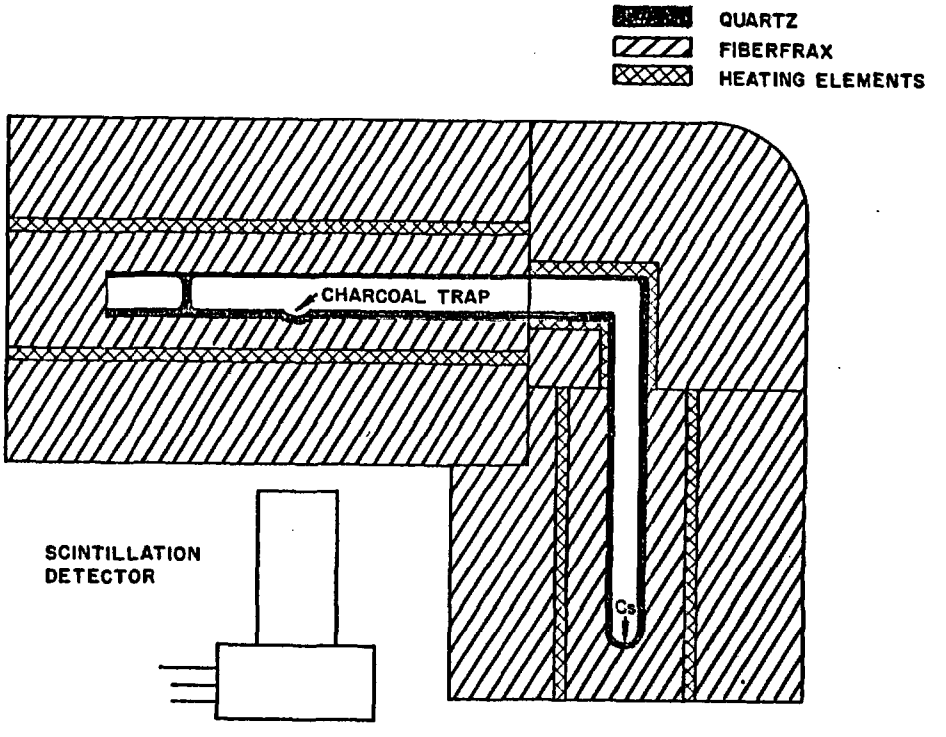

FIGURE 50

CESIUM ABSORPTION ON CHARCOAL AS A FUNCTION OF CESIUM VAPOR PRESSURE

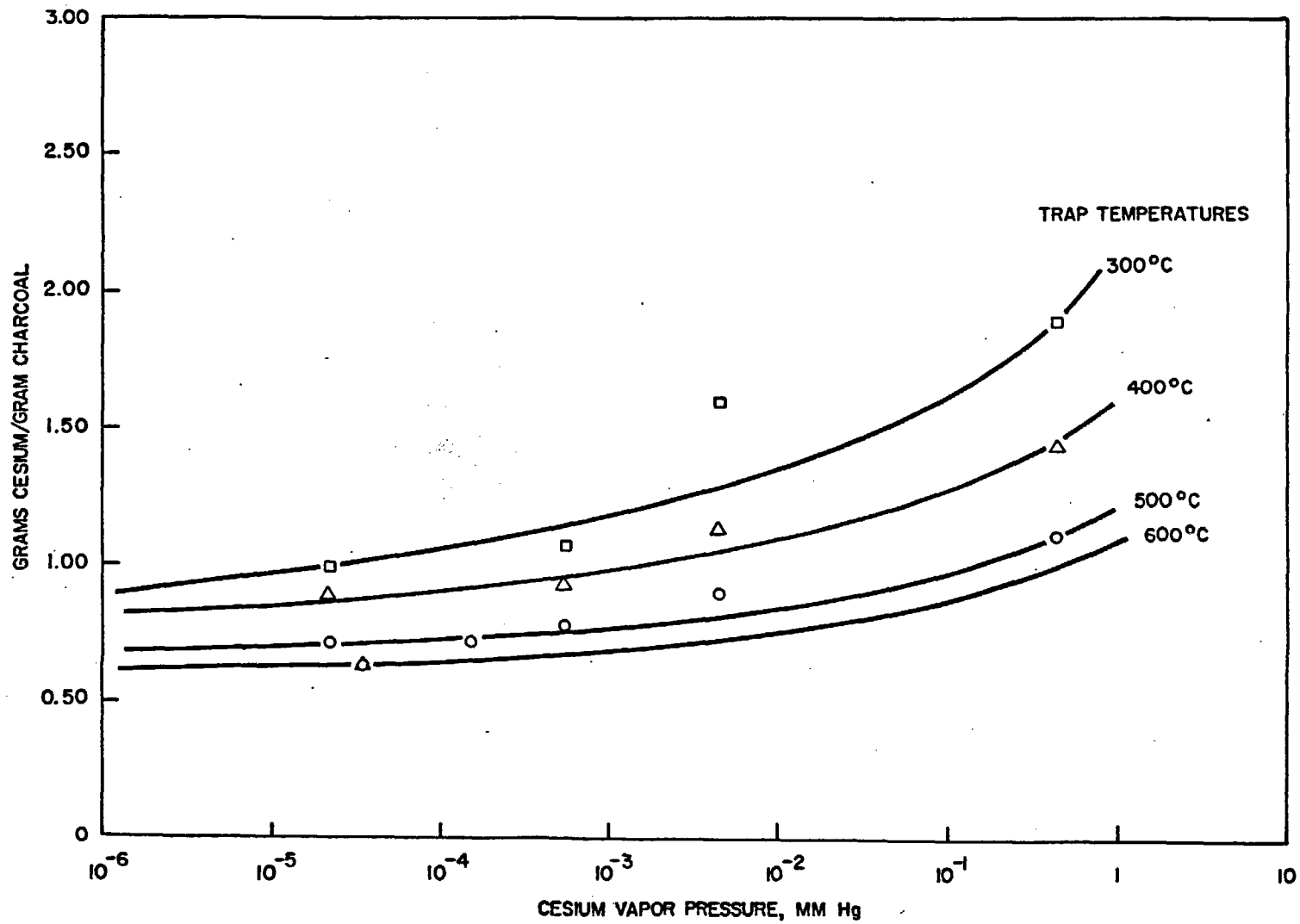

FIGURE 51

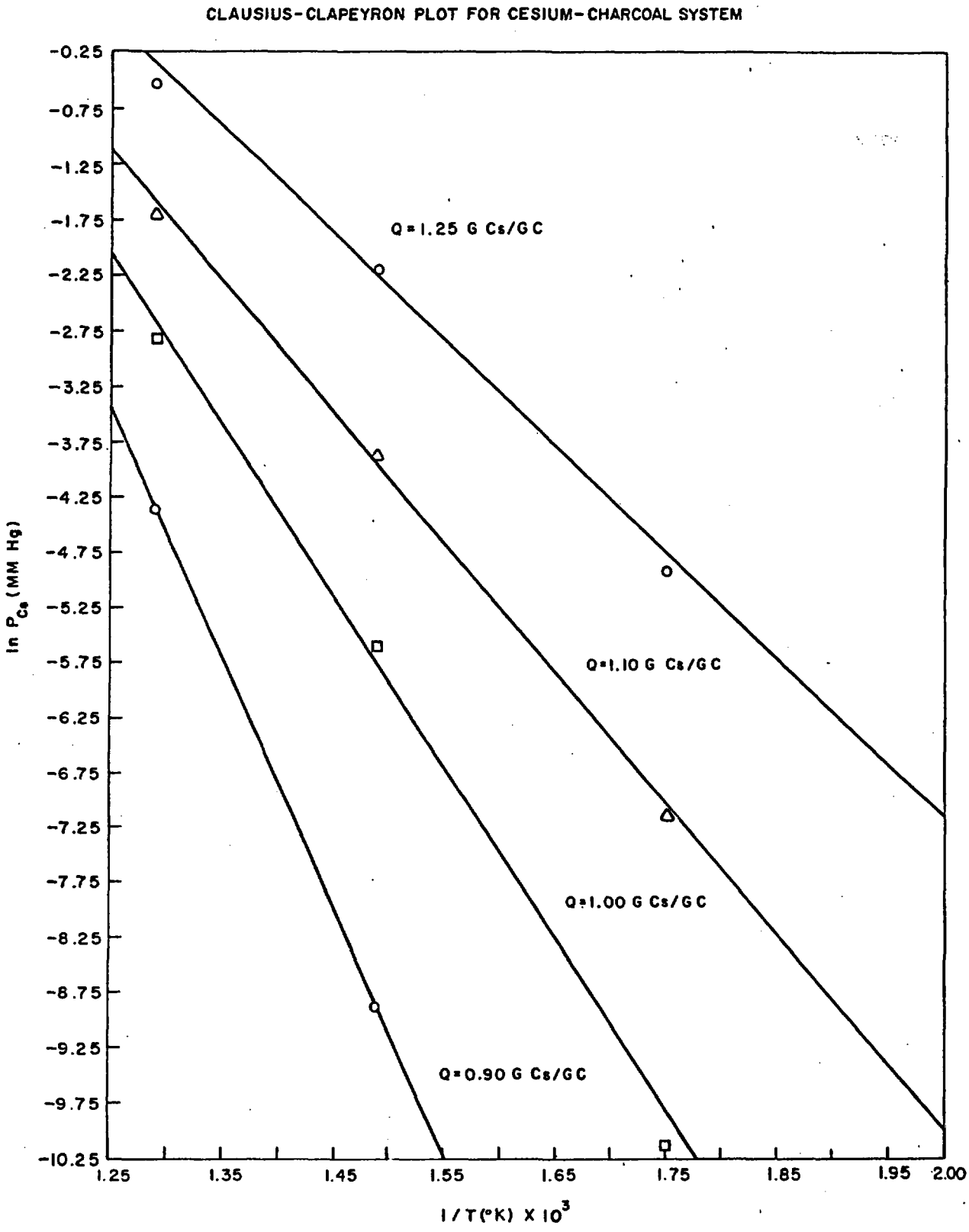
CLAUSIUS-CLAPEYRON PLOT FOR CESIUM-CHARCOAL SYSTEM
Q = 1.25 G Cs/G C
Q = 1.10 G Cs/G C
Q = 1.00 G Cs/G C
Q = 0.90 G Cs/G C
ln P_{Cs} (MM Hg)
-0.25
-0.75
-1.25
-1.75
-2.25
-2.75
-3.25
-3.75
-4.25
-4.75
-5.25
-5.75
-6.25
-6.75
-7.25
-7.75
-8.25
-8.75
-9.25
-9.75
-10.25
1.25
1.35
1.45
1.55
1.65
1.75
1.85
1.95
2.00
1/T(°K) X 10^3

FIGURE 52

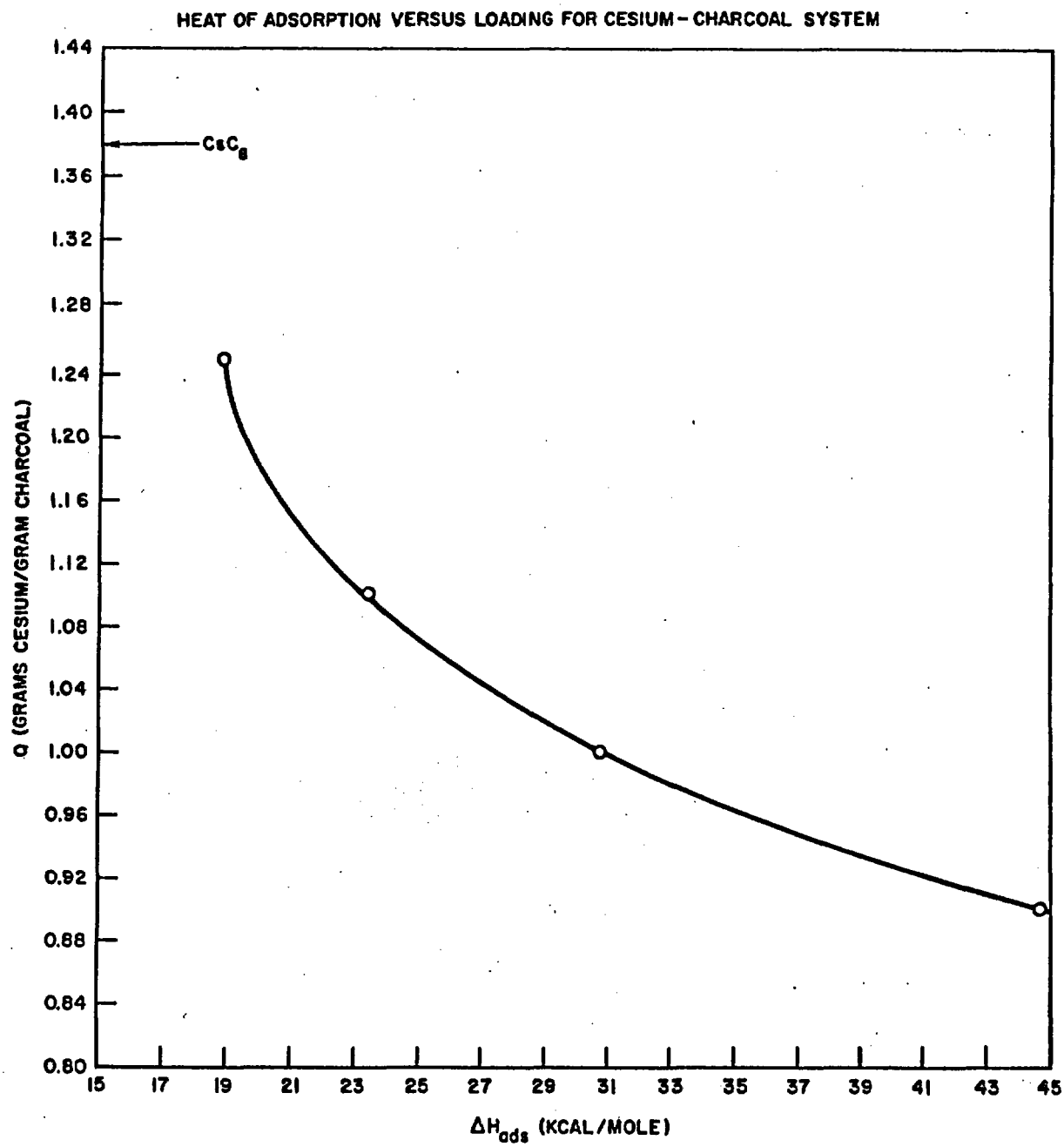
HEAT OF ADSORPTION VERSUS LOADING FOR CESIUM - CHARCOAL SYSTEM
Q (GRAMS CESIUM/GRAM CHARCOAL)
1.44
1.40
1.36
1.32
1.28
1.24
1.20
1.16
1.12
1.08
1.04
1.00
0.96
0.92
0.88
0.84
0.80
CsC8
15
17
19
21
23
25
27
29
31
33
35
37
39
41
43
45
ΔHads (KCAL/MOLE)

FIGURE 53

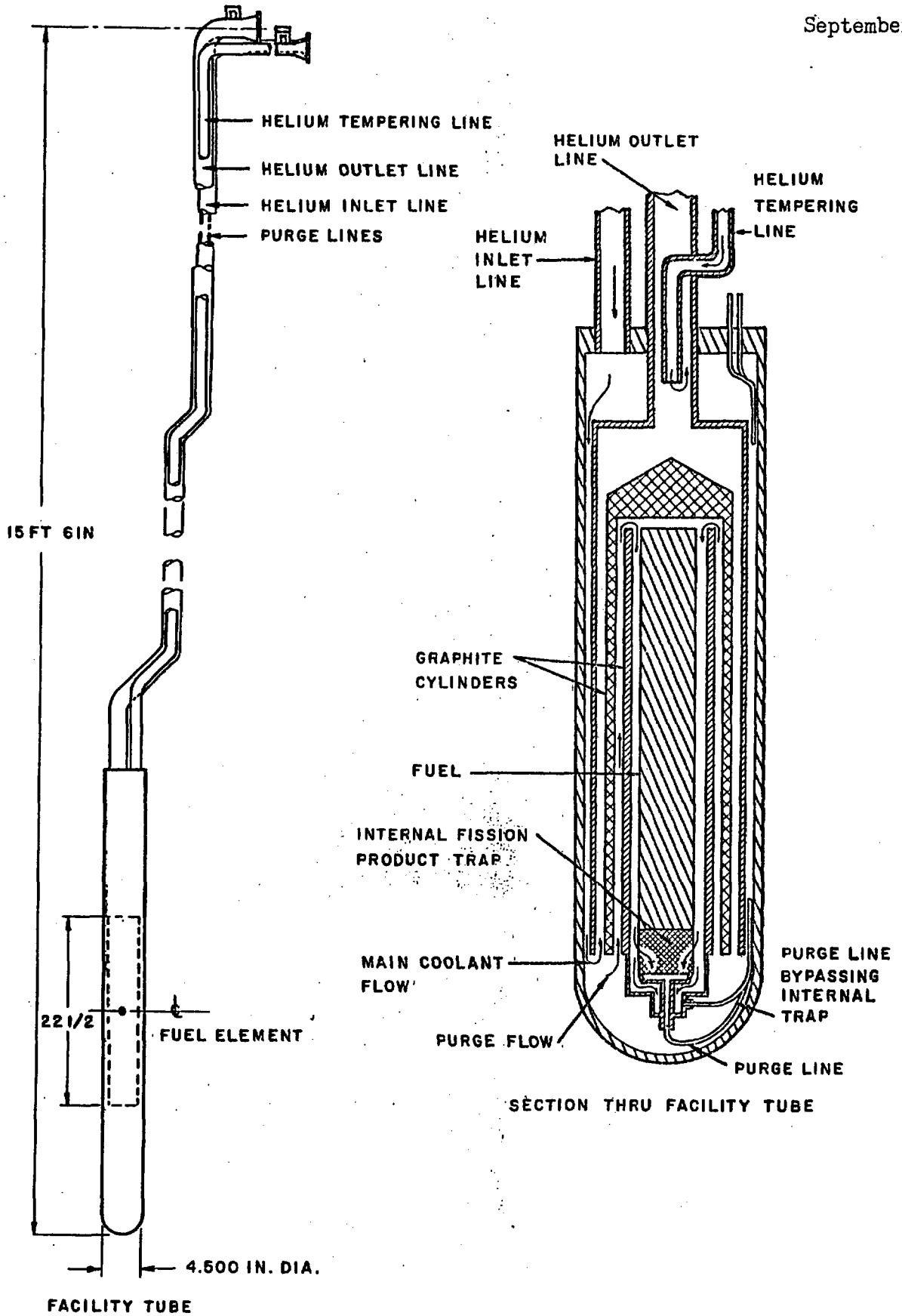

FACILITY TUBE & FUEL DIAGRAM

FIGURE 54

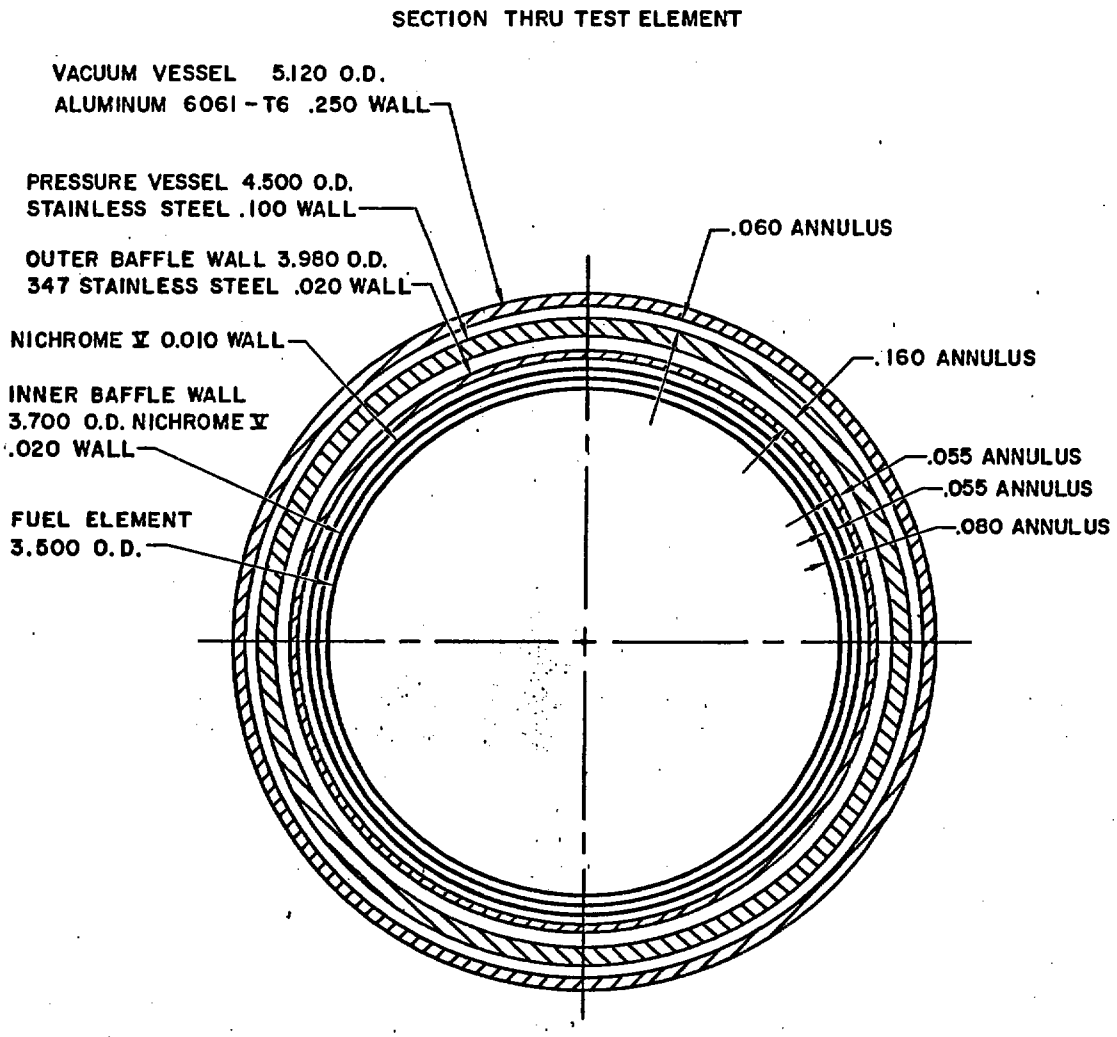
SECTION THRU TEST ELEMENT
VACUUM VESSEL 5.120 O.D.
ALUMINUM 6061-T6 .250 WALL
PRESSURE VESSEL 4.500 O.D.
STAINLESS STEEL .100 WALL
OUTER BAFFLE WALL 3.980 O.D.
347 STAINLESS STEEL .020 WALL
NICHROME V 0.010 WALL
INNER BAFFLE WALL
3.700 O.D. NICHROME V
.020 WALL
FUEL ELEMENT
3.500 O.D.
.060 ANNULUS
.160 ANNULUS
.055 ANNULUS
.055 ANNULUS
.080 ANNULUS

FIGURE 55

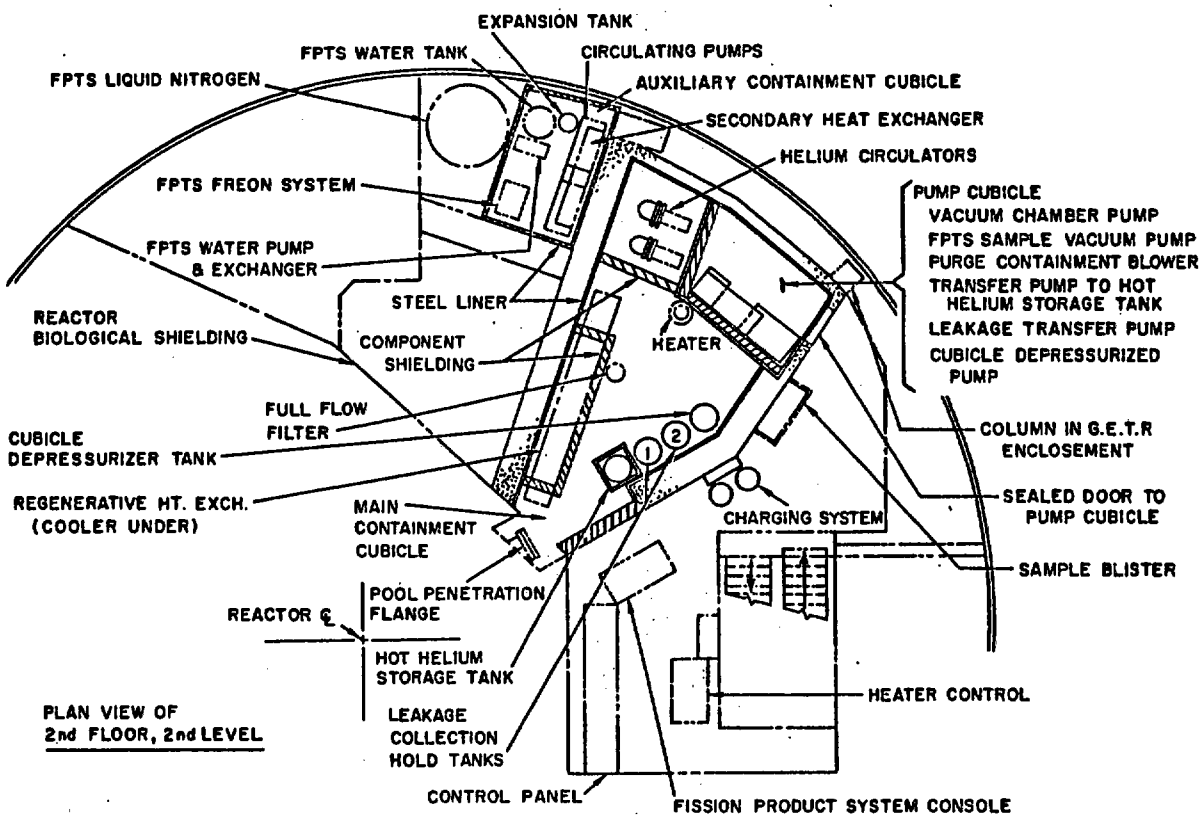
EXPANSION TANK
FPTS WATER TANK
CIRCULATING PUMPS
FPTS LIQUID NITROGEN
AUXILIARY CONTAINMENT CUBICLE
SECONDARY HEAT EXCHANGER
HELIUM CIRCULATORS
FPTS FREON SYSTEM
PUMP CUBICLE
VACUUM CHAMBER PUMP
FPTS SAMPLE VACUUM PUMP
PURGE CONTAINMENT BLOWER
TRANSFER PUMP TO HOT HELIUM STORAGE TANK
LEAKAGE TRANSFER PUMP
CUBICLE DEPRESSURIZED PUMP
FPTS WATER PUMP & EXCHANGER
STEEL LINER
REACTOR BIOLOGICAL SHIELDING
COMPONENT SHIELDING
HEATER
FULL FLOW FILTER
CUBICLE DEPRESSURIZER TANK
COLUMN IN G.E.T.R ENCLOSEMENT
REGENERATIVE HT. EXCH. (COOLER UNDER)
MAIN CONTAINMENT CUBICLE
CHARGING SYSTEM
SEALED DOOR TO PUMP CUBICLE
SAMPLE BLISTER
POOL PENETRATION FLANGE
REACTOR ℄
HOT HELIUM STORAGE TANK
HEATER CONTROL
PLAN VIEW OF 2nd FLOOR, 2nd LEVEL
LEAKAGE COLLECTION HOLD TANKS
CONTROL PANEL
FISSION PRODUCT SYSTEM CONSOLE
OUT-OF-POOL EQUIPMENT

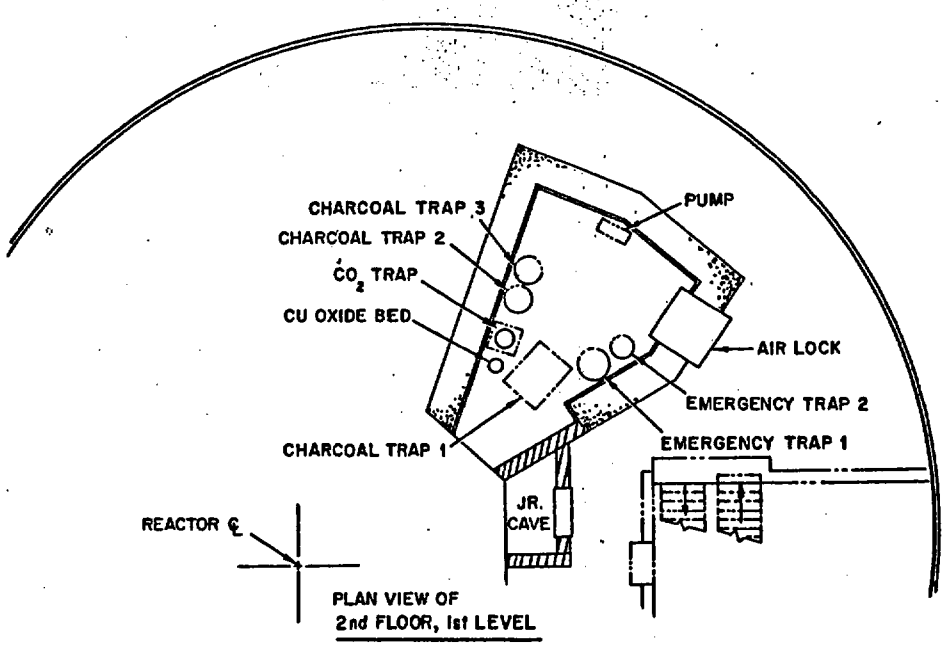
CHARCOAL TRAP 3
PUMP
CHARCOAL TRAP 2
CO_2 TRAP
CU OXIDE BED
AIR LOCK
EMERGENCY TRAP 2
CHARCOAL TRAP 1
EMERGENCY TRAP 1
JR. CAVE
REACTOR ℄
PLAN VIEW OF 2nd FLOOR, 1st LEVEL

FIGURE 56

A	AREA MARKED "A" INDICATES REVISION		
B	AREA MARKED "B" ARE REVISED		
C	AREAS MARKED "C" ARE REVISED		
D	AREAS MARKED "D" ARE REVISED		
E	AREAS MARKED "E" ARE REVISED		

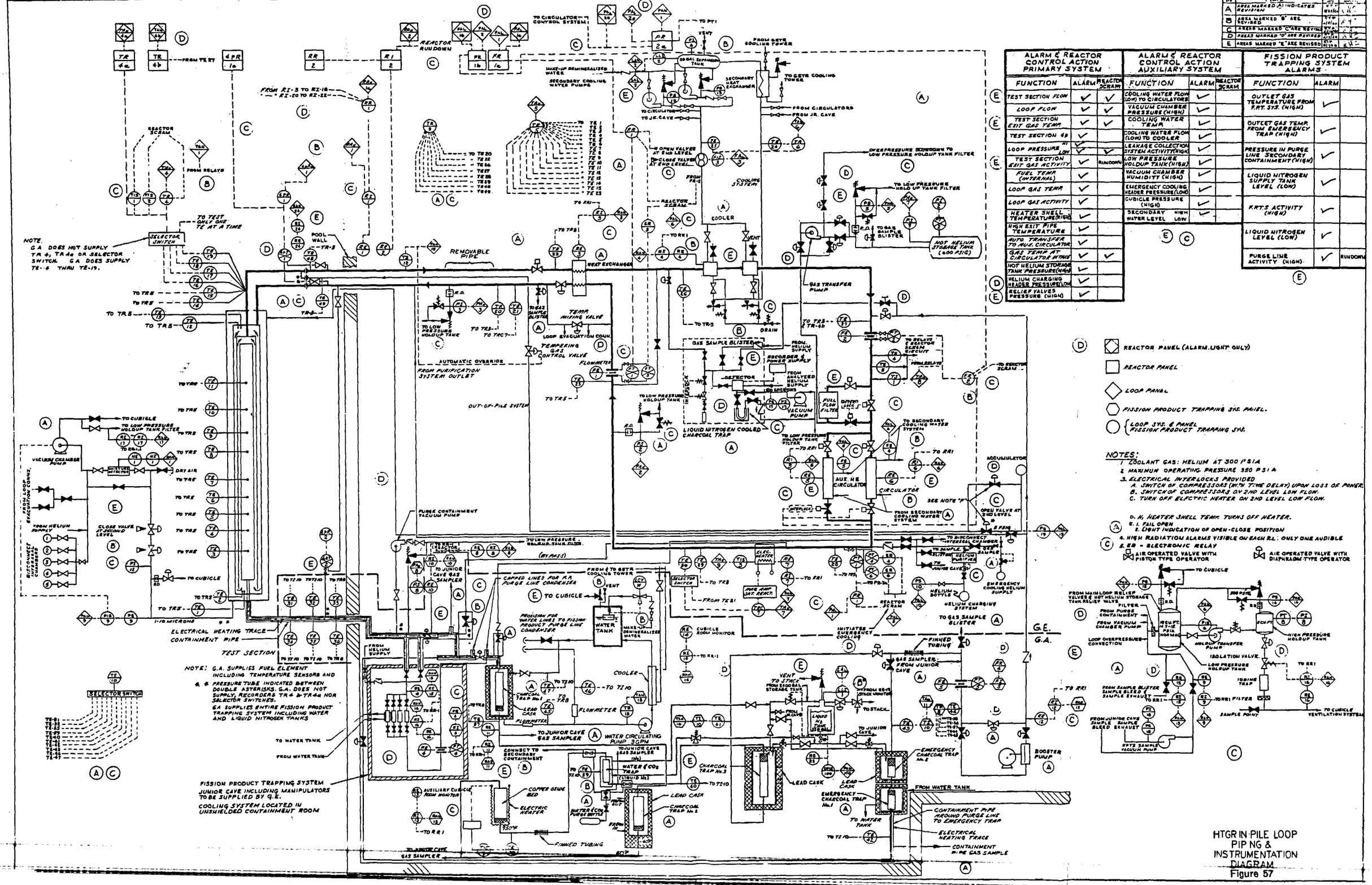

ALARM & REACTOR CONTROL ACTION PRIMARY SYSTEM		
FUNCTION	ALARM	REACTOR SCRAM
TEST SECTION FLOW	✓	✓
LOOP FLOW	✓	✓
TEST SECTION EXIT GAS TEMP.	✓	✓
TEST SECTION ΔP	✓	
LOOP PRESSURE HI	✓	
LOOP PRESSURE LOW	✓	✓
TEST SECTION EXIT GAS ACTIVITY	✓	RUNDOWN
FUEL TEMP. (INTERNAL)	✓	
LOOP GAS TEMP.	✓	
LOOP GAS ACTIVITY	✓	
HEATER SHELL TEMPERATURE (HIGH)	✓	
HIGH EXIT PIPE TEMPERATURE	✓	
AUTO TRANSFER TO AUX. CIRCULATOR	✓	
GAS TEMP. AT CIRCULATOR ATMOS	✓	✓
HOT HELIUM STORAGE TANK PRESSURE (HIGH)	✓	
HELIUM CHARGING HEADER PRESSURE (LOW)	✓	
RELIEF VALVES PRESSURE (HIGH)	✓	

ALARM & REACTOR CONTROL ACTION AUXILIARY SYSTEM		
FUNCTION	ALARM	REACTOR SCRAM
COOLING WATER FLOW (LOW) TO CIRCULATORS	✓	
VACUUM CHAMBER PRESSURE (HIGH)	✓	
COOLING WATER TEMP.	✓	
COOLING WATER FLOW (LOW) TO COOLER	✓	
LEAKAGE COLLECTION SYSTEM ACTIVITY (HIGH)	✓	
LOW PRESSURE HOLDUP TANK (HIGH)	✓	
VACUUM CHAMBER HUMIDITY (HIGH)	✓	
EMERGENCY COOLING HEADER PRESSURE (LOW)	✓	
CUBICLE PRESSURE (HIGH)	✓	
SECONDARY WATER LEVEL HIGH	✓	
SECONDARY WATER LEVEL LOW	✓	

FISSION PRODUCT TRAPPING SYSTEM ALARMS		
FUNCTION	ALARM	
OUTLET GAS TEMPERATURE FROM F.P.T. SYS. (HIGH)	✓	
OUTLET GAS TEMP. FROM EMERGENCY TRAP (HIGH)	✓	
PRESSURE IN PURGE LINE SECONDARY CONTAINMENT (HIGH)	✓	
LIQUID NITROGEN SUPPLY TANK LEVEL (LOW)	✓	
F.P.T.S ACTIVITY (HIGH)	✓	
LIQUID NITROGEN LEVEL (LOW)	✓	
PURGE LINE ACTIVITY (HIGH)	✓	RUNDOWN

HTGR IN PILE LOOP
PIPING &
INSTRUMENTATION
DIAGRAM
Figure 57

1. Macro-Meteorology: Data collection and evaluation from records of five Weather Bureau Class A Stations within an eighty mile radius of the reactor site.

2. Micro-Meteorology: Data collection and evaluation of weather information collected at Holtwood Dam (Approximately six miles upstream of the reactor site.)

3. Site-Meteorology: A main and auxiliary weather station on the reactor site has been established. These stations consist of two towers equipped with aerovane indicators and recorder, matched termisters with recorder, recording rain gauge and hygrothermograph.

4. Macro-Hydrology: Evaluation of data, concerning Susquehanna River flows, Chesapeake Bay area, and Conowingo Pond.

5. Micro-Hydrology: Extensive dye studies are being conducted in the Conowingo Pond at various conditions to determine the flow patterns in the Conowingo Pond.

6. Geology: Core borings have been made on grids at and adjacent to the reactor site covering approximately 390,000 square feet of land area.

7. Seismology: Inquiry made of the Geophysics Division, U. S. Department of Commerce and the Maryland State Geologist, Dr. J. T. Singewald.

8. Radiation Monitoring Program: Applicant has agreed to participate in the Water Quality Network Program conducted by the U. S. Public Health Service. Participation in this program, which is now in operation, consists of using Conowingo Hydro Plant as a sampling station in the USPHS National Network. Quarterly checks will be made at Holtwood Dam to correlate the results obtained there with the results obtained at Conowingo. Since engaging the services of Nuclear Science and Engineering Company as consultants in the environmental radiation monitoring program, the erection of equipment at all sampling locations has been completed in all the stations shown in Table I-11 (Appendix B) and Figure I-9 (Appendix A). The overall environmental radiation monitoring program is summarized in Table I-12 (Appendix B).

As of June 1960 samples have been taken as follows:

Item	Samples
Air particulate	64 (one week's duration each)
Surface water	6
Well water	3
Silt	2
Earth	5
Milk	3 (separate farms)
Shell fish	3 (independent beds)
Cat fish	1 (Conowingo Pond)

approximately twelve miles upstream from Holtwood on the Susquehanna River; the U.S. Weather Bureau Station at Lancaster, Pennsylvania; and a cooperative U.S. Weather Bureau Station at the Police Barracks near Conowingo Dam. A limited amount of surface and upper air information is also available from the Aberdeen Proving Grounds near Aberdeen, Maryland; and water temperatures are recorded regularly at Conowingo Dam.

Only data from Holtwood Dam will be presented herein. Emphasis will be placed upon the wind record. This parameter was analyzed first, since it was expected to exhibit the most obvious differences from the regional climatic averages. Additional information will be developed concerning the diurnal distribution of various wind velocities, the frequency of various intensities of precipitation, and the variability of temperature.

Records at Holtwood Dam were examined for the interval October, 1949 through September, 1954. Wind direction and speed, dry-bulb temperature, water temperature, precipitation, and a description of current weather conditions were obtained four times a day: at 0100, 0700, 1300, and 1900, E.S.T. This constitutes a total of approximately 7,300 hourly observations. The data were hand-punched into IBM cards to facilitate statistical analysis.

Table II-5 (Appendix B), shows the occurrence of wind speed as a function of wind direction. Data are presented for each season, and for the year as a whole. It should be noted that Table II-5 (Appendix B) is identical in form to Table II-1 (Appendix B), which presents comparable statistics for the region surrounding the lower Susquehanna Valley.

The tremondous effect of the Valley on the local wind regime is obvious. As might be expected, a substantial channeling of the wind up and downstream is observed. At Holtwood Dam, the axis of the channel runs approximately 30° west of north. For the year as a whole, down channel winds (from the north or northwest) occur 47% of the time; up channel winds (from the south or southeast) occur 43% of the time. After allowing for the occurrence of calms, winds at a substantial angle to the axis of the channel are observed only 7% of the time. The high frequency of up-channel winds is all the more noticeable since for the surrounding area winds from the southeast were less frequent than from any other direction.

In addition to the channeling of the wind, a slight reduction in wind speed is observed when the data in Table II-5 (Appendix B) are compared with the regional averages. The decrease is not as substantial

and matched thermisters were installed approximately 13 meters above ground elevation and 50 meters above the level of the primary weather station. Output signals are carried by cable to the primary weather station, where the data are recorded. The elevation of the auxiliary weather station would be slightly above the top of a 150-foot stack at the proposed reactor site.

Due to the difficulty of obtaining early delivery of the thermisters and the related recording equipment, the program of observation was not fully under way until March, 1960. Nevertheless, wind records at three levels have been obtained regularly since August 1, 1959.

A program of abstracting local meteorological data from the instrument records was inaugurated on September 1, 1959. Wind, temperature, and precipitation are read from the charts at six hourly intervals: at 0100, 0700, 1300, and 1900 E.S.T. These data are transferred to punch cards. As the number of observations accumulates, pertinent statistical summaries can easily be tabulated. In addition, these cards will be used to relate observations at the reactor site to simultaneous weather conditions at Holtwood Dam six miles upstream, and also to prevailing weather conditions as observed at the five Class A Weather Stations in the surrounding region. While extensive studies of this type cannot be undertaken for some time, due to lack of sufficient local data, they may ultimately be of considerable value in developing satisfactory monitoring and operating procedures. Meanwhile, even a limited amount of data from the site will be of considerable help in interpreting local wind, temperature, and diffusion regimes.

4. Micro-meteorology of the Reactor Site. A great deal can be said about micro-meteorological conditions at the reactor site on the basis of the Holtwood data and a knowledge of the micro-meteorology of other similar locations. It might be expected that at the reactor site the wind direction would be up or down channel a great preponderance of the time, as at Holtwood. However, the local situation is complicated by the fact that here the shore line of the pond is being dealt with, rather than a location out in the channel which is comparatively free from topographic influence. Thus, the local wind regime may be modified by drainage winds which move down Rock Run Creek during periods of nocturnal cooling. Conversely, in the afternoon when the surrounding land is heated more than the water, there may be a stronger component of the wind on shore. The distance to which such on-shore winds may develop and move up Rock Run Creek is not at present known.

The relative temperature of the immediate shore line and the pond will also be of the utmost importance. When the pond is colder than the shore line there will be a tendency for air to subside over the pond and spread out over the bordering land areas. This air will eddy against the hills and return over the channel at higher elevations. When the pond is warmer than the shore line a reverse eddy is to be expected, with rising air over the channel and descending currents along the borders of the channel. Eddies of this type have been observed in many locations. They are described, for example, in a report on meteorological diffusion at Shippingport, Pennsylvania.[3] Cross-channel eddies of the sort described above may be expected to intensify, partially counter-balance, or reverse the direction of the nocturnal katabatic flow down Rock Run Creek.

In addition to these expected and fairly predictable circulations, there will be a host of minor eddies associated with the local topography. The slopes of the hills bordering the pond will heat and cool at different rates, depending on their exposure, vegetal covering, the time of day, the season of the year, the degree of cloudiness, and many other parameters. The eddies set up by this differential heating and cooling will tend to be advected up or down channel by the prevailing winds. The result will be a complex wind structure near the shore line which is not at all similar in detail, at least, to the wind regimes in mid-channel.

The anemometer records at the reactor site should exhibit wind variations substantially greater than those recorded at Holtwood. Although the prevailing up and down channel flow should be discernible, winds at a comparatively high angle to the axis of the pond will be more common. In addition, the average wind speed should be considerably reduced below that observed at Holtwood. A preliminary analysis of anemometer records at the reactor site is contained in Section 5, Page II - 10.

Additional micro-meteorological data pertaining to the reactor site will be accumulated by a careful program of observation and instrumentation. This program is directed toward answering such questions as: (a) To what extent are wind speeds reduced? (b) How frequently is a wind at a large angle to the channel actually observed? (c) What is the intensity and diurnal variation of the drainage wind down Rock Run Creek and the afternoon reverse flow? (d) What is the intensity and rate of development of the cross-channel circulation associated with temperature differences between the pond and the bordering shore line? Quantitative answers to such questions will add to an understanding of the local diffusion process.

3. See Footnote 2, Supra Page II - 4.

5. Preliminary Analysis of Anemometer Records at the Reactor Site. Wind observations at Peach Bottom for the fall of 1959 and the winter of 1960 are summarized in Tables II-6(A), II-6(B) and II-6(C) (Appendix B). The six months of data for each of three observational sites constitute an extremely small statistical sample, which is restricted to the colder half of the year. These data should be used with considerable caution. Nevertheless, it is clear from a preliminary analysis that the wind regimes show many of the attributes expected in advance on the basis of a general knowledge of micrometeorology. As expected, the winds at Peach Bottom are lighter, and show a smaller degree of channeling parallel to the axis of the pond.

The mean wind speed of all three anemometers for the six-month period is 5.3 mi/hr at Peach Bottom, compared to 6.6 mi/hr for the winter and fall seasons at Holtwood Dam. A substantial increase in frequency of calms is noted: 12% at Peach Bottom compared to 4% at Holtwood. This may be due in part to the method of observation. The Peach Bottom anemometer records have been examined visually to estimate the average wind speed over a period of one hour preceding the time of observation. In principle, the data at Peach Bottom and at Holtwood are therefore comparable. However, it is difficult to estimate the averate flow accurately for extremely low wind speeds, and statistics on the frequency of calm conditions at Peach Bottom should therefore be used with caution. It may be noted in this connection that winds of less than 4 mi/hr are observed at Peach Bottom 42% of the time as compared with 36% at Holtwood. These latter statistics may offer a better comparison of the two wind regimes.

The decrease in wind channeling is quite large. At Holtwood, it has already been noted that the wind is almost parallel to the channel or is calm a total of 93% of the time. The comparable figure at Peach Bottom is 61%. This has been accompanied by a substantial angle to the shoreline. On the average the wind is from the west 23% of the time, an order of magnitude larger than the 2% measured at Holtwood.

The prevalence of a large number of off-shore winds, and the comparative infrequency of on-shore flow, may be related to the season of observation. The data in Tables II-6(A), II-6(B) and II-6(C) (Appendix B) are for the cold half of the year only. During the fall and winter months, the pond is generally warmer than the surrounding air. This would naturally lead to a cross-channel circulation with rising air over the pond and off-shore flow at the site. It will be significant to note possible changes in the wind fields during the spring and summer months when the comparative temperatures of the water in the pond and the air are reversed.

A comparison of the three levels of observation at Peach Bottom reveals some interesting results. As might be expected, the anemometer which shows the lowest wind speeds is the one located approximately ten meters above the ground near the shore of the pond. There is surprisingly little difference, however, between the mean wind speed at this station and at the hillside station. The latter anemometer is located only thirteen meters above the ground, but is at an elevation of about fifty meters above the site of the primary weather station. The anemometer recording the highest air movement is the one at thirty meters elevation above the primary weather station.

It is interesting to note that the same trend is not discernible in the number of calms observed. In this category, the smallest number of calms is recorded at the hillside station: 10% for the six-month interval, as compared with 11% at the 30-meter anemometer and 15% at the lowest anemometer. It is questionable whether this statistic is as important as the frequency of occurrence of light winds of less than 4 mi/hr: 42% at the hillside anemometer; 36% at the 30-meter level; and 50% at the lowest level.

There is a steady increase in wind variability with elevation above the pond. At each elevation four of the most frequent observations are winds from the northwest, west, southeast, and calm. The percentage of observations in these four categories total 88% at the lowest level; 82% at the 30-meter level; and 61% at the hillside station. Two comparatively infrequent wind directions are southwest and northeast. The percentage of observations in these two categories is 5% at the lowest level, 10% at the 30-meter level and 23% at the hillside station. Upon proceeding to higher elevations above the pond, the variability of wind speed apparently increases until it eventually becomes comparable to that of the surrounding region. The region of transition seems to extend well below the top of the hills surrounding the pond, since the hillside anemometer is located more than 100 feet below the crest of the hills bordering the pond.

The above comments are developed from inspection of a relatively short period of record. The continuing program of observation will provide a rapidly increasing reservoir of data concerning the micrometeorology of the reactor site.

6. Winds Associated with Period of Precipitation. Before concluding the general discussion of the climatology of the Peach Bottom reactor site and the surrounding region, it will be important to mention briefly the wind regimes associated with periods of precipitation. These data are of particular significance in evaluating rainout as a possible source of contamination of the Conowingo pond and the surrounding area.

Two sets of precipitation wind roses have been prepared: one for the average of five Class A Weather Bureau Stations in the surrounding region, Table II-7 (Appendix B), and one for Holtwood Dam, Table II-8 (Appendix B). Again, four observations a day were considered over a total period of five years. In preparing the wind roses for the region, an observation was included if any one of the five Class A Weather Stations reported precipitation within an hour of the time of observation. In preparing the wind roses for Holtwood Dam, the weather at the single station was used as the deciding factor. A total of 1948 observations in the region was classified as occurring with precipitation. This constitutes about 27% of all observations. On the other hand, only 383 observations were classified as occurring with precipitation at Holtwood Dam. This constitutes only slightly more than 5% of the total number. This discrepancy seems to be somewhat larger than can be explained solely on the basis of the number of stations involved. One probable factor is the absence of an observer at the Holtwood Station, coupled with the fact that the triple-register does not show accumulations of precipitation less than .01 inch.

A wind rose of the regional geostrophic wind direction and speed is shown in Table II-9 (Appendix B); the same parameter for periods of precipitation is shown in Table II-7 (Appendix B). Examination of these tables indicates that periods of rainfall tend to be associated with somewhat higher wind speeds. The increase is approximately four miles per hour. Furthermore, the occurrence of winds of less than four miles per hour is reduced by a factor of two to three. As might be expected, there is an increase in the frequency of geostrophic winds from the east and southeast, and a corresponding decrease in the frequency of winds from the west and northwest. Nevertheless, the occurrence of precipitation is not overwhelmingly associated with a geostrophic wind from any particular direction.

The annual wind rose for periods of precipitation at Holtwood also exhibits a decrease in wind speed from 6.9 to 6.0 mi/hr; compare Tables II-5 and II-8 (Appendix B). The frequency of winds of less than 4 mi/hr is reduced from 40% to 28% and this change is most noticeable during the fall season. It was anticipated that periods of rainfall at Holtwood would tend to be associated with up-channel flow. For all Holtwood observations, the occurrence of down-channel winds is 47%, of up-channel winds 43% and of calms 3%. For the 383 cases of concurrent precipitation, there were 41% down-channel winds, 51% up-channel winds and 1% calm. The increased frequency of up-channel flow is evident, but the association is not as substantial as had been expected.

Probably this condition will be rare. It has been seen that the usual meteorological situation involves a wind up or down channel. Under stagnant conditions when the temperature of the water is high, eddies will tend to form which will carry the stack effluent inland. It is, however, rather unlikely that these eddies will be strong enough, will extend far enough inland, and will have a sufficiently weak return flow to make this situation critical. It may be possible to check this by smoke tests conducted on the site during appropriate weather conditions.

Subject to such verification, it will be assumed that a substantial movement of stack effluents up Rock Run Creek and its tributary will occur only under those rare conditions when the average wind flow is across the channel, almost at right angles to its axis. This might be associated with a synoptic situation for which the gradient wind over the region as a whole is strong from the northeast. Whether or not such an association actually occurs can be determined from climatological studies now under way.

Assume that during a period of approximately 16 hours the wind blows continuously across channel, forcing the stack effluent up Rock Run Creek and its tributary. It may be noted parenthetically that such an extended period of cross-channel flow has not been observed in the five years of record examined at Holtwood Dam. It will also be assumed that the wind speed is sufficiently low and the stability is sufficiently high to prevent movement of the effluent far out of the channel, away from the site boundary.

Under such circumstances a crude estimate of the relative dilution at location C can be obtained from volumetric considerations. The width of the channel is approximately 150 meters; a reasonable length over which the effluent could be spread is of the order of 1500 meters; the depth of the cloud is assumed to be 40 meters; and it is assumed that 50% of the effluent remains within this volume. Finally, the volume is itself reduced 50% on the assumption of a uniform slope towards the channel. On this basis the average relative dilution for the entire cloud would be approximately 6×10^{-3} sec/m^3. For maximum concentrations, this average value must be increased substantially. Perhaps a reasonable estimate of the maximum relative dilution under such circumstances would be 3×10^{-2} sec/m^3. Again, it must be emphasized that this is an order of magnitude estimate only.

One final point needs to be considered. When the source is diffuse, extending from the ground to the top of the secondary containment, conditions will be somewhat modified. There is no object, however, in preparing elaborate computations for this case. Concentrations

if it is assumed that the cloud depth extends to 65 meters and the wind speed is 1 m/sec. This is a reasonable, though probably a conservative, estimate.

No estimate of relative dilution will be made for off-site locations up Rock Run Creek and its tributary under conditions of normal nocturnal inversion. During the night drainage winds probably will occur, moving downward toward the pond. In addition, there is usually at least a small wind component parallel to the channel. These facts would imply that the opportunity for a substantial amount of effluent to move far inland up Rock Run Creek is very low. It might tend to occur only under large-scale meteorological conditions which lead to a cross-channel flow over the entire reservoir. Wind records at Holtwood indicate that a persistent regime of this kind is extremely rare. This possibility need not be considered, therefore, at the present time.

3. Average Relative Dilutions

For investigating the probable effects of accidents at locations which are off-site but in the immediate vicinity of the reactor, it is useful to have estimates of the average value of the relative dilution to be expected at a single point. To obtain such data, relative dilutions associated with normal daytime (unstable) lapse rates are required.

Under lapse conditions it is reasonable to use Sutton's Equation, with $n = 0.20$. A typical value of $\bar{u}$ is 3 m/sec (about 7 mph) directed up or down channel. The values C_y and C_z are assumed to be 0.40 and 0.30 $(\text{meters})^{n/2}$, respectively. These values are one to two times larger than would be expected at comparable wind speeds in regions of low topographic relief -- a ratio smaller than that assumed for stable regimes, since the correction associated with "macro-viscous" effects decreases with increasing instability. These values of meteorological parameters lead to a relative dilution of 10^{-5} sec/m^3 along the axis of the plume at the site boundary ($x = 10^3$m). Due to the strong mixing and to organized vertical circulations, no distinction will be drawn between locations at pond elevation and on slopes bordering the channel.

An estimate can now be obtained of the relative dilution at a point near the pond at the site boundary under "average" weather conditions. If a typical nocturnal regime yields a relative dilution of 3×10^{-4} sec/m^3, and a typical daytime regime yields 10^{-5} sec/m^3, a reasonable average value would be about 2×10^{-4} sec/m^3 if the plume were always oriented in the same direction. This takes into account the fact that nocturnal relative dilutions will occasionally be substantially

by the year 2000 the demand for water in Baltimore City and its environs will have increased to the point that Baltimore's upland sources will have to be supplemented, more or less continuously by water drawn from the Susquehanna River.

F. Conowingo Pond Circulation and Displacement Time

The circulation and mixing and the displacement time of water in Conowingo Pond are the primary hydrologic factors governing the concentration of non-conservative contaminants that might be discharged or washed into the pond or might fall out over its surface. Since relatively little is known concerning the displacement and mixing of waters in Conowingo Pond and the upper Chesapeake Bay special studies are now being conducted to provide additional information. This work is directed, therefore, toward answering questions regarding the dispersion and movement of any contamination which might enter the reservoir at the Peach Bottom site. Field data required to answer some of the questions concerning thermal structure and circulation in the Pond are being gathered under a research program conducted by the Chesapeake Bay Institute (CBI) of the John Hopkins University. Also considerable data already exist on salt distribution in the upper bay.

The following is a brief discussion of the additional field program, as well as of the analytical work being carried on specifically for the purpose of predicting the distribution of any low level activity which might be regularly discharged with the condenser water, and the impact of an accidental release of activity into or over the reservoir.

The additional field data being collected over and above that contemplated in the Conowingo Pond study by CBI involve for the most part tracer dye studies and additional current studies.

This program involves five separate weeks of field work, two which were completed during the summer of 1959 and a third completed in the spring of 1960. In the summer of 1959 observations were taken during periods of maximum thermal stratification and low river flow, while in May of 1960 high flow conditions (average of about 100,000 cfs for a five day period) and only slight vertical temperature gradients prevailed. Additional observations in the River and upper Chesapeake Bay below Conowingo Dam may be required.

During each of these week-long survey periods a fluorescent dye, Rhodamine B Extra, is introduced into the pond near the Peach

Bottom site. The time-spacial distribution of concentration of the tracer material is then determined. The choice of Rhodamine B Extra as the tracer material results from an extensive search for a fluorescent material which has an excitation and fluorescent spectrum suitable for rapid field measurement of concentration without interference from naturally occurring fluorescent materials or from suspended materials. The wave length of 5460 Å which excites Rhodamine B Extra to maximum fluorescence does not measurably excite natural fluorescent organic materials and is much less scattered by the fine suspended material than would be the case for exciting light of shorter wave length. Suitable filters are available to effectively separate any scattered fraction of the exciting wave band from the wave band of maximum fluorescence which is centered at 5850 Å. Using a portable fluorimeter, it is possible to detect this tracer material down to a concentration of 3×10^{-5} ppm in the field, even under conditions of varying background, fluorescence, and turbidity.

Based upon present knowledge of diffusion in a flow pattern such as exists in Conowingo Reservoir, it is estimated that the probable concentration,in ppm, just upstream from the dam at the center of the diffusing volume, will be approximately equal to 2×10^{-5} times the number of pounds of dye introduced near the Peach Bottom site. Thus, with a release of 50 lbs, the peak concentration in the diffusion volume after travel down-reservoir to the vicinity of the proposed Baltimore City intake will be about 1×10^{-3} ppm. Since 3×10^{-5} ppm can be detected and 1×10^{-4} ppm can be measured to an accuracy of about 10%, the vertical and horizontal distribution about the center of the diffusing volume should be readily obtained by this technique all the way to the turbine intakes. Auxiliary observations would include the temperature and conductivity distribution in the reservoir as well as current observations using free drifting drogues.

The data obtained on the special field surveys outlined above, together with data collected under the CBI study, is being analyzed to provide estimates of the distribution of any contamination which might be released into the reservoir from the plant site , for several selected indicator conditions of stratification and river flow. The manner in which any activity would be carried through the reservoir and into the upper bay will be evaluated from the field data.

The experimental data collected in the summer of 1959 involves time and space distribution of concentration from an instantaneous release of a contaminated volume. In the spring of 1960 a continuous discharge over a period of 102 hours, which was sufficient to establish a steady state distribution, was completed.

A picture of the concentration distribution in time and space in the pond which would result from a nearly instantaneous release of a given amount of activity for three representative stratification and flow conditions will result from the analytical studies. In addition, the steady state distribution in space for a continuous discharge at a given rate, for the same three river flow conditions, will be calculated.

Salinity information already available from CBI will be utilized to determine the pertinent mixing parameters for computation of the likely distribution of activity in the upper bay resulting from an accidental release from the plant site.

G. Preliminary Estimates of Dispersion in Conowingo Pond

The data collected to date on the above described field program is being analyzed, although some field observations remains to be obtained. A study of the material available does allow an estimate of dispersion within Conowingo Pond to be made, using approximate solutions to the pertinent advective-diffusive equations.

This study is restricted to conditions relatively unfavorable to rapid dispersion to the pond. In summer thermal stratification develops which greatly restricts vertical mixing. Much of the vertical extent of the pond is therefore not available as dilution water for radioactive materials which might enter the pond.

Consideration is given to three different cases involving discharge of radioactive materials to the pond. First the case of a nearly instantaneous release of activity into the pond at the condenser outfall is considered. Such a release might occur as a result of the accidental rupture of a tank containing collected "drips", or in some other manner not specified here. The local volume contaminated by such a release will move downstream with the flow, and will diffuse into an ever-increasing volume with ever-decreasing concentrations. The time-space variations in concentration about the center of the horizontally dispersing volume after release in a medium of infinite horizontal extent can be expressed by:

$$C(r, t) = \frac{M}{2\pi D P^2 t^2} \exp\left[-\frac{r^2}{2P^2t^2}\right] \qquad (1)$$

where C (r, t) is the concentration at distance $\underline{r}$ from the center of the contaminated volume at time t; $\underline{M}$ is the source strength; $\underline{D}$ the thickness of the layer in which vertical mixing is restricted by thermal stratification; and $\underline{P}$ is a constant "diffusion velocity".

The Conowingo Pond of course is not of infinite horizontal extent. The boundary conditions at the sides of the pond can be satisfied by reflecting the above solution from the shores. This is accomplished by considering the dispersion from two pseudo sources which are located as mirror images of the true source on land on either side of the pond, and adding the contribution from all three sources.

For present purposes the pond is considered as having a rectangular surface area, 1,500 meters wide and 15,000 meters from the source to the dam. Designating the velocity, directed toward the dam as $\underline{U}$, the distance from the west shore to the point of release as $\underline{a}$, and the distance from the point of release to the east shore as $\underline{b}$, equation

(1) becomes, in a rectalinear coordinate system with the x-axis directed downstream and the y-axis laterally across the pond, centered at the point of release and positive toward the east shore:

$$\frac{C}{M} = \frac{1}{2\pi D P^2 t^2} \exp\left[-\frac{(x-Ut)^2}{2P^2t^2}\right] \left\{\exp\left[-\frac{y^2}{2P^2t^2}\right] + \exp\left[-\frac{(y-2a)^2}{2P^2t^2}\right] + \exp\left[-\frac{(y^2+2b)}{2P^2t^2}\right]\right\} \tag{2}$$

Here the condition of reflection at the side boundaries has been included.

The source is not a true point source, since mechanical dilution will have occurred within the condenser discharge prior to release. The fact that there is thus a finite, rather than a theoretical infinite, initial concentration may be treated by introducing a pseudo time correction which represents the time which would have been required by natural dispersion to reduce the concentration to the actual initial concentration. If V_c represents the volume of condenser discharge which has been mechanically mixed with the source prior to release, then the initial concentration is simply $C_o = M/V_c$. The pertinent form of equation (2) is

$$\frac{C}{C_o} = \frac{t_o^2}{(t+t_o)^2} \exp\left[-\frac{(x-Ut)^2}{2P^2t^2}\right] \left\{\exp\left[-\frac{y^2}{2P^2t^2}\right] + \exp\left[-\frac{(y-2a)^2}{2P^2t^2}\right] + \exp\left[-\frac{(y+2b)^2}{2P^2t^2}\right]\right\} \tag{3}$$

where the time correction term, t_o, is given by

$$t_o = \frac{1}{P}\sqrt{\frac{V_c}{2\pi D}} \tag{4}$$

The ratio of concentration, in curies/m^3, to the amount of activity released, in curies, has been computed from equations (3) and (4) for the following conditions:

(a) Flow and vertical mixing are considered to be restricted by thermal stratification to a layer 5 meters thick (i. e. D = 5 meters).

(b) The flow is taken at 5,000 cfs (case 1a) and at 50,000 cfs (case 1b).

(c) The volume V_c of condenser discharge initially mixed with the contaminant is taken as $2 \times 10^3 m^3$. Note that the choice of this parameter is important only in the early stages of dispersion.

(d) The diffusion velocity, P, is taken at 3×10^{-3} meters/sec. Preliminary evaluation of the dye release data from the summer of 1959 indicate that the diffusion velocity under conditions of relatively low flow and consequent hydro-power peaking discharges from the reservoir is about 7×10^{-3} m/sec. The data obtained from the continuous dye discharge made in May, 1960, under conditions of a steady discharge through the turbines as well as some spill through the flood gates, with a total flow averaging about 100,000 cfs, gives a preliminary estimate for P of between 2×10^{-3} and 3×10^{-3} m/sec. It appears quite definite that the large scale eddy motion set up in the reservoir in summer by the peaking discharge patterns is a very effective contributor to dispersion, and under these conditions the diffusion velocity, P, is larger than under conditions of high continuous flow through the reservoir. The value of 3×10^{-3} m/sec selected for P for these computations thus appears applicable to the case of 50,000 cfs discharge, but is conservative by at least a factor of two for the low flow case.

(e) The point of release is taken at 500 meters from the west shore.

Conditions (a) and (b), together with an assumed constant width of 1,500 meters, provide the information that the center of the dispersing contaminated volume would reach the vicinity of the Baltimore water intake in about 10 days for case (1a) and in about one day for case (1b).

Table III-6 (Appendix B) lists the computed ratios of concentration to the amount of activity discharged as a function of relative position about the center of the diffusing volume for 12 hours, 1 day, 5 days, and 10 days. Here $x' = x - Ut$, and hence $x' = 0$, $Y = 0$ is the center of the contaminated volume. For case (1a) x' is located about 750 meters below the discharge point at 12 hours, 1,500 meters downstream at 1 day, halfway to the dam at 5 days, and at the dam in 10 days. For case (1b) the center is located one halfway to the dam at 12 hours, and at the dam at one day. The distribution appears to extend downstream from the dam as if the reservoir continued on downstream.

The second case for which initial computations have been made is for a continuous discharge of activity with the condenser cooling water. This might be a normal operating condition, in which case the amount released would presumably be kept at very low levels, or it might be a temporary condition resulting from a slow leak.

The pertinent equation for a continuous point source, having a strength per unit time of Q_r, discharged into a current U along the x-axis, is given by:

$$C(x,y) = \frac{Q_r}{2\sqrt{2\pi}\,DP\,(x^2+y^2)^{1/2}} \exp\left[-\frac{U^2y^2}{2P^2(x^2+y^2)}\right]\left\{1+\Phi\left(\frac{xU}{\sqrt{2}\,P(x^2+y^2)^{1/2}}\right)\right\} \quad (5)$$

Again, this equation must be reflected at the east and west shores in order to satisfy the side boundary conditions. If the solution is applied only to distances of 1 km or more downstream, the point source assumption is reasonably valid.

Equation (5) has been utilized to compute the steady state distribution of the ratio C/Q_r for the following conditions:

(a) The mixing and flow is restricted by thermal stability to a layer 5 meters thick;

(b) the velocity U is taken at 2×10^{-2}m/sec corresponding to a flow of 5,000 cfs.

Table III-7 (Appendix B) lists the values of the ratio C/Q_r for these conditions at selected values of the lateral coordinate from -5×10^{-2}m (the west shore) to $+10^3$m (the east shore) and for selected vales of the longitudinal coordinate downstream to a distance 10 kilometers below the outfall. The location of the outfall again was assumed to be 500 meters from the west shore and 1,000 meters from the east shore. As a result of the effects of the side boundaries, the distribution becomes uniformly spread out across the pond fairly rapidly in the downstream direction.

In the lower pond the concentration will become simply that which would result from complete mixing of the steady rate of discharge of material with the assumed steady inflow of fresh water. Thus, with the assumed flow, (Q_f), of 5,000 cfs (141 m^3/sec), the final steady state concentration would be given by:

$$C = \frac{Q_r}{Q_f} = \frac{Q_r}{141}$$

or the ratio C/Q_r is given by

$$C/Q_r = 7.1 \times 10^{-3}$$

for C in curies/m^3 and Q_r in curies per second. It is seen from Table III-7 (Appendix B) that this concentration has been nearly reached 10 kilometers below the discharge point.

In both cases treated above, the flow and mixing were assumed to be restricted to a layer 5 meters thick, though no condition was placed on the actual depth at which this layer occurred. In the upper end of the pond the five meter interval would extend from the surfact to the bottom. However, at about 10 kilometers above the dam, the depth changes relatively rapidly. The depth interval within which the flow will be contained depends on the temperature of the waters in the upper end of the reservoir and on the thermal stratification in the lower pond. Studies to date indicate that under various combinations of weather history the later which flows through the lower pond and out through the turbines may occur in almost any depth interval from surfact to bottom. The values of dilution ratio given in Tables III-6 and III-7 (Appendix B) then apply to the 10 meter layer within which the flow is confined, which may occur at any depth dependent on the previous and current weather situations.

The third case treated is that of washout of activity, which had previously been released to the atmosphere, onto the surface of the pond in direct rainfall. The initial distribution of washout on the surface is assumed to be that described in the meteorological section for the case of an inversion with low wind velocities up or down the canyon containing the pond. The surface concentration of activity, in curies per unit surface area, is related to the distance up or downstream from the atmospheric source by the relationship

$$\zeta = \zeta_o e^{-\alpha |x|} \tag{6}$$

where ζ_o is the maximum washout concentration, and occurs at the locale of the source. For the particular meteorological situation assumed, α has a value of about $2.5 \times 10^{-4} m^{-1}$.

In order to treat the dilution of this surface source of varying concentration along the pond, a modified form of a line source equation for diffusion has been utilized. The concentration $\underline{C}$ at a distance $\underline{x}$ from an instantaneous line source of total strength $\underline{M}$ and confined length $\underline{l}$, a time $\underline{t}$ after release, is given by

$$C = \frac{M}{\sqrt{2\pi}\, DlPt} \exp\left[-\frac{x'^2}{2P^2t^2}\right] \tag{7}$$

ENVIRONMENTAL RADIATION SAMPLING STATIONS

PEACH BOTTOM ATOMIC POWER STATION
PHILADELPHIA ELECTRIC COMPANY

FIGURE I - 9

VI. (Cont'd) Page

C. Liquid Effluents VI - 4

D. Solid Wastes VI - 7

VII. PLANT SAFETY ANALYSIS

A. Introduction and Summary VII - 1

B. Incidents Involving the Reactor VII - 2

C. Incidents Involving the Fission Product Trapping System VII - 20

D. Safety Considerations Relating to Fuel Handling VII - 31

E. Plant Behavior Under Abnormal Conditions Arising External to the Plant VII - 37

F. Environmental Consequences of Accidents VII - 40

APPENDIX A - Figures

APPENDIX B - Radioactive Inventories

APPENDIX C - Calculations of Core Heat-Up Following Loss of Normal Cooling

APPENDIX D - Steam Generator Tube Rupture Calculations

APPENDIX A (Cont'd)

FIGURES

*Figure D-1 - Effect of Steam Addition on an Isolated Helium Coolant Loop and Dump Tank System

*Figure D-2 - Effect of Steam Addition on Unisolated Helium Coolant Loop and Dump Tank System

*Figure D-3 - Transient Steam and Water Quantities Following Rupture of Helium Coolant System and One Steam Tube

* Located in Appendix D

made so that an annealing system can be installed if it should later prove to be necessary. The provision which is being made is the inclusion of blind flanges on both sides of the compressor discharge valves. The flanges can be removed and an electrical heating system can be located between the flanges. By use of this heating system, the gas temperature can be raised from 633 F (compressor discharge temperature) to approximately 850 F. The piping layout and the clearances between the pressure vessel and the shielding are being designed to accommodate thermal expansions consistent with an 850 F annealing temperature.

Coupons from the steel plate used in making the pressure vessel will be located within the vessel and removed periodically to provide an early check on radiation damage. Should these coupons indicate a faster trend toward embrittlement of the vessel than expected, then the vessel can be annealed before a dangerous situation develops.

The criterion for prevention of embrittlement of the vessel steel is to limit the rise in transition temperature to 100 F by setting a minimum temperature for the vessel wall during operation. The minimum wall temperatures during reactor operation required to satisfy this criterion are shown in Figure 46.

7. Control Rods and Drives

a. Introduction and Summary

The 40 MW HTGR will normally be controlled by 36 control rods each worth about .006 Δk reactivity on the average, the maximum rod worth being about .010 Δk. Each control rod will be driven by a control rod drive which, for scram purposes, will be a self-contained system not dependent on any external equipment other than the supply of a scram signal in the form of interruption of an electric current.

The control rod absorbers will be made of a refractory material, boron-carbide-loaded graphite, supported on a gas-cooled metal support tube.

8. Control Rods and Control Rod Drives

a. Control Rods

The present reference design, which is shown in Figure 6, consists of six boron carbide loaded carbon cylinders, each about 13-1/2 inches long, supported on a center support rod made of type 321 stainless steel. The concentration of boron in the carbon is in the range 20-30 per cent by weight, the boron existing as uniformly dispersed particles of boron carbide of diameter less than 50 microns. The support rod is flexibly jointed by knuckle joints located approximately every 15 inches along the length of the rod to provide flexibility in the control rod. This flexibility allows for any misalignment which may be introduced by differential thermal expansion and/or reactor vessel manufacturing tolerances. Within the reactor, the control rod slides in a graphite guide tube of about 3-1/2 inches O. D. by 2-1/2 inches I. D. by 12 feet long.

The control rod is connected to its drive unit by means of a push rod. The control rod is held to the push rod by means of a mechanical latch which can be released only by first opening the casing of the control rod drive and removing the power unit. Conversely, reattachment of the power unit to the drive is not possible with the latch open. Subsequent to the removal and reattachment of a control rod, correct operation of the latching mechanism is established by using the fuel transfer machine (Page II-18) to check that the control rod cannot be lifted. The control rod guide tube is held to the core grid plate by means of another mechanical latch.

It should be noted that the absorber material does not slide in contact with the guide tube since the outside diameter of the absorber material is less than the outside diameters of the knuckle joints. Possible adverse effects of impacts which might arise as a result of small amounts of play in the knuckle joints will be avoided by limiting the downward acceleration of the control rod to less than one g under all normal circumstances, including deceleration at the end of the scram stroke.

An alternate design for the control rod is under investigation simultaneously with the reference design described above. The alternate design, Figure 6A, involves the use of a small diameter support rod constructed of a high-temperature alloy. The necessary degree of flexibility of the control rod as a whole would result from the low flexural rigidity of the small diameter support rod.

Cooling of the control rods will be accomplished by diverting a small fraction (2% to 5%) of the helium coolant flowing through the core into the control rod guide tubes. The coolant enters the guide tube through holes in the region below the core grid plate, and divides into two parallel flow paths: a portion flows upward in the space between the guide tube and the control rod itself; the remainder flows downwards and enters the control rod support rod at or near its bottom, regardless of the position of the control rod. This latter coolant then flows upward within the control rod, cooling the support rod in the process. All of the control rod coolant discharges from the top of the guide tube into the plenum chamber above the top of the core, mixing with the main coolant stream at that location. Figure 6B shows the coolant flow pattern for the two limiting cases of a control rod fully inserted and fully withdrawn.

The division of control rod coolant flow between the paths inside and outside the absorber will vary with control rod position. When a control rod is fully inserted, the majority of its coolant will flow through the metal support rod, and its calculated maximum temperature under normal full power operation is close to 1000 F. If there were a reduction in primary coolant flow through the core, then there would also be a reduction of coolant flow through the control rods and their support rods. Such reducations in primary coolant flow are discussed in detail on page VII - 5, Section C.1. Since under reduced coolant flow the reactor would be scrammed immediately, the resulting rise in temperature of the control rod support rods would be negligible.

In the highly unlikely case of complete loss of coolant flow the following sequence of events would occur: the reactor would be scrammed immediately; as a consequence of the stored heat in the fuel elements the temperature equilibration radially across the fuel elements would result in an approximate maximum surface temperature of 3000 F in about three minutes for the hottest fuel elements (see page VII-6, Section C.2.); the control rods and therefore their support rods would overheat as a consequence, resulting in failure of some support rods after a few minutes time. Nevertheless, the control rods could not drop out of the reactor. Such a failure in any of the control rods would occur at a point within the rod more than 3 feet above the core grid plate and the control rod is held in place by its push rod and guide tube. Only in the incredible case of a subsequent failure of the push rods could the control rods leave the core. Such subsequent failure of the push rods would require this complete loss of coolant flow to prevail for many hours, a condition which is considered incredible with the separate parallel cooling circuits and multiple backup power sources.

Subsequent to any occurrence of reduced coolant flow the reactor operating procedure will specify a mandatory inspection of control rods to determine the extent, if any, of the damage which may have occurred. It should be noted that the fuel handling equipment is designed to remove a control rod and its guide tube together as one assembly, and that either a periscope or a television system will be provided for inspecting reactor core components within the reactor after shutdown.

The design of the control rod support will be selected in the winter of 1960-61, and the control rod will be test operated in hot helium, together with the prototype control rod drive, during the period May 1961 through April 1962, as detailed in Section II, Part L.

Both designs for the control rod presently being considered involve the use of uncanned boron carbide in carbon. The irradiation program now under way to determine the irradiation stability of this material is also described in Section II, Part L.4.

b. Control Rod Drives

(1) Mechanical Design

The present reference design for the control rod drive is based on a system utilizing an axial piston type hydraulic motor with hydraulic fluid as the prime mover for both the regulating and scram functions.

Figure 6C illustrates schematically the mechanical and hydraulic arrangement and circuitry of the drive. The system is comprised of the following major components: an outer containment or pressure shell, terminating at, and integral with, the pressure vessel; a screw actuator mechanism supported and contained within a tubular shell, co-axially fitting inside the pressure shell; a hydraulic power unit attached to the lower extremity of the pressure shell; a push rod arrangement, with its lower end attached to the screw actuator mechanism and the upper end attached to, and supporting, the control rod absorber element.

The outer pressure containment is essentially one continuous tubular member, welded to the bottom of the reactor vessel, with the power unit attached to the lower end by means of a mechanically sealed service disconnect, all of which forms a completely sealed unit. In the biological shield region the outer containment diameter is increased by means of a bolted on sleeve of a high nickel steel material. It provides a step configuration to the air gap between the drive containment and the concrete shield clearance hole for the purpose of reducing neutron streaming through this void.

The linear actuator portion of the drive is supported and packaged within a tubular member, fitting co-axially within the outer pressure shell. The purpose of this arrangement is to provide a convenient means of removing and servicing the mechanism without disturbing the outer drive containment. The ball-nut and lead-screw are located within this support tube. The screw is retained and supported by a combination of radial and thrust bearings at the lower end. The recirculating ball-nut is attached to the lower end of a hollow push rod. The push rod is splined or keyed to the support tube to restrain the nut against rotation. Rotation of the screw will thus cause the ball-nut to translate in an axial direction raising or lowering the hollow push rod.

At the lower end of the actuator, a rod backstopping device is located. It is a cam type self-energizing mechanical clutch that is torque and direction sensitive. The screw is splined to the clutch output end, and the external case of the clutch is keyed to the support tube. Torque applied to the input end is transmitted unrestricted to the screw in either direction. However, torque generated from the output or screw end is positively blocked at the clutch. The purpose of this device is to prevent the control rod from drifting downwards in the case of failure of the hydraulic motor. It also restrains the screw from rotating when the motor unit is detached for servicing.

Normally, the entire drive containment including the hydraulic power unit is pressurized with helium at a pressure slightly above reactor pressure. During removal of the hydraulic power unit for service, pressure is retained in the actuator containment region by means of a rotary seal between the screw and support tube, and a static seal arrangement between the support tube and outer shell.

The lower end of the support tube is anchored to an adjustment device that will allow raising and lowering of the entire actuator mechanism, independent of ball screw actuation. The purpose of this adjustment feature is to provide a means of actuating the latches that connect the absorber portion of the control rod to the drive.

A hydraulic power unit is attached to the lower end of the outer pressure shell. Connection is made by a gas tight mechanical joint that is readily separated for servicing. The power unit consists of an outer pressure shell containing a hydraulic motor, a deceleration valve, a gear and mechanism arrangement to actuate the deceleration valve, and a gear drive to actuate position transmitters, limit switches, etc.

Below and external to the pressure shell, but part of the power unit, is an integral valve and manifold assembly. This consists of flow control valves, a directional regulating control valve and a scram control valve. Flow connections between valves are accomplished by ported sub-plates that anchor and support the valves. Replaceable static seals between valve mounting faces and sub-plates effectively eliminate fluid leakage. Attached to the bottom end of the valve manifold or sub-plate is a piston type hydraulic accumulator.

The basic hydraulic drive circuit, its principle of operation and associated components are also schematically illustrated in Figure 6C. The hydraulic motor is of the axial piston type. External fluid leakage from the motor is prevented by a double shaft seal arrangement, where the volume between the seals is vented to the external oil reservoir. The motor shaft is splined to the input end of the rod backstopping clutch. The position transmitters, limit switches, etc., are driven by gears connecting to the motor shaft. In a similar fashion, the deceleration valve actuator is driven. This gear train will be of rugged design, capable of absorbing full motor output in a jammed or stalled condition without damage.

The hydraulic motor provides two modes of control rod operation: normal, controlled regulation at a relatively slow speed, and rapid insertion at high or scram velocity. This is accomplished by running the motor at two different flow rates. Regulating motion is controlled by restricted low volume delivery ports and externally controlled directional valving. Scram is controlled by large high volume delivery ports, a one-directional control valve and a deceleration valve.

The deceleration valve throttles the flow of oil leaving the hydraulic motor during the last two feet of rod insertion travel. The mechanical drive between the motor and this valve progressively closes the fluid exhaust orifice so as to bring the rod velocity down to zero with less than 1 g deceleration.

Regulation is accomplished by a two direction, three position control valve. In the de-energized or null position all ports are blocked. Valve position will be determined by either electric solenoid actuation or electric closed loop servo control.

Scram will be controlled by a spring offset two position valve. During normal rod operation, this valve is held in the closed position by an energized solenoid. De-energizing the solenoid shifts the valve into the open or scram position. The energy for performing the scram function is stored in the form of an inert gas charged hydraulic accumulator. A piston type accumulator is used in order to monitor stored fluid supply volume by instrumenting the approximate position of the piston. In addition, gas and fluid pressure will be monitored as well as the presence of fluid in the gas volume region.

The hollow push rod, its lower end attached to the ball-nut, terminates at the top in the form of a mechanical latch. This latch connects to the upper solid push rod. Referring to Figure 6C, the latch operates as follows. To disconnect this latch, the control rod is fully withdrawn and the power unit removed to provide access to the lower end of the actuator support tube. The support tube is anchored to a vertical adjustment fitting. This fitting is manipulated to cause the support tube to descend a fixed distance. This allows the nut and hollow push rod to drop down below the normal lower stopping point. This also pulls the latch down to a position where latching balls "A" will align with groove "B". Retainer sleeve for balls "A" will seat against a shoulder of the outer tube, causing balls "A" to cam out into groove "B", while the remainder of the latch mechanism continues downward an additional slight amount until balls "C" align with groove "D". This allows the hollow push rod to separate from the upper solid rod. The solid rod is prevented from dropping out by the previously mentioned step in the outer tube.

The top of the solid push rod terminates in the form of a mechanical latch that connects to the absorber portion of the control rod. Again referring to Figure 6C, the latch operates as follows. To disconnect this latch the control rod is fully inserted. As in the operation of the lower latch, the power unit has to be removed to provide access to the actuator support tube adjustment device. In this case, however, the support tube is raised above its normal position. The adjustment screw is rotated manually to raise the nut and push rod above its normal upper stopping point. This raises the latch assembly to a point where balls "E" align with groove "F" and cam outward allowing the push rod section to continue further. Push rod movement continues until balls "G" align with groove "H", and the shoulder of the push rod seats against the bottom of the ball retainer sleeve. An upward movement of the control rod will then cam balls "G" into groove "H" and allow its complete separation from the push rod.

To assure that all mechanical latches are engaged upon reassembly of a drive unit, the position of the actuator support tube is mechanically interlocked to the power unit attachment. In other words, it is impossible for the power unit to be secured in place unless the actuator support tube is in its normal operational position.

The control rod and graphite guide sleeve are designed to be removed together as one unit. With reference to Figure 6C, it will be noted that the guide sleeve seats in a universal type swivel joint. The sleeve is anchored to this joint by a bayonet pin type connection. Removal requires a small rotary motion applied to the guide sleeve by the fuel transfer machine. This disengages the bayonet locking pins and allows vertical withdrawal.

(2) Operation

The operating principle of the drive system is as follows. The drive and mechanism region inside the outer pressure shell is pressurized with buffer helium to a pressure slightly above reactor pressure. This serves two functions: it provides a balancing force to counteract the downward force exerted on the control rod by reactor pressure; and it provides a means of preventing fission products from the reactor entering the drive region by maintaining a flow of buffer helium from the drive containment to the reactor vessel.

Figure 6C illustrates the basic hydraulic equipment of the drive unit. Fluid pressure for normal regulation or controlled movement of the rod is supplied by auxiliary equipment, external to the sub-pile room and not shown in the figure. (This external pump system also maintains the scram accumulators at proper volume and pressure.) Upward and downward movement is determined by the spool position of regulating control valve "K". The present plan is to have a group of the centrally positioned rods in the core actuated by a closed loop electric servo control and the remainder of the rods adjusted by manual electric solenoid control.

During normal operation the scram control valve "L" is held energized, blocking the ports between the accumulator and motor. An emergency insertion or scram will call for a shut-off signal. In other words, all control circuits to the drive are de-energized. This will cause the regulating control valve to return to the null or closed position and the scram control valve to return to its full open position. Accumulator discharge will then provide the high volume flow to accelerate and drive the hydraulic motor at scram velocity. Gas pressure in the accumulator circuit after scram would be at least 40 per cent of maximum operating pressure. Deceleration is normally accomplished by the mechanically interlocked deceleration valve "M" during the last 2 feet of rod travel. If the deceleration valve seized in the open position, although such failure is extremely unlikely, the deceleration valve transmission would smoothly stall the motor through a torsion bar coupling. Top and bottom extremities of the rod travel will be cushioned by light rate springs to absorb residual energy resulting from end of stroke rod creep due to intentional leakage built into the deceleration valve.

Valves will be constructed so as to prevent pressure buildup in the motor ports from internal valve leakage which could conceivably cause the motor to drift with the system in the static condition. In addition, porting of the valves, especially the scram valve, will be such that inadvertent external action or component failure will make rapid or scram velocity withdrawal of the rod impossible.

Figure 6C indicates a number of check valves and external shut-off valves. Isolation valve "N" provides for deactivating a faulty rod or drive. Only one rod will be permitted to become inactive without immediate corrective action. Non-return check valves "O" and "P" prevent system or accumulator discharge if external pressure lines or pumps were to fail, thus maintaining the capability for all drives to scram even if there were a loss of pressure in the auxiliary supply system. Non-return check valve "Q" will be designed to prevent failure in the closed position. The helium buffer line is equipped with a non-return type of check valve to prevent a pressure loss in the drive containment in the case of rupture of the helium line. The orifice size of the buffer helium port is of such small size, that even without a check valve, the pressure drop in the drive containment would be so gradual that non-emergency corrective action could be taken.

The possible malfunctions which can occur in the hydraulic circuit are minor and will not require an automatically initiated scram. These situations will normally be taken care of by appropriate corrective action by the plant operators. The only potentially serious situation that would initiate an automatic scram would be the case where the supply system oil pressure dropped to a minimum level. In this case scram would be instrumented to be automatic with a minimum of delay, in order to utilize accumulator pressure before it is dissipated into the system. A standard checking procedure will be adopted during certain shutdown periods where each rod will be withdrawn individually and scrammed. This will assure that scram valves and accumulator pistons are free and functioning normally. In every case the design will be such as to fail safe on the loss of proper functioning.

The control rod drive is designed to provide the following operating characteristics:

a. Normal regulating rod speed .....approx. 0.125 ft./sec.
b. Maximum regulating acceleration up or down....<1g
c. Maximum scram rod speed.....10 ft./sec.
d. Maximum scram acceleration 3g
e. Normal maximum scram deceleration.....<1g
f. Total system response delay time.....approx. 100 milliseconds
g. Total rod stroke..... 8 ft.

(3) Auxiliary Equipment

(a) Fluid Systems

The external or auxiliary equipment will consist of a fluid pressure supply system, a fluid return or reservoir system and a pressure regulating control circuit. The pressure supply will be provided by two parallel electric motor driven pump units. One pump will provide sufficient capacity for normal regulating control and accumulator recharging. The other pump will act as a standby and will be switched on automatically if the system pressure should fall below 90 per cent of normal; or, it can be driven in parallel if greater capacity should be needed. With one pump the re-charging time for the accumulators after a scram would be about 1-1/2 minutes. Interlocks will

HTGR PROJECT
TARGET SCHEDULE
CONTROL RODS

LEGEND

- ● INFORMATION TRANSMITTED
- ■ COMPLETION OR DECISION
- ▲ DELIVERY
- ⊗ PLACE ORDER FOR COMPONENT

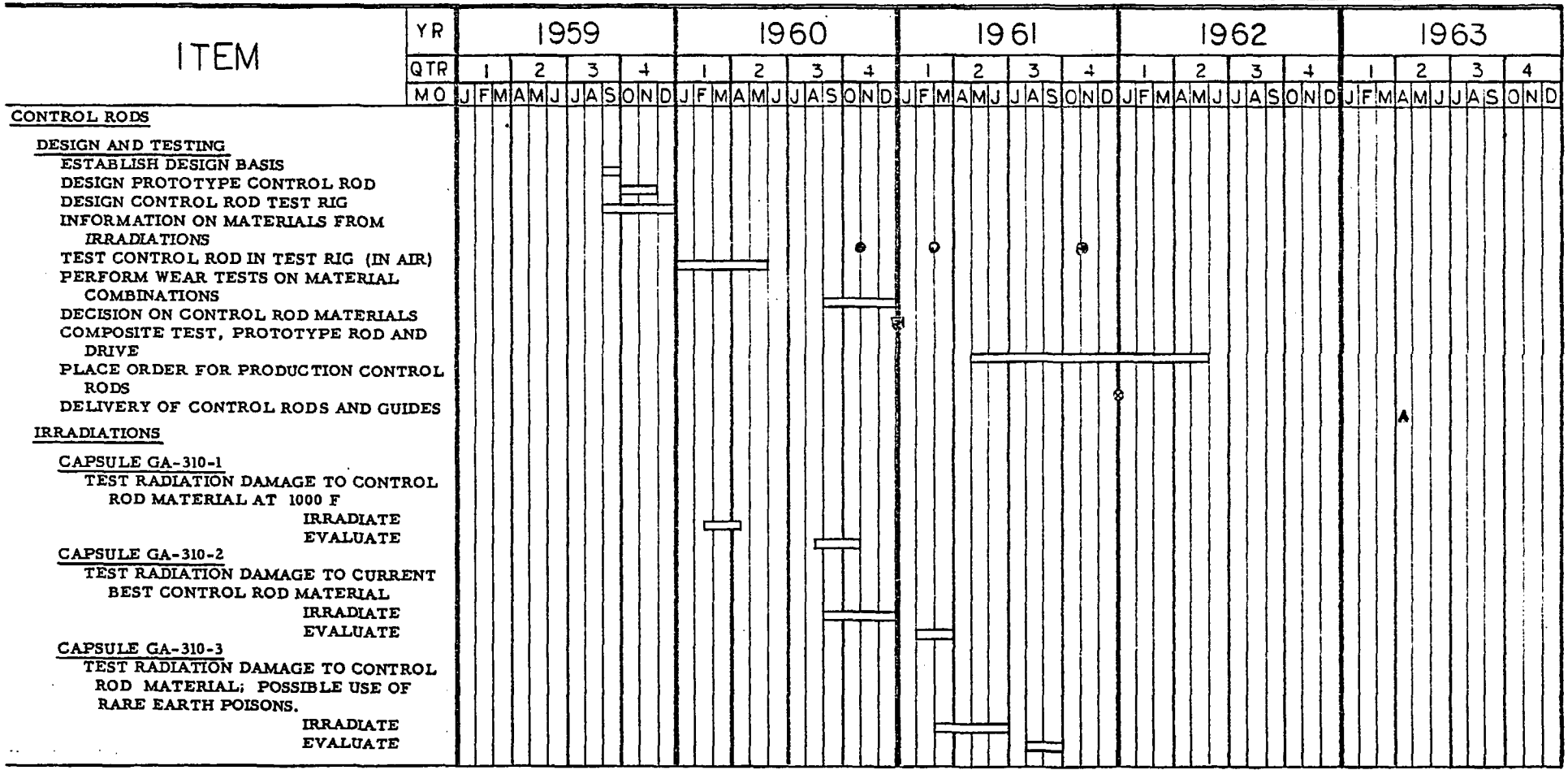

September, 1960

b. Control Rod Drives

(1) Background

The choice of a hydraulic type of drive has been based on a number of factors, an important one being reliability. Component selection has been based on the use of heavy duty industrial type units that have a history of successful operation for long periods with no maintenance. Ten million to twenty million cycles are readily obtained by industrial valves which far exceed the duty cycle they would be subjected to in this application. All components will be selected to operate well below their normal continuous duty rating. Components will be selected, modified or designed if necessary, to provide minimum leakage and maximum fail safe characteristics.

Hydraulics have been developed over the years into extremely reliable and versatile systems, that have found application in practically every field requiring some form of power transmission. Hydraulics have been chosen because of their high reliability, high power to size ratio, high flexibility, and high signal to power response capabilities. Hydraulic rotary output drives have acquired a reputation of long and reliable life in mobile equipment, such as, earth movers, tractors, military vehicles, etc., where operating environment and servicing conditions have been less than desirable. Industrial applications, such as machine tools have required extremely long life, far in excess of the duty life expected in the control rod drives. High power output precision control requirements have been met by hydraulics, such as: aircraft and missile control systems; sea, ground and airborne radar antenna and gun laying systems; and the more recent machine tool applications using programmed automatic control. Components and systems have been developed to meet near zero leakage requirements and are now commonplace.

In addition, to assure high reliability, a high degree of cleanliness will be maintained in the circuit by a high efficiency filtration system. Extreme cleanliness will be initially insured at installation by suitable cleaning procedures of the equipment and piping prior to final assembly.

Fluid selection will be based on its suitability for use in this hydraulic system, its resistance to radiation damage and possessing a low vapor pressure property. Radiation level in the sub-pile room will be relatively low and will not present a problem with most hydraulic fluids even under many years of exposure. Vapor pressure of the order of one-tenth of a micron at operating temperature is considered desirable in order to keep diffusion into the buffer helium at an acceptable level. Several standard hydraulic fluids possess vapor pressures meeting this requirement and have excellent lubricating properties as well.

Grease type lubricants meeting similar requirements in regard to radiation and vapor pressure will be used in bearings, clutches, etc. located in the power unit region. Material combinations for the ball screw and nut, and ball splines will be selected from experimental test results that will allow operation under conditions requiring a minimum of lubrication.

(2) Program and Schedule

The proposed drive system is fundamentally straightforward mechanically. The hydraulic circuit consists of reliable and well proven components. Because of the application, a comprehensive development and test program for the entire drive system has been planned and is currently under way.

(a) Wear Tests on Material Combinations

Although it is planned to lubricate most of the mechanisms, there are certain points where it may be difficult to assure lubrication over long periods without frequent inspection and maintenance. In these instances it is intended to select material combinations that offer minimum friction and maximum wear and galling resistance. This becomes particularly important where the operating environment is an inert and dry atmosphere such as helium.

At the present time a friction-wear test is under way which will provide valuable information on the behavior of various material combinations operating in a helium atmosphere. The test will check materials with various finishes and hardnesses running dry. It will also check the life or permanency of certain antifriction coatings, such as dry film type lubricants if these are found to be necessary.

Among combinations to be tested are pairs of materials selected from the following:

a. 416 stainless steel - hardened.
b. 416 stainless steel - heavily nitrided.
c. 52100 steel-chromized.
d. Stellite No. 3
e. Stellite No. 25
f. Tungsten carbide
g. 440C stainless - hardened
h. Graphite

Other materials will be included in the program as found necessary.

(b) Component Tests

a. Ball Nut and Screw

A test setup is now being built to determine the dynamic behavior of various ball nut and screw configurations. The screws will be run at various accelerations and velocities to determine stability and critical speed effects. In addition, the test will be performed in a helium atmosphere at temperatures up to 200 F to acquire friction and wear data, which is above the design operating temperature. The test rig will use a hydraulic motor drive to provide the required accelerations and velocities, but will not simulate the hydraulic circuit proposed for the actual control rod drive. These tests are expected to run to the end of 1960.

b. Other Components and Sub Components

Tests will be run to check function and reliability of various mechanisms and assemblies such as latches, clutches, override snubbers, rotary face-seal, etc., by the end of 1960. Cycling tests to check reliability, life, leakage, etc. of hydraulic components will also be run. In addition to the component tests, a prototype hydraulic system will be built and thoroughly tested for function, response, reliability, leakage, etc. The latter system will be ordered during this period and will be placed in operation in the early part of 1961.

(c) Full Scale Prototype Test

Completion of construction of the full scale prototype test facility is scheduled for April, 1961. Figure 58 shows a view of the test facility presently under construction. Construction of the complete prototype drive system is scheduled to be completed by the same time. Testing of the entire system is planned for the period May 1961 through April 1962.

The main test will simulate full scale reactor operation of the entire system complete with the prototype control rod absorber element. Reactor simulation will provide pressurized helium environment with expected temperature gradients. Complete control and monitoring instrumentation proposed for the actual plant installation will be duplicated. Additional instrumentation as necessary will be used to control and record variables essential to the system and the test. The test will provide data on overall system integrity, response, performance, duty life, wear rates if detectable, and reliability. It is planned to subject the rod/drive combination to at least 10^6 inches of random motions at regulating speed, and at least 5000 scram operations starting from various rod positions. The latter number is five times as many scrams as are expected to occur in the life of a control rod drive. The test will be carried to the point of destruction of some important feature if this can be done in a reasonable period of time.

Naturally, all control rod drives and their associated components will receive an exhaustive series of check-out tests in situ at the Peach Bottom site prior to initial reactor operation with a pure helium atmosphere in the reactor. These tests will embrace both hot and cold conditions and at least 100 scrams per rod during which the rod drive performance will be monitored, especially from the point of view of excessive accelerations.

(d) Schedule

The target schedule for the control rod drive development and testing program is shown in the chart on the following page.

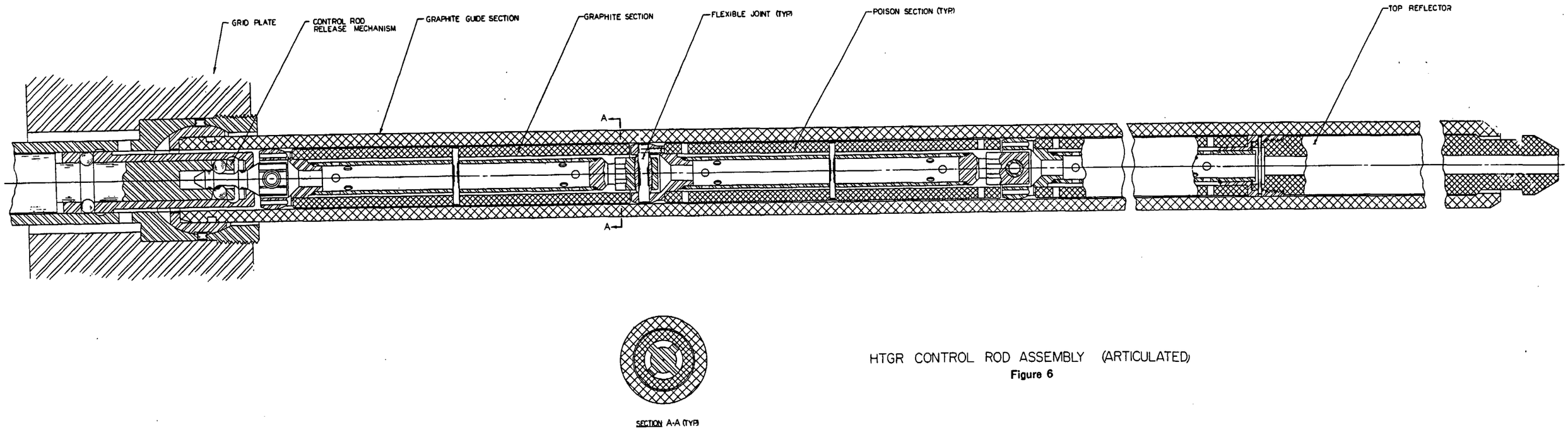

HTGR CONTROL ROD ASSEMBLY (ARTICULATED)

Figure 6

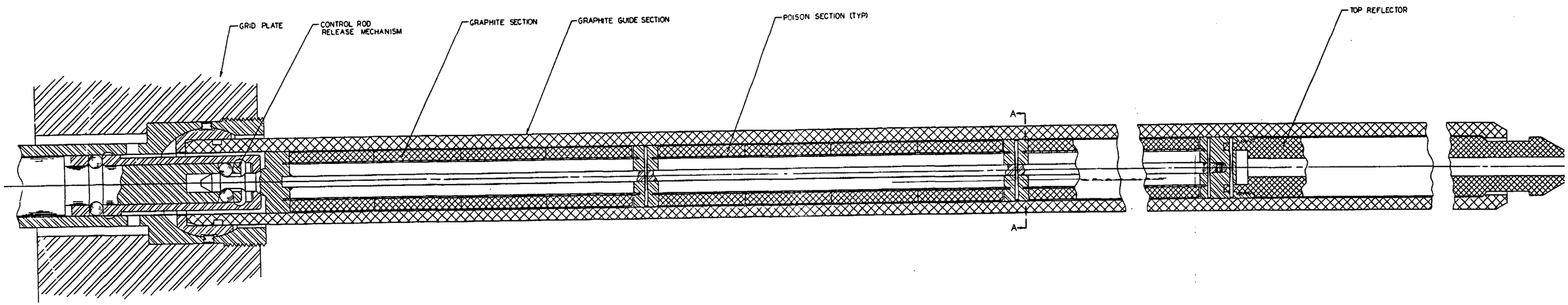

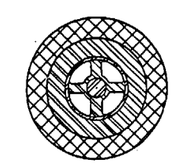

SECTION A-A
(TYP FOR ALL SECTIONS)

HTGR CONTROL ROD ASSEMBLY (FLEXIBLE)

Figure 6A

SEP 1960

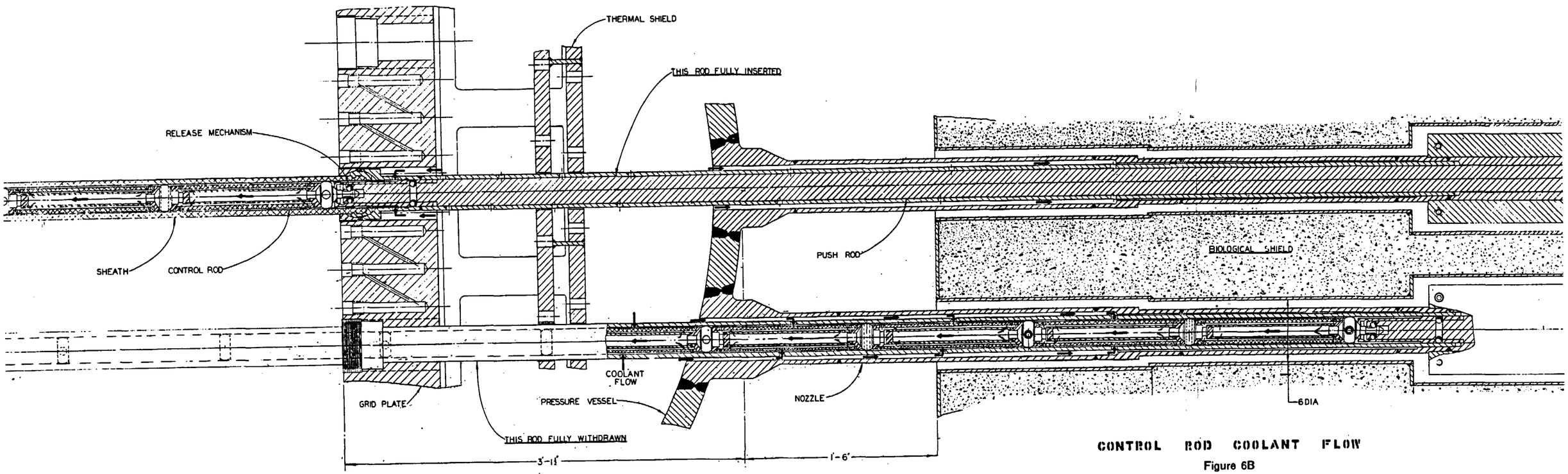

CONTROL ROD COOLANT FLOW

Figure 6B

HTGR HYDRAULIC MOTOR CONTROL ROD DRIVE

September 1960

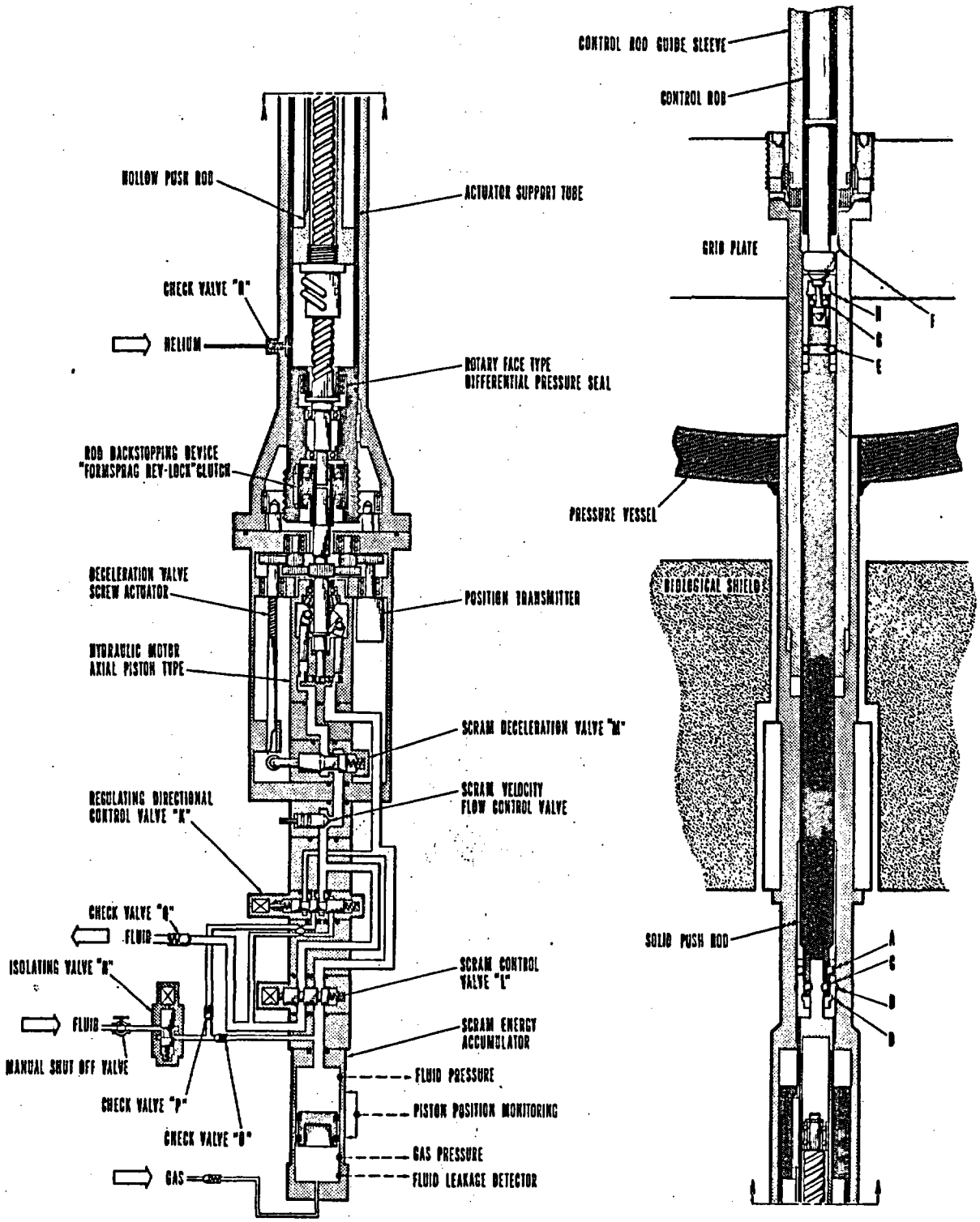

FIGURE 6C

HTGR REACTOR EQUIPMENT TEST FACILITY

September 1960

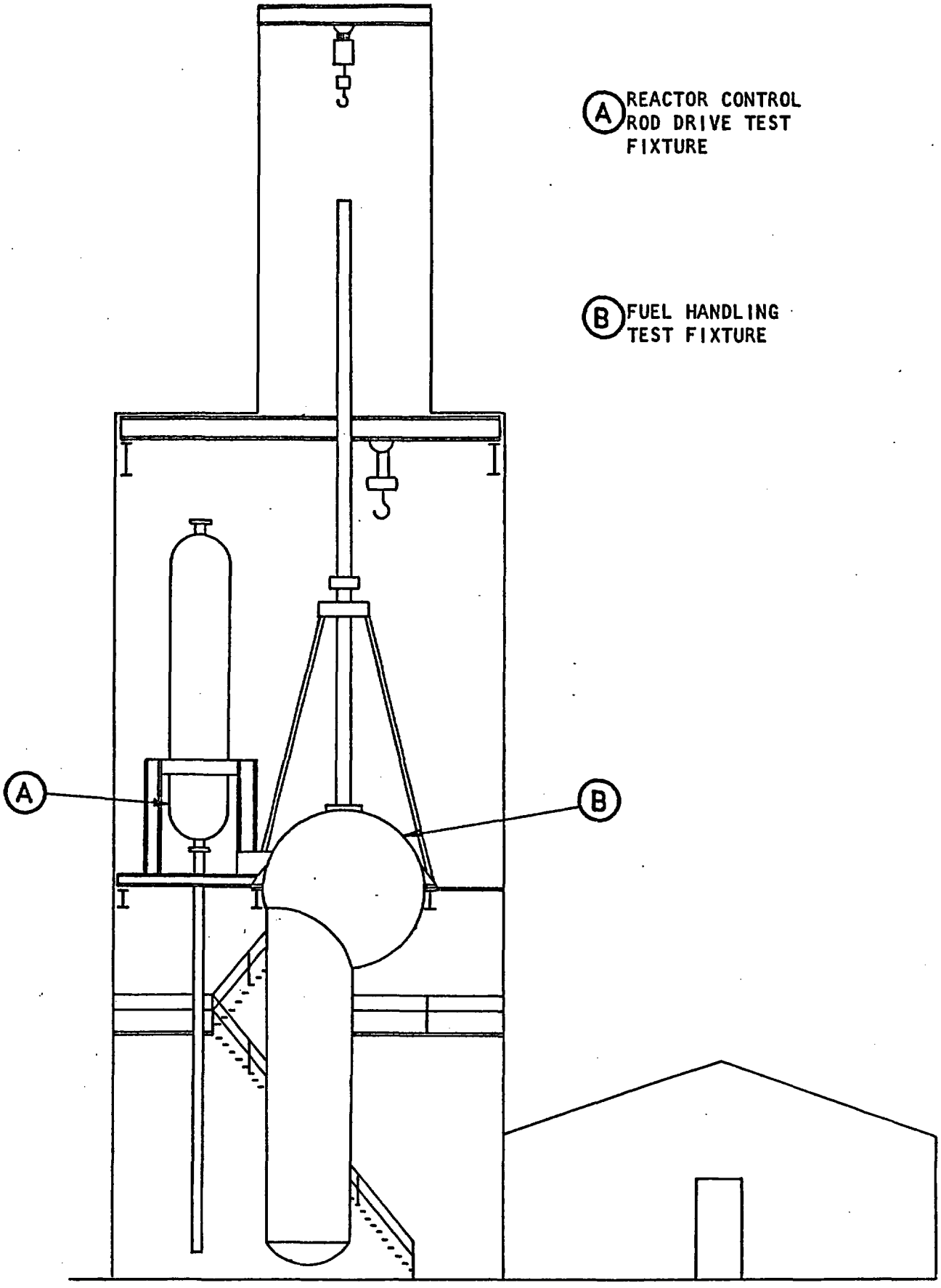

FIGURE 58

HTGR PROJECT
TARGET SCHEDULE
CONTROL ROD DRIVES

LEGEND

- ⊖ INFORMATION TRANSMITTED
- ■ COMPLETION OR DECISION
- ▲ DELIVERY
- ⊗ PLACE ORDER FOR COMPONENT

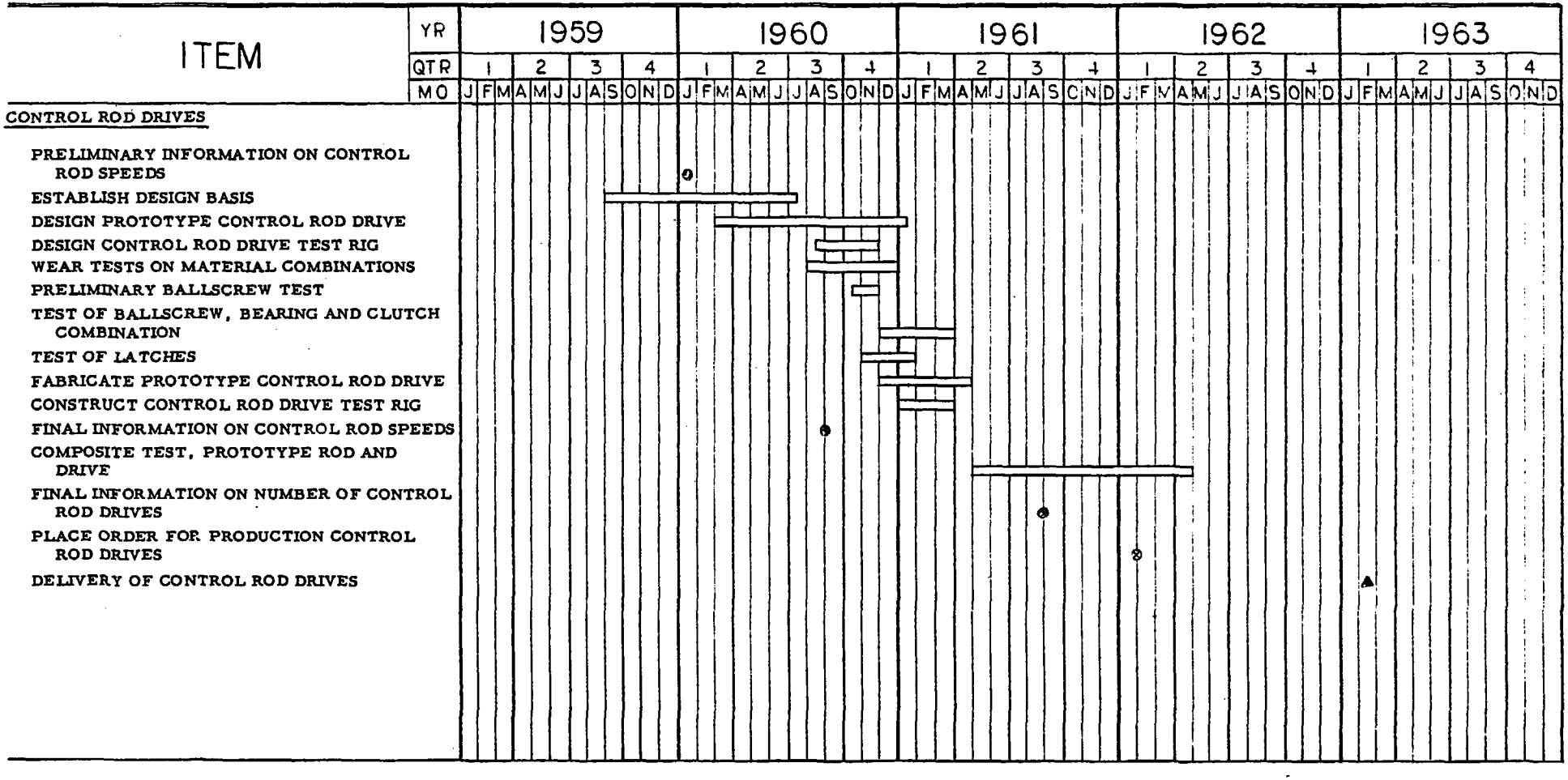

September, 1960

OBSOLETE PAGES

8. Control Rods and Control Rod Drives

a. Control Rods

The present reference design, which is shown in Figure 6, consists of six boron carbide loaded carbon cylinders, each about 13-1/2 inches long, supported on a center support rod made of type 321 stainless steel. The concentration of boron in the carbon is in the range 20-30 per cent by weight, the boron existing as uniformly dispersed particles of boron carbide of diameter less than 50 microns. The support rod is flexibly jointed by knuckle joints located approximately every 15 inches along the length of the rod to provide flexibility in the control rod. This flexibility allows for any misalignment which may be introduced by differential thermal expansion and/or reactor vessel manufacturing tolerances. Within the reactor, the control rod slides in a graphite guide tube of about 3-1/2 inches O. D. by 2-1/2 inches I. D. by 12 feet long.

The control rod is connected to its drive unit by means of a push rod. The control rod is held to the push rod by means of a mechanical latch which can be released only by first opening the casing of the control rod drive and removing the power unit. Conversely, reattachment of the power unit to the drive is not possible with the latch open. Subsequent to the removal and reattachment of a control rod, correct operation of the latching mechanism is established by using the fuel transfer machine (Page II-18) to check that the control rod cannot be lifted. The control rod guide tube is held to the core grid plate by means of another mechanical latch.

It should be noted that the absorber material does not slide in contact with the guide tube since the outside diameter of the absorber material is less than the outside diameters of the knuckle joints. Possible adverse effects of impacts which might arise as a result of small amounts of play in the knuckle joints will be avoided by limiting the downward acceleration of the control rod to less than one g under all normal circumstances, including deceleration at the end of the scram stroke.

An alternate design for the control rod is under investigation simultaneously with the reference design described above. The alternate design, Figure 6A, involves the use of a small diameter support rod constructed of a high-temperature alloy. The necessary degree of flexibility of the control rod as a whole would result from the low flexural rigidity of the small diameter support rod.

Cooling of the control rods will be accomplished by diverting a small fraction (2% to 5%) of the helium coolant flowing through the core into the control rod guide tubes. The coolant enters the guide tube through holes in the region below the core grid plate, and divides into two parallel flow paths: a portion flows upward in the space between the guide tube and the control rod itself; the remainder flows downwards and enters the control rod support rod at or near its bottom, regardless of the position of the control rod. This latter coolant then flows upward within the control rod, cooling the support rod in the process. All of the control rod coolant discharges from the top of the guide tube into the plenum chamber above the top of the core, mixing with the main coolant stream at that location. Figure 6B shows the coolant flow pattern for the two limiting cases of a control rod fully inserted and fully withdrawn.

The division of control rod coolant flow between the paths inside and outside the absorber will vary with control rod position. When a control rod is fully inserted, the majority of its coolant will flow through the metal support rod, and its calculated maximum temperature under normal full power operation is close to 1000 F. If there were a reduction in primary coolant flow through the core, then there would also be a reduction of coolant flow through the control rods and their support rods. Such reducations in primary coolant flow are discussed in detail on page VII - 5, Section C.1. Since under reduced coolant flow the reactor would be scrammed immediately, the resulting rise in temperature of the control rod support rods would be negligible.

In the highly unlikely case of complete loss of coolant flow the following sequence of events would occur: the reactor would be scrammed immediately; as a consequence of the stored heat in the fuel elements the temperature equilibration radially across the fuel elements would result in an approximate maximum surface temperature of 3000 F in about three minutes for the hottest fuel elements (see page VII-6, Section C.2.); the control rods and therefore their support rods would overheat as a consequence, resulting in failure of some support rods after a few minutes time. Nevertheless, the control rods could not drop out of the reactor. Such a failure in any of the control rods would occur at a point within the rod more than 3 feet above the core grid plate and the control rod is held in place by its push rod and guide tube. Only in the incredible case of a subsequent failure of the push rods could the control rods leave the core. Such subsequent failure of the push rods would require this complete loss of coolant flow to prevail for many hours, a condition which is considered incredible with the separate parallel cooling circuits and multiple backup power sources.

Subsequent to any occurrence of reduced coolant flow the reactor operating procedure will specify a mandatory inspection of control rods to determine the extent, if any, of the damage which may have occurred. It should be noted that the fuel handling equipment is designed to remove a control rod and its guide tube together as one assembly, and that either a periscope or a television system will be provided for inspecting reactor core components within the reactor after shutdown.

The design of the control rod support will be selected in the winter of 1960-61, and the control rod will be test operated in hot helium, together with the prototype control rod drive, during the period May 1961 through April 1962, as detailed in Section II, Part L.

Both designs for the control rod presently being considered involve the use of uncanned boron carbide in carbon. The irradiation program now under way to determine the irradiation stability of this material is also described in Section II, Part L.4.

b. Control Rod Drives

(1) Mechanical Design

The present reference design for the control rod drive is based on a system utilizing an axial piston type hydraulic motor with hydraulic fluid as the prime mover for both the regulating and scram functions.

Figure 6C illustrates schematically the mechanical and hydraulic arrangement and circuitry of the drive. The system is comprised of the following major components: an outer containment or pressure shell, terminating at, and integral with, the pressure vessel; a screw actuator mechanism supported and contained within a tubular shell, co-axially fitting inside the pressure shell; a hydraulic power unit attached to the lower extremity of the pressure shell; a push rod arrangement, with its lower end attached to the screw actuator mechanism and the upper end attached to, and supporting, the control rod absorber element.

The outer pressure containment is essentially one continuous tubular member, welded to the bottom of the reactor vessel, with the power unit attached to the lower end by means of a mechanically sealed service disconnect, all of which forms a completely sealed unit. In the biological shield region the outer containment diameter is increased by means of a bolted on sleeve of a high nickel steel material. It provides a step configuration to the air gap between the drive containment and the concrete shield clearance hole for the purpose of reducing neutron streaming through this void.

The linear actuator portion of the drive is supported and packaged within a tubular member, fitting co-axially within the outer pressure shell. The purpose of this arrangement is to provide a convenient means of removing and servicing the mechanism without disturbing the outer drive containment. The ball-nut and lead-screw are located within this support tube. The screw is retained and supported by a combination of radial and thrust bearings at the lower end. The recirculating ball-nut is attached to the lower end of a hollow push rod. The push rod is splined or keyed to the support tube to restrain the nut against rotation. Rotation of the screw will thus cause the ball-nut to translate in an axial direction raising or lowering the hollow push rod.

At the lower end of the actuator, a rod backstopping device is located. It is a cam type self-energizing mechanical clutch that is torque and direction sensitive. The screw is splined to the clutch output end, and the external case of the clutch is keyed to the support tube. Torque applied to the input end is transmitted unrestricted to the screw in either direction. However, torque generated from the output or screw end is positively blocked at the clutch. The purpose of this device is to prevent the control rod from drifting downwards in the case of failure of the hydraulic motor. It also restrains the screw from rotating when the motor unit is detached for servicing.

Normally, the entire drive containment including the hydraulic power unit is pressurized with helium at a pressure slightly above reactor pressure. During removal of the hydraulic power unit for service, pressure is retained in the actuator containment region by means of a rotary seal between the screw and support tube, and a static seal arrangement between the support tube and outer shell.

The lower end of the support tube is anchored to an adjustment device that will allow raising and lowering of the entire actuator mechanism, independent of ball screw actuation. The purpose of this adjustment feature is to provide a means of actuating the latches that connect the absorber portion of the control rod to the drive.

A hydraulic power unit is attached to the lower end of the outer pressure shell. Connection is made by a gas tight mechanical joint that is readily separated for servicing. The power unit consists of an outer pressure shell containing a hydraulic motor, a deceleration valve, a gear and mechanism arrangement to actuate the deceleration valve, and a gear drive to actuate position transmitters, limit switches, etc.

Below and external to the pressure shell, but part of the power unit, is an integral valve and manifold assembly. This consists of flow control valves, a directional regulating control valve and a scram control valve. Flow connections between valves are accomplished by ported sub-plates that anchor and support the valves. Replaceable static seals between valve mounting faces and sub-plates effectively eliminate fluid leakage. Attached to the bottom end of the valve manifold or sub-plate is a piston type hydraulic accumulator.

The basic hydraulic drive circuit, its principle of operation and associated components are also schematically illustrated in Figure 6C. The hydraulic motor is of the axial piston type. External fluid leakage from the motor is prevented by a double shaft seal arrangement, where the volume between the seals is vented to the external oil reservoir. The motor shaft is splined to the input end of the rod backstopping clutch. The position transmitters, limit switches, etc., are driven by gears connecting to the motor shaft. In a similar fashion, the deceleration valve actuator is driven. This gear train will be of rugged design, capable of absorbing full motor output in a jammed or stalled condition without damage.

The hydraulic motor provides two modes of control rod operation: normal, controlled regulation at a relatively slow speed, and rapid insertion at high or scram velocity. This is accomplished by running the motor at two different flow rates. Regulating motion is controlled by restricted low volume delivery ports and externally controlled directional valving. Scram is controlled by large high volume delivery ports, a one-directional control valve and a deceleration valve.

The deceleration valve throttles the flow of oil leaving the hydraulic motor during the last two feet of rod insertion travel. The mechanical drive between the motor and this valve progressively closes the fluid exhaust orifice so as to bring the rod velocity down to zero with less than 1 g deceleration.

Regulation is accomplished by a two direction, three position control valve. In the de-energized or null position all ports are blocked. Valve position will be determined by either electric solenoid actuation or electric closed loop servo control.

Scram will be controlled by a spring offset two position valve. During normal rod operation, this valve is held in the closed position by an energized solenoid. De-energizing the solenoid shifts the valve into the open or scram position. The energy for performing the scram function is stored in the form of an inert gas charged hydraulic accumulator. A piston type accumulator is used in order to monitor stored fluid supply volume by instrumenting the approximate position of the piston. In addition, gas and fluid pressure will be monitored as well as the presence of fluid in the gas volume region.

The hollow push rod, its lower end attached to the ball-nut, terminates at the top in the form of a mechanical latch. This latch connects to the upper solid push rod. Referring to Figure 6C, the latch operates as follows. To disconnect this latch, the control rod is fully withdrawn and the power unit removed to provide access to the lower end of the actuator support tube. The support tube is anchored to a vertical adjustment fitting. This fitting is manipulated to cause the support tube to descend a fixed distance. This allows the nut and hollow push rod to drop down below the normal lower stopping point. This also pulls the latch down to a position where latching balls "A" will align with groove "B". Retainer sleeve for balls "A" will seat against a shoulder of the outer tube, causing balls "A" to cam out into groove "B", while the remainder of the latch mechanism continues downward an additional slight amount until balls "C" align with groove "D". This allows the hollow push rod to separate from the upper solid rod. The solid rod is prevented from dropping out by the previously mentioned step in the outer tube.

The top of the solid push rod terminates in the form of a mechanical latch that connects to the absorber portion of the control rod. Again referring to Figure 6C, the latch operates as follows. To disconnect this latch the control rod is fully inserted. As in the operation of the lower latch, the power unit has to be removed to provide access to the actuator support tube adjustment device. In this case, however, the support tube is raised above its normal position. The adjustment screw is rotated manually to raise the nut and push rod above its normal upper stopping point. This raises the latch assembly to a point where balls "E" align with groove "F" and cam outward allowing the push rod section to continue further. Push rod movement continues until balls "G" align with groove "H", and the shoulder of the push rod seats against the bottom of the ball retainer sleeve. An upward movement of the control rod will then cam balls "G" into groove "H" and allow its complete separation from the push rod.

To assure that all mechanical latches are engaged upon reassembly of a drive unit, the position of the actuator support tube is mechanically interlocked to the power unit attachment. In other words, it is impossible for the power unit to be secured in place unless the actuator support tube is in its normal operational position.

The control rod and graphite guide sleeve are designed to be removed together as one unit. With reference to Figure 6C, it will be noted that the guide sleeve seats in a universal type swivel joint. The sleeve is anchored to this joint by a bayonet pin type connection. Removal requires a small rotary motion applied to the guide sleeve by the fuel transfer machine. This disengages the bayonet locking pins and allows vertical withdrawal.

(2) Operation

The operating principle of the drive system is as follows. The drive and mechanism region inside the outer pressure shell is pressurized with buffer helium to a pressure slightly above reactor pressure. This serves two functions: it provides a balancing force to counteract the downward force exerted on the control rod by reactor pressure; and it provides a means of preventing fission products from the reactor entering the drive region by maintaining a flow of buffer helium from the drive containment to the reactor vessel.

Figure 6C illustrates the basic hydraulic equipment of the drive unit. Fluid pressure for normal regulation or controlled movement of the rod is supplied by auxiliary equipment, external to the sub-pile room and not shown in the figure. (This external pump system also maintains the scram accumulators at proper volume and pressure.) Upward and downward movement is determined by the spool position of regulating control valve "K". The present plan is to have a group of the centrally positioned rods in the core actuated by a closed loop electric servo control and the remainder of the rods adjusted by manual electric solenoid control.

During normal operation the scram control valve "L" is held energized, blocking the ports between the accumulator and motor. An emergency insertion or scram will call for a shut-off signal. In other words, all control circuits to the drive are de-energized. This will cause the regulating control valve to return to the null or closed position and the scram control valve to return to its full open position. Accumulator discharge will then provide the high volume flow to accelerate and drive the hydraulic motor at scram velocity. Gas pressure in the accumulator circuit after scram would be at least 40 per cent of maximum operating pressure. Deceleration is normally accomplished by the mechanically interlocked deceleration valve "M" during the last 2 feet of rod travel. If the deceleration valve seized in the open position, although such failure is extremely unlikely, the deceleration valve transmission would smoothly stall the motor through a torsion bar coupling. Top and bottom extremities of the rod travel will be cushioned by light rate springs to absorb residual energy resulting from end of stroke rod creep due to intentional leakage built into the deceleration valve.

Valves will be constructed so as to prevent pressure buildup in the motor ports from internal valve leakage which could conceivably cause the motor to drift with the system in the static condition. In addition, porting of the valves, especially the scram valve, will be such that inadvertent external action or component failure will make rapid or scram velocity withdrawal of the rod impossible.

Figure 6C indicates a number of check valves and external shut-off valves. Isolation valve "N" provides for deactivating a faulty rod or drive. Only one rod will be permitted to become inactive without immediate corrective action. Non-return check valves "O" and "P" prevent system or accumulator discharge if external pressure lines or pumps were to fail, thus maintaining the capability for all drives to scram even if there were a loss of pressure in the auxiliary supply system. Non-return check valve "Q" will be designed to prevent failure in the closed position. The helium buffer line is equipped with a non-return type of check valve to prevent a pressure loss in the drive containment in the case of rupture of the helium line. The orifice size of the buffer helium port is of such small size, that even without a check valve, the pressure drop in the drive containment would be so gradual that non-emergency corrective action could be taken.

The possible malfunctions which can occur in the hydraulic circuit are minor and will not require an automatically initiated scram. These situations will normally be taken care of by appropriate corrective action by the plant operators. The only potentially serious situation that would initiate an automatic scram would be the case where the supply system oil pressure dropped to a minimum level. In this case scram would be instrumented to be automatic with a minimum of delay, in order to utilize accumulator pressure before it is dissipated into the system. A standard checking procedure will be adopted during certain shutdown periods where each rod will be withdrawn individually and scrammed. This will assure that scram valves and accumulator pistons are free and functioning normally. In every case the design will be such as to fail safe on the loss of proper functioning.

The control rod drive is designed to provide the following operating characteristics:

a. Normal regulating rod speed .....approx. 0.125 ft./sec.
b. Maximum regulating acceleration up or down....<1g
c. Maximum scram rod speed.....10 ft./sec.
d. Maximum scram acceleration 3g
e. Normal maximum scram deceleration.....<1g
f. Total system response delay time.....approx. 100 milliseconds
g. Total rod stroke..... 8 ft.

(3) Auxiliary Equipment

(a) Fluid Systems

The external or auxiliary equipment will consist of a fluid pressure supply system, a fluid return or reservoir system and a pressure regulating control circuit. The pressure supply will be provided by two parallel electric motor driven pump units. One pump will provide sufficient capacity for normal regulating control and accumulator recharging. The other pump will act as a standby and will be switched on automatically if the system pressure should fall below 90 per cent of normal; or, it can be driven in parallel if greater capacity should be needed. With one pump the re-charging time for the accumulators after a scram would be about 1-1/2 minutes. Interlocks will

prevent withdrawal of any rods subsequent to a scram until the normal accumulator pressure is reestablished.

The fluid return or reservoir system will be maintained pressurized at the same pressure as the drive containment. This is to prevent the possibility of any significant leakage of contaminated helium into the hydraulic system.

Gas pressure supply for the accumulators will be in the form of bottled nitrogen located in the auxiliary equipment compartment. It will be available at a pressure higher than system fluid pressure. During initial charging of the accumulators with fluid pumps off, gas pressure will be supplied at about 40 per cent of normal fluid system pressure prior to topping off with the fluid pressure pumps. During reactor operation, with system fluid pumps operating at normal, instrumentation indication that the accumulator piston is too low would mean a probable escape of accumulator gas. For this condition gas would be available at above normal system pressure to bring the piston back to the correct position.

(b) Instrumentation

Pressure and flow regulating control will consist of a panel mounted with shut-off valves, pressure regulating valves, pressure gages, fluid temperature indicators and reservoir fluid level alarms.

Instrumentation of the hydraulic system external to the reactor containment region will indicate the following conditions which may require corrective action by the plant operators.

a. Presence of excess fluid in the pressure containment of the power unit.

b. Presence of excess fluid in the gas region of the hydraulic accumulators.

c. Insufficient fluid in the accumulators indicated by the accumulator piston position.

d. Difference between accumulator gas pressure and system hydraulic pressure.

e. System fluid pressure too low.

f. Fluid temperature too high.

g. Insufficient fluid volume in reservoir.

h. Insufficient fluid pressure in reservoir.

4. Control Rods and Control Rod Drives

a. Control Rods

(1) Control Rod Tests

A reference design control rod has been built (without boron in the carbon) and operated in a cold air test through approximately 10,000 normal insertion and withdrawal cycles during which the control rod was required to negotiate a sudden change in direction of one degree as it slid from a steel guide tube into a graphite guide tube and back again.

The articulated control rod behaved very smoothly throughout this test. The amount of wear in the graphite guide tube was measured to be of the order of 0.0002 inches while the stainless steel surfaces that had been sliding against the inside surface of the graphite guide tube were found to have been worn away to the extent of about 0.0005 inches.

Wear tests in a hot, pure helium environment on combinations of materials which may be used in the control rod have begun and are scheduled for completion by the end of 1960.

(2) Irradiation of Control Rod Materials

Various samples of carbon and graphite materials containing boron carbide were irradiated in the GETR during February, March and April, 1960, with an integrated thermal flux of about 5×10^{19} at temperatures in the range 1000 F to 1500 F. Boron contents from 10 per cent to 30 per cent by weight were used. Evaluation of the irradiated samples is currently under way but it has been established that the samples maintained their integrity and that shrinkage was small. Irradiation of a second set of samples is about to begin. It is intended that the integrated thermal flux in this case be about 10^{20}. Evaluation of these samples should take place in the spring of 1961. Additional irradiations of samples of control rod absorber material are scheduled for the period March to July, 1961, with evaluation to follow in the months of August and September, 1961.

(3) Schedule

A detailed schedule is shown in the table below.

HTGR PROJECT
TARGET SCHEDULE
CONTROL RODS

LEGEND

- ● INFORMATION TRANSMITTED
- ■ COMPLETION OR DECISION
- ▲ DELIVERY
- ⊗ PLACE ORDER FOR COMPONENT

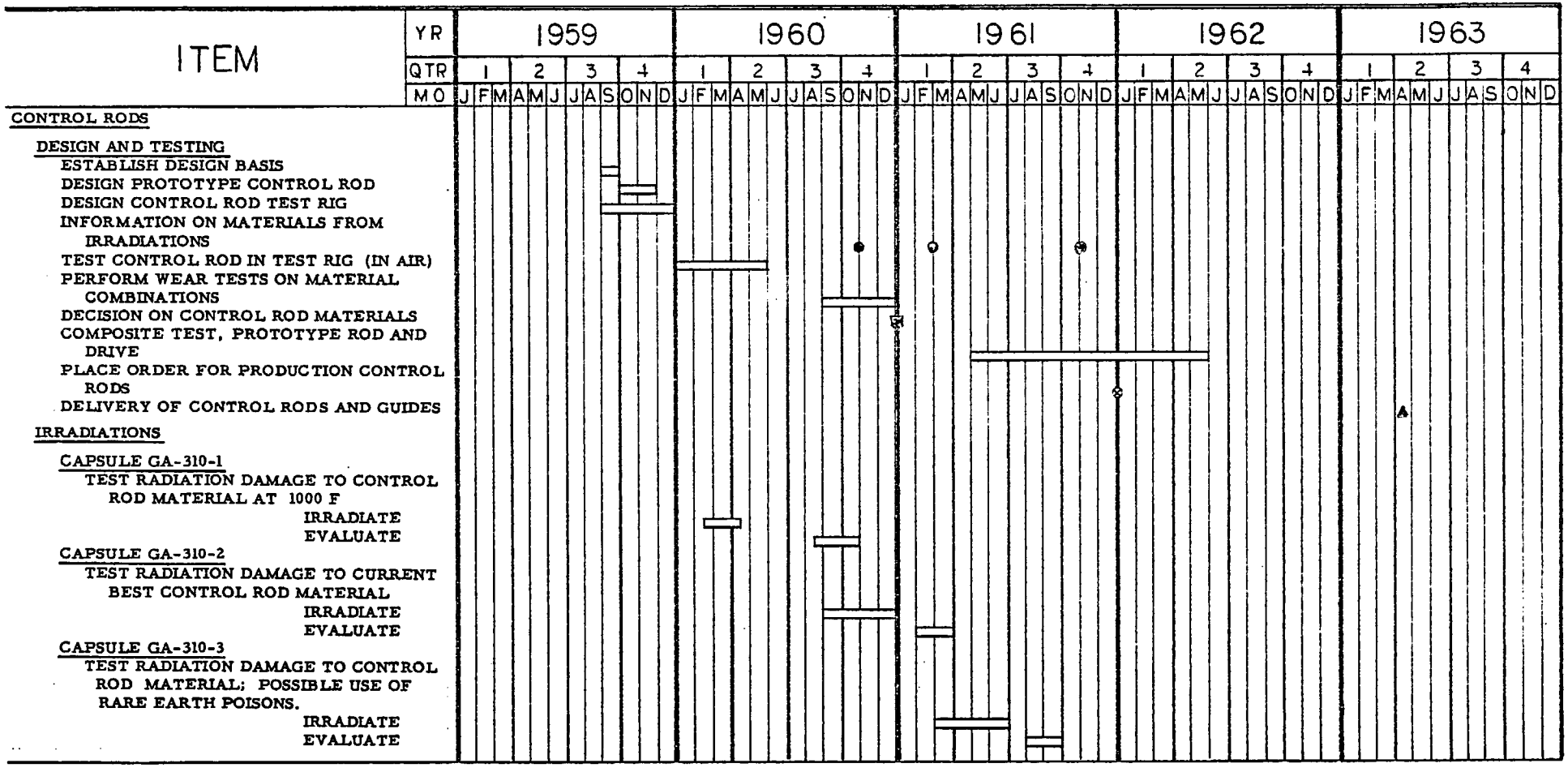

September, 1960

b. Control Rod Drives

(1) Background

The choice of a hydraulic type of drive has been based on a number of factors, an important one being reliability. Component selection has been based on the use of heavy duty industrial type units that have a history of successful operation for long periods with no maintenance. Ten million to twenty million cycles are readily obtained by industrial valves which far exceed the duty cycle they would be subjected to in this application. All components will be selected to operate well below their normal continuous duty rating. Components will be selected, modified or designed if necessary, to provide minimum leakage and maximum fail safe characteristics.

Hydraulics have been developed over the years into extremely reliable and versatile systems, that have found application in practically every field requiring some form of power transmission. Hydraulics have been chosen because of their high reliability, high power to size ratio, high flexibility, and high signal to power response capabilities. Hydraulic rotary output drives have acquired a reputation of long and reliable life in mobile equipment, such as, earth movers, tractors, military vehicles, etc., where operating environment and servicing conditions have been less than desirable. Industrial applications, such as machine tools have required extremely long life, far in excess of the duty life expected in the control rod drives. High power output precision control requirements have been met by hydraulics, such as: aircraft and missile control systems; sea, ground and airborne radar antenna and gun laying systems; and the more recent machine tool applications using programmed automatic control. Components and systems have been developed to meet near zero leakage requirements and are now commonplace.

In addition, to assure high reliability, a high degree of cleanliness will be maintained in the circuit by a high efficiency filtration system. Extreme cleanliness will be initially insured at installation by suitable cleaning procedures of the equipment and piping prior to final assembly.

Fluid selection will be based on its suitability for use in this hydraulic system, its resistance to radiation damage and possessing a low vapor pressure property. Radiation level in the sub-pile room will be relatively low and will not present a problem with most hydraulic fluids even under many years of exposure. Vapor pressure of the order of one-tenth of a micron at operating temperature is considered desirable in order to keep diffusion into the buffer helium at an acceptable level. Several standard hydraulic fluids possess vapor pressures meeting this requirement and have excellent lubricating properties as well.

Grease type lubricants meeting similar requirements in regard to radiation and vapor pressure will be used in bearings, clutches, etc. located in the power unit region. Material combinations for the ball screw and nut, and ball splines will be selected from experimental test results that will allow operation under conditions requiring a minimum of lubrication.

(2) Program and Schedule

The proposed drive system is fundamentally straightforward mechanically. The hydraulic circuit consists of reliable and well proven components. Because of the application, a comprehensive development and test program for the entire drive system has been planned and is currently under way.

(a) Wear Tests on Material Combinations

Although it is planned to lubricate most of the mechanisms, there are certain points where it may be difficult to assure lubrication over long periods without frequent inspection and maintenance. In these instances it is intended to select material combinations that offer minimum friction and maximum wear and galling resistance. This becomes particularly important where the operating environment is an inert and dry atmosphere such as helium.

At the present time a friction-wear test is under way which will provide valuable information on the behavior of various material combinations operating in a helium atmosphere. The test will check materials with various finishes and hardnesses running dry. It will also check the life or permanency of certain antifriction coatings, such as dry film type lubricants if these are found to be necessary.

Among combinations to be tested are pairs of materials selected from the following:

a. 416 stainless steel - hardened.
b. 416 stainless steel - heavily nitrided.
c. 52100 steel-chromized.
d. Stellite No. 3
e. Stellite No. 25
f. Tungsten carbide
g. 440C stainless - hardened
h. Graphite

Other materials will be included in the program as found necessary.

(b) Component Tests

a. Ball Nut and Screw

A test setup is now being built to determine the dynamic behavior of various ball nut and screw configurations. The screws will be run at various accelerations and velocities to determine stability and critical speed effects. In addition, the test will be performed in a helium atmosphere at temperatures up to 200 F to acquire friction and wear data, which is above the design operating temperature. The test rig will use a hydraulic motor drive to provide the required accelerations and velocities, but will not simulate the hydraulic circuit proposed for the actual control rod drive. These tests are expected to run to the end of 1960.

b. Other Components and Sub Components

Tests will be run to check function and reliability of various mechanisms and assemblies such as latches, clutches, override snubbers, rotary face-seal, etc., by the end of 1960. Cycling tests to check reliability, life, leakage, etc. of hydraulic components will also be run. In addition to the component tests, a prototype hydraulic system will be built and thoroughly tested for function, response, reliability, leakage, etc. The latter system will be ordered during this period and will be placed in operation in the early part of 1961.

(c) Full Scale Prototype Test

Completion of construction of the full scale prototype test facility is scheduled for April, 1961. Figure 58 shows a view of the test facility presently under construction. Construction of the complete prototype drive system is scheduled to be completed by the same time. Testing of the entire system is planned for the period May 1961 through April 1962.

The main test will simulate full scale reactor operation of the entire system complete with the prototype control rod absorber element. Reactor simulation will provide pressurized helium environment with expected temperature gradients. Complete control and monitoring instrumentation proposed for the actual plant installation will be duplicated. Additional instrumentation as necessary will be used to control and record variables essential to the system and the test. The test will provide data on overall system integrity, response, performance, duty life, wear rates if detectable, and reliability. It is planned to subject the rod/drive combination to at least 10^6 inches of random motions at regulating speed, and at least 5000 scram operations starting from various rod positions. The latter number is five times as many scrams as are expected to occur in the life of a control rod drive. The test will be carried to the point of destruction of some important feature if this can be done in a reasonable period of time.

Naturally, all control rod drives and their associated components will receive an exhaustive series of check-out tests in situ at the Peach Bottom site prior to initial reactor operation with a pure helium atmosphere in the reactor. These tests will embrace both hot and cold conditions and at least 100 scrams per rod during which the rod drive performance will be monitored, especially from the point of view of excessive accelerations.

(d) Schedule

The target schedule for the control rod drive development and testing program is shown in the chart on the following page.

HTGR PROJECT
TARGET SCHEDULE
CONTROL ROD DRIVES

LEGEND

- ● INFORMATION TRANSMITTED
- ■ COMPLETION OR DECISION
- ▲ DELIVERY
- ⊗ PLACE ORDER FOR COMPONENT

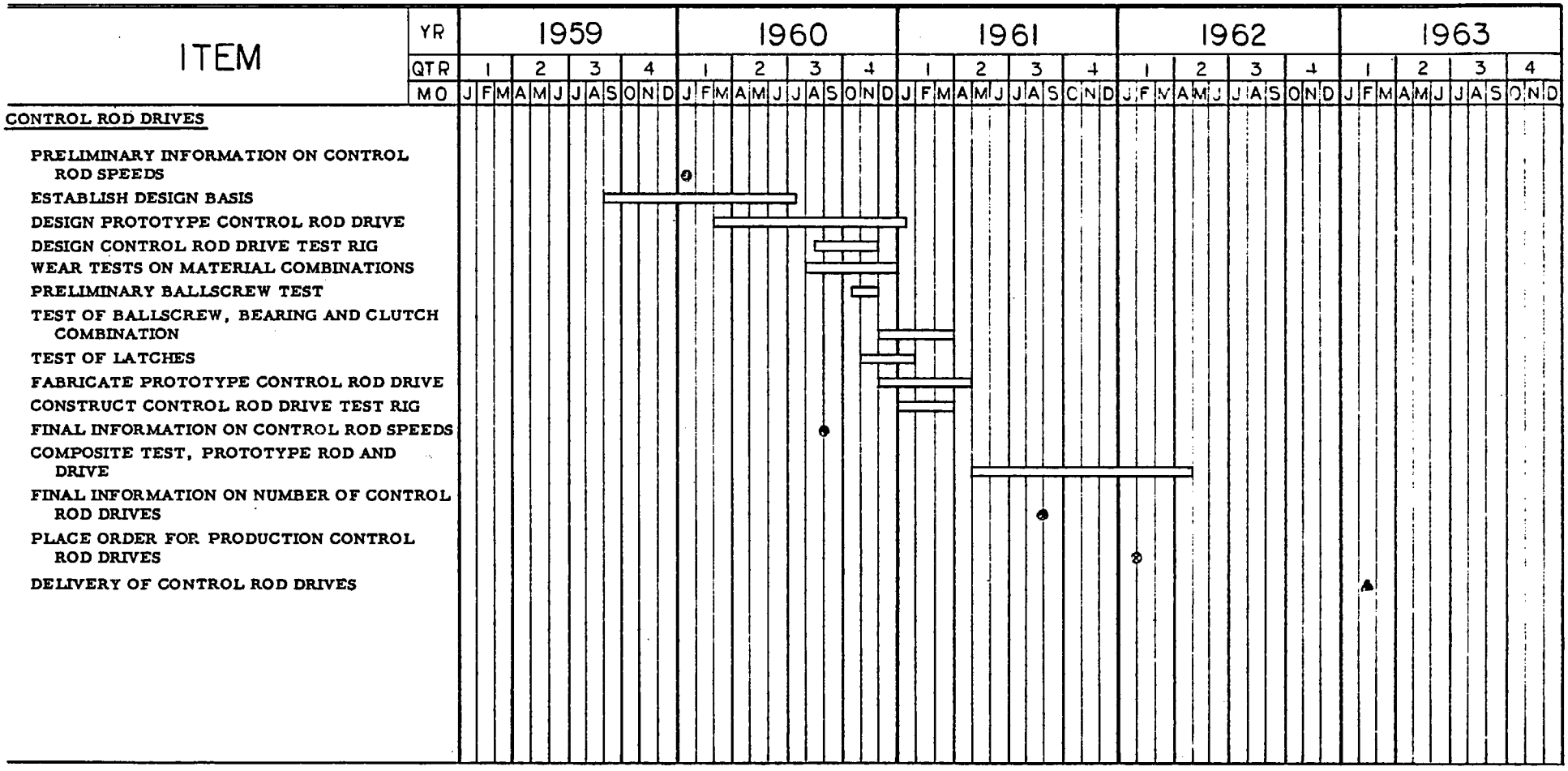

September, 1960

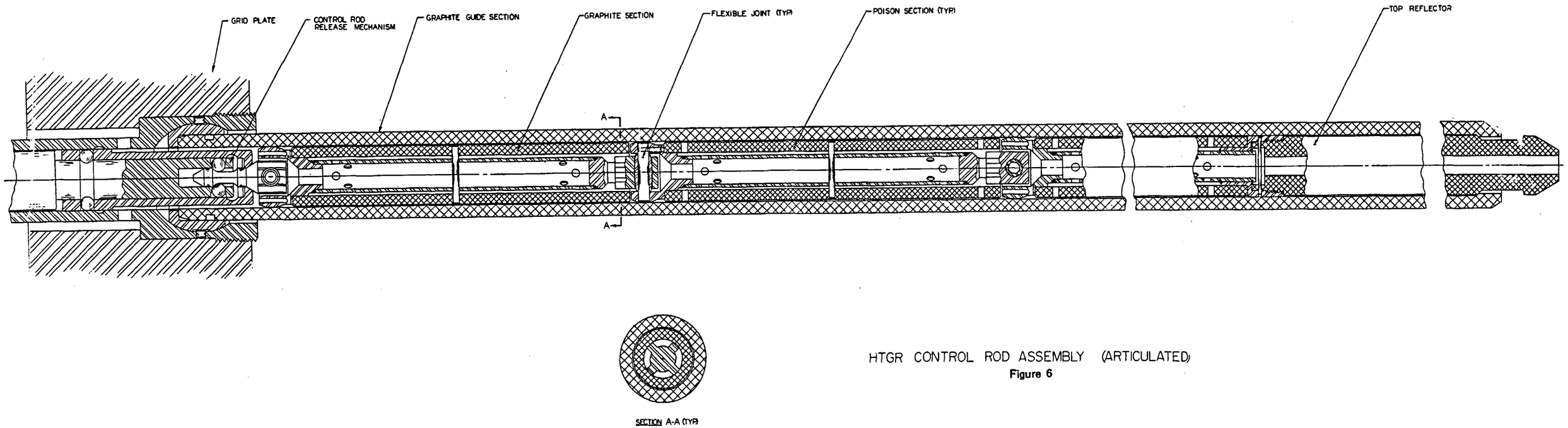

HTGR CONTROL ROD ASSEMBLY (ARTICULATED)

Figure 6

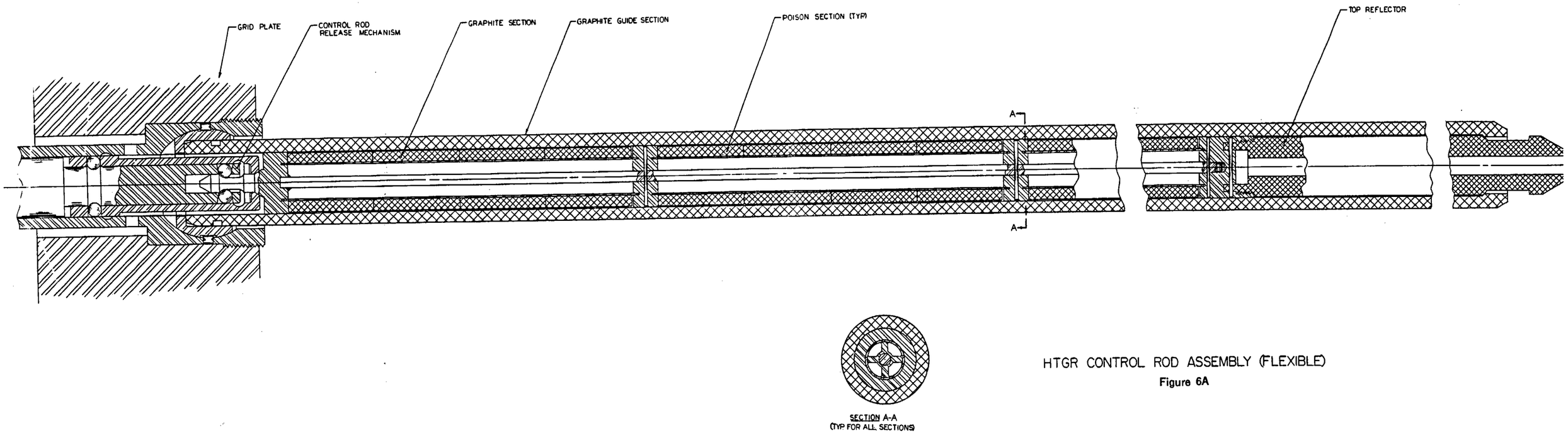

HTGR CONTROL ROD ASSEMBLY (FLEXIBLE)

Figure 6A

SEP 1960

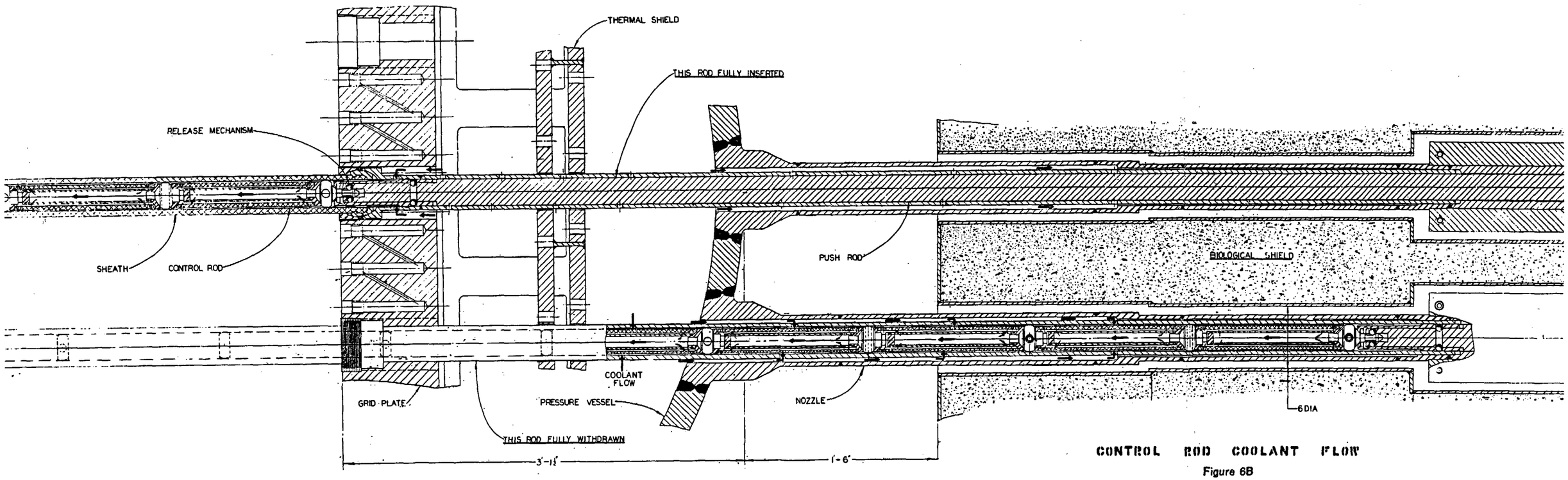

CONTROL ROD COOLANT FLOW

Figure 6B

HTGR HYDRAULIC MOTOR CONTROL ROD DRIVE

September 1960

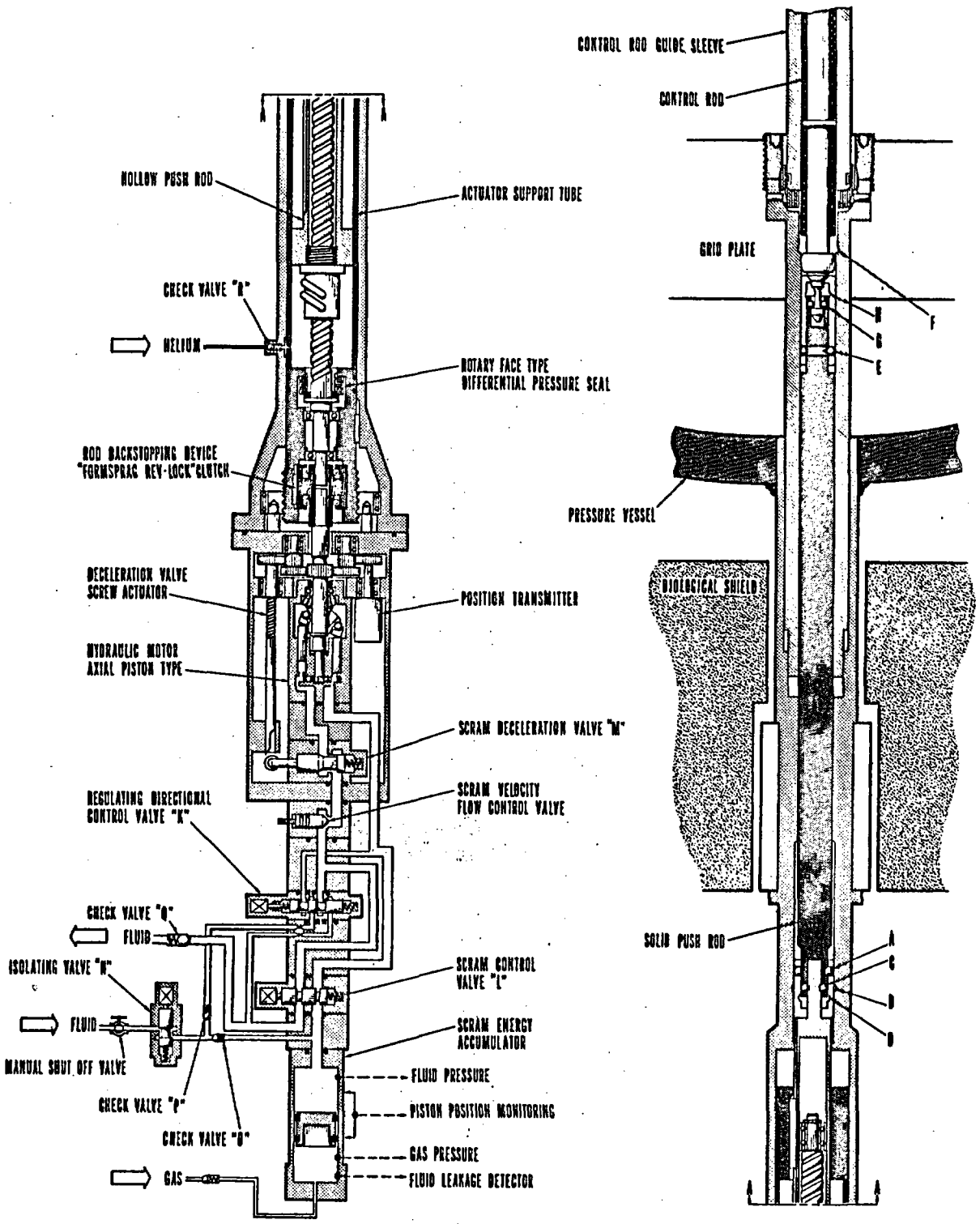

FIGURE 6C

HTGR REACTOR EQUIPMENT TEST FACILITY

September 1960

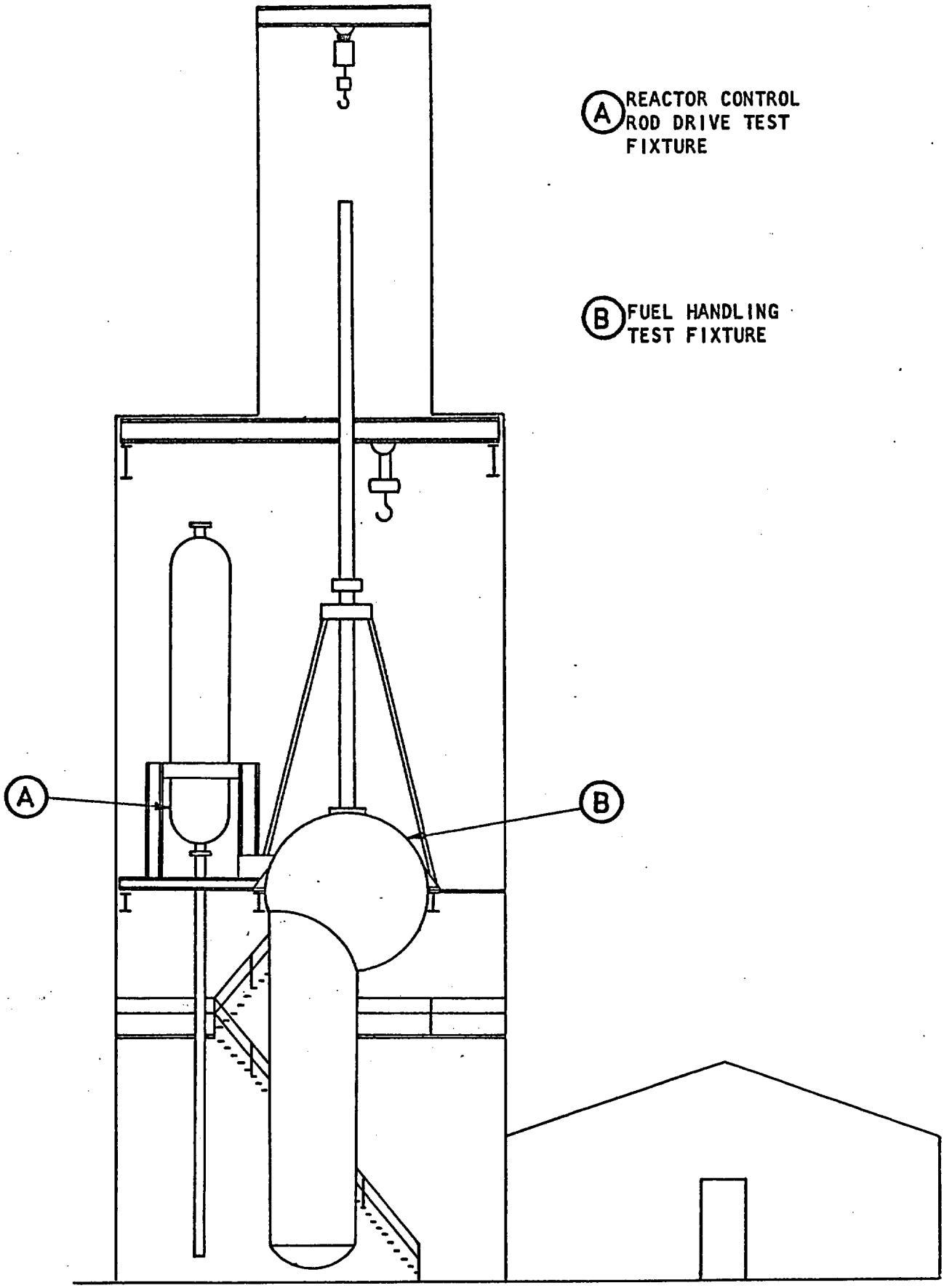

FIGURE 58